DOSE RESPONSE RELATIONSHIP BETWEEN THE CHEMICAL COMPOSITION OF 2.4 MICROMETER PARTICLES AND HUMAN LUNG CELLS (A549) CYTOKINE EXPRESSION

by

Alice J. Kardjaputri
B.Sc.(Hons), Carleton University, 2005

THESIS SUBMITTED IN PARTIAL FULFILMENT OF
THE REQUIREMENTS FOR THE DEGREE OF

MASTER OF SCIENCE

In the
Department of
Chemistry

SIMON FRASER UNIVERSITY

Summer 2009

APPROVAL

Name: Alice J. Kardjaputri

Degree: Master of Science

Title of Thesis: Dose Response Relationship Between Chemical Composition Of 2.4 Micrometer Particles And Human Lung Cells (A549) Cytokine Expression

Examining Committee:

Chair — Dr. David J. Vocadlo
Associate Professor, Department of Chemistry

Dr. George R. Agnes
Senior Supervisor
Professor, Department of Chemistry

Dr. Hua-Zhong(Hogan) Yu
Supervisor
Associate Professor, Department of Chemistry

Dr. Robert A. Britton
Supervisor
Assistant Professor, Department of Chemistry

Dr. Charles J. Walsby
Internal Examiner
Assistant Professor, Department of Chemistry

Date Defended/Approved: March 27, 2009

Declaration of
Partial Copyright Licence

ABSTRACT

Inhalation of ambient particulate matter is a factor in the pathogenesis of cardiovascular and pulmonary diseases. A goal of this thesis was to identify specific chemical components of particulate matter most significant in its causing adverse health effects. To address this issue, instrumentation and methodology were developed with which one could design, create, levitate and deposit 2.4±0.1 μm diameter particles of known chemical composition onto lung cells, *in vitro*, followed by the monitoring of downstream human lung cell (A549) response. An outcome of the method development process was an investigation of two disparate components hypothesized to be significant factors in particulate matter toxicity, endotoxin and soluble metals. The effect of incorporating these components, separately, into carbon particles on cytokine expression from lung cells was measured. Through immunocytochemistry studies of the expression of intercellular adhesion molecule (ICAM)-1, it was learned that endotoxin and metal salt both effect its upregulation and their relative toxicity were determined to be 9.0×10^{-5} versus 4.4×10^{-3} per particle number per pg of LPS and Zn, respectively. Additionally, another biomolecule not yet identified but observed using MALDI-TOF-MS (m/z= 8.3 kDa) was upregulated by A549 cells incubated with these particle types.

DEDICATION

.

For mommy and Cecil

ACKNOWLEDGEMENTS

The support of my senior supervisor Dr. George Agnes has been exceptional. His guidance, humour, and support and a willingness to let me “prove him wrong” created an atmosphere in which I was able to strive; and for that, my gratitude can not be overstated.

I would also like to acknowledge Dr. van Eeden, Dr. J. Hogg, Dr. S Hayashi from the iCAPTURE Centre at St. Paul’s Hospital, for all of the informative discussions where she explained what my results actually meant. I would also like to thank all of the others at iCAPTURE that helped guide me in the right direction and make me feel at home: John Gosselink and John McDonough.

I would like to thank my many co-workers from over the years. Particularly, I would like to thank Allen E. Haddrell (whose work in the development of the WaSP methodology truly made this thesis possible), Neil Draper (for his willingness to always help), Mariana Cruz (for her insight and for editing my thesis), and other lab mates who make the work environment more interesting.

And of course, the support of my family and friends especially Ms. Jenny Tam throughout my studies has been incredible. Through all of the unforeseen events of the past few years, without their steadfast support, I have no idea how this would have ever been finished.

TABLE OF CONTENTS

LIST OF FIGURES

LIST OF TABLES

LIST OF ABBREVIATIONS

AC	alternating current
BD	Beta defensin
C	Celsius
CCL	Chemokine ligand
CFCAS	Canadian Foundation for Climate and Atmospheric Science
cm	centimetre
DC	direct current
EDLT	electrodynamic levitation trap
ELISA	enzyme linked immunosorbant assay
EPA	Environmental Protection Agency
g	gram
GC-MS	gas chromatography-mass spectrometry
h	hour
Hz	hertz
iCAPTURE	Imaging, Cell Analysis, and Phenotyping Toward Understanding Responsive, Reparative, Remodelling, and Recombinant Events
IL	interleukin
IR	infrared

K	Kelvin
k	Boltzmann constant
kHz	kilohertz
L	litre
m/z	mass to charge ratio
M	matrix
MALDI	matrix assisted laser desorption/ionization
MCP	Monocyte Chemoattractant Protein
MHz	megahertz
MS	mass spectrometry
mL	millilitre
mm	millimeter
mmol	millimole
mol	mole
NF-κB	nuclear Factor-κB
ng	nanogram
nm	nanometer
NO_3	nitrate radical
NSERC	Natural Sciences and Engineering Research Council of Canada
OH	hydroxyl radical
pg	picogram

PIP	proinflammatory potential
QIT	quadrupole ion trap
RF	radio frequency
ROS	reactive oxygen species
s	second
SFU	Simon Fraser University
T	temperature
TLF	time lag focusing
TNF-α	Tumour Nucrosis Factor-α
TOF	time of flight
UBC	University of British Columbia
°	degree
µL	microlitre
µm	micrometer

CHAPTER 1
INTRODUCTION

Clean air is a basic health requirement for achieving a healthy life style. Conversely, epidemiological evidence links exposure to ambient particulate matter and the pathogenesis of respiratory and cardiovascular diseases such as asthma, chronic obstructive pulmonary disease (COPD), arrhythmia, congestive heart failure, and myocardial infarction.[1-3] There are many sources of both natural and anthropogenic emissions of particulate matter, such as forest fires, volcanoes, and the combustion of fossil fuels. Particulates and gaseous emissions due to anthropogenic activities have increased dramatically with population increase and economic development of nations over the last century. Emissions due to anthropogenic activity is believed to be a significant factor for the observed progressive change locally and globally in the troposphere's chemical composition with respect to minor (low concentration) components.[3] How these emissions influence human health, and change in climate, is the subject of intense research activity world-wide.

Epidemiology studies have repeatedly demonstrated an association between exposure to particulate matter and numerous indices of human morbidity and mortality. Beyond a few size catagories, little information is available regarding how particulate chemical composition may affect, chronically and/or acutely, the cells of the respiratory tract, causing for example, oxidative stress and inflammation, which can through the mediators secreted by those cells invoke response in other tissues. Tools with which

hypotheses can be addressed using *in vitro* strategies that lead to contributions of relevant knowledge to this air quality issue are needed. Specifically, knowledge of the relative potential as to how each of the many different particulate types to effect differential expression of biomarkers is needed. Such information could permit improved understanding, and ideally extrapolation of the relative exposure risk to human health to the varied ambient particle sources. Introduced and used in the work described in this thesis is an apparatus that enabled the generation of particle populations where the particle chemical composition, the size of the particles, and the number of particles in each population is known, and then that population can be delivered to a lung cell culture to initiate a dose-response experiment.

1.1 Particulate matter

Analysis of ambient particles sampled from the troposphere have shown that they are a mixture of solid and/or liquid particles of various sizes, < 10 μm in diameter (PM_{10}), and that they have heterogeneous composition. Based on the location where ambient particles of various size tend to deposit onto the air-cell interface of the human respiratory tract, ambient particles are usually catagorized into three general size bins: particle aerodynamic diameter between 2.5 and 10 μm as $PM_{2.5-10}$ (coarse), particle aerodynamic diameter <2.5 μm as $PM_{2.5}$ (fine), and aerodynamic diameter <0.1 μm as ultrafine particles (PM_{UF}).

Ambient particles are also often categorized based on their source, either primary or secondary. Primary sources of particulate matter are those that directly introduce pre-existing particles into the troposphere. Primary particles tend to dominante the coarse fraction of PM (eg. 2.5-10 μm) and generally tend to not agglomerate in the troposphere.[4]

There are natural and anthropogenic sources of primary particles. Natural sources include volcanic eruptions, sea sprays, wind-driven suspension of soil or mineral dusts, and biological materials. Biological materials found in ambient particles include, for example, fragments of plants, micro-organisms, and pollens.[5-7] Anthropogenic sources of primary particles include biomass burning, vehicular generated dusts, and incomplete combustion of fossil fuels.[8,9] Anthropogenic activity that involves mechanical break-up of large materials by processes that include grinding or crushing are also sources of primary particles.[4,10]

Secondary ambient particles are produced as an outcome of oxidative chemical reactions in the troposphere.[4,10] The formation of secondary particles in the troposphere occurs through nucleation, and requires ions or clusters as nuclei, which can be followed by growth (eg. accumulation mode) through condensation of other compounds dependent on local atmospheric conditions.[11] There are two types of secondary particle formation: homogeneous and heterogeneous.[11] Homogeneous (self nucleation) particle formation is a result of favorable collisions of gasesous compounds.[11] Heterogeneous nucleation, or ion-induced, occurs when a gaseous ion serves as a nuclei for the condensation of gaseous compounds.[11]

1.2 Lungs

Discussion of the human respiratory system, with respect to particulate air pollution, frequently involves separate description of the upper and the lower respiratory tracts. The upper respiratory tract includes the nasal passages, pharynx and the larynx. The lower respiratory tract is composed of the trachea, the bronchi and lungs. The primary function of the upper respiratory tract is to filter, humidify, and adjust the

temperature of inspired air. The primary function of the lower respiratory tract is to transfer gaseous species (eg. O_2, CO_2, and H_2O) into and out of the blood stream.

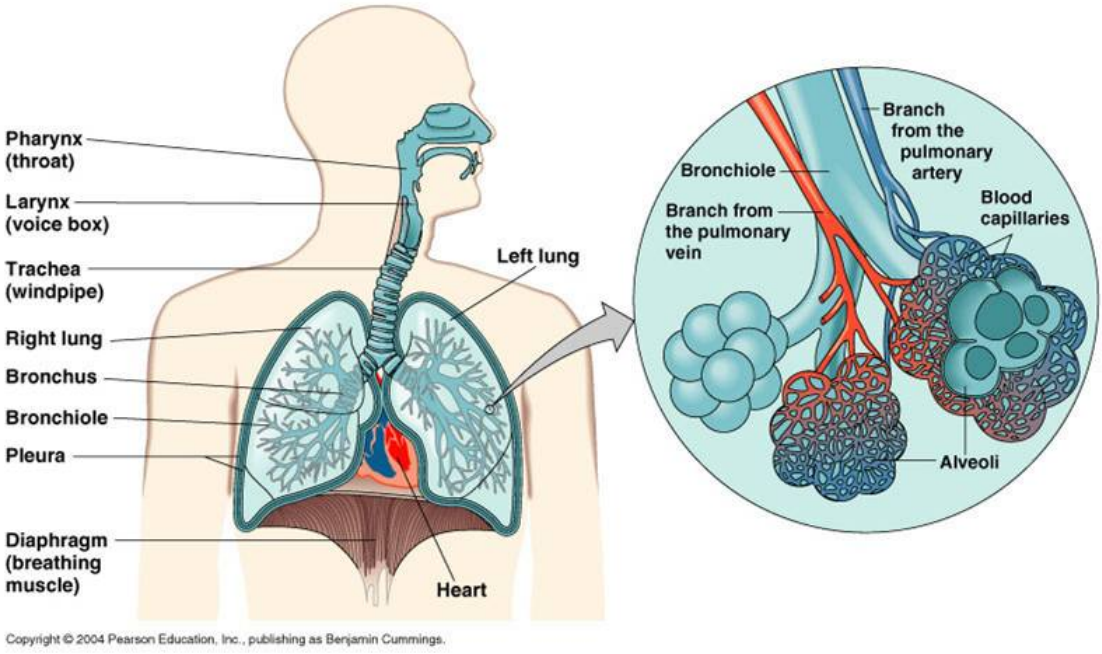

Figure 1.1 Depiction of respiratory tract physiology. (Figure used unmodified)

The upper respiratory system is well evolved to remove particles using cilia. It is believed that coarse particles tend to deposit in the upper respiratory tract. In moving further into the respiratory tract, entering the lower respiratory tract, the trachea divides into left and right primary bronchi, which themselves further divide into smaller airways, bronchioles. The bronchioles then further divide into a series of transitional airways involved in gaseous exchange. At each branching point, in addition to the alveolar region, there is a possibility for particles suspended in the inhaled air to deposit and interact directly with tissue, possibly causing injury. Lung cells that are injured as a result of

their contact with particles display this through a variety of signalling pathways, such as NF-κB and apoptosis. Because several epidemiology studies have correlated $PM_{2.5}$, which is believed to deposit predominantly in the lower respiratory tract, with adverse effects on human health, many *in vitro* dose-response studies have used cells and tissues from the lower respiratory tract.

1.3 Inflammation

The lungs are constantly being challenged by toxic gases, PM_{10}, and infectious agents such as viri, fungi, bacteria, and parasites. The infectious agents, or portions thereof, can also be harboured in or carried on other particulate matter. It has been demonstrated that exposure to PM_{10} results in systemic inflammation. Inflammation, a complex biological process, involves secretion of numerous pro-inflammatory mediators by injured cells. Cytokines are a class of pro-inflammatory mediators that are expressed following the activation of biological signal transduction cascades. Sustained exposure to inflammation, either chronic or acute, can lead to detrimental outcomes such as tissue remodelling from the action of mediators that include matrix metalloproteinases.

Lung cells communicate their injury by the secretion of mediators. Cytokines are but one class of mediators, and cytokines effect responses in other tissues and organs. It has been demonstrated that systemic inflammation, for the case of dosing humans with ambient particles, is known to involve the secretion of cytokines that elicit the release of either granulocytes (non-specific immunity) or lymphocytes (specific immunity) from the bone marrow. Upon arrival to the site of injury, leukocytes are activated, with a notable example of this being the transformation of monocytes into macrophages. In the case of atherosclerosis, the action of these potent agents of the immune system is thought to be a

factor in the pathogenesis of lesions, causing or promoting them to form, grow, and in the extreme to rupture, possibly leading to thrombosis.

1.4 Nuclear Factor (NF-κB) pathway

NF-κB is a transcription factor. The NF-κB pathway, which has been shown to be activated following exposure to PM_{10}, is a major pro-inflammatory gene found in numerous cell types that when activated results in the transcription of mRNA of numerous pro-inflammatory mediators including TNF-α, IL-1β, IL-6, and intercellular adhesion molecule (ICAM)-1.[12-15] As alluded to in the preceding paragraph, NF-κB is a key player in an individual's immune response, and as such it is involved in the translation and secretion of mediators that are involved in cell proliferation. The activation of the NF-κB has been identified in disorders including cancer, autoimmune diseases, viral infection, and abnormal immune development.[16-19]

The activation and regulation of the NF-κB pathway can be monitored directly through measurement of RNA transcription, and also indirectly by following the expression of pro-inflammatory mediators that are not necessarily linearly related to RNA abundance. An understanding as to which environmental stimulants cause the activation of this pathway may give some insight into their toxicity. Thus, the focus of this thesis became the study of the relationships between the chemical composition of a particle and its effect on this major pro-inflammatory pathway, as determined through the measurement of one mediator, intercellular adhesion molecule (ICAM)-1. The dose-response relationship was also monitored using soft ionization mass spectrometry as another readout tool, in an attempt to monitor other mediator differential expression.

1.5 Intercellular Adhesion Molecule (ICAM)-1

ICAM-1 is a cell surface glycoprotein expressed in numerous cell types. It is expressed by lung epithelial cells[20], leukocytes, and endothelial cells (though technically described as vascular cellular adhesion molecule (VCAM-1)). ICAM-1 is expressed in the membranes of resting (eg. not stimulated) cells at low numbers, but upon stimulation by cytokines, such as interleukin-1β and tumour necrosis factor (TNF)-α, its expression is upregulated. As will be shown in later chapters, ICAM-1 expression in A549 cells stimulated through their incubation with tumor necrosis factor (TNF)-α, as a positive control was arbitrarily assigned a normalized ICAM-1 expression value of 1. On that relative scale, resting A549 cells had an ICAM-1 expression level of ~0.3.

The systemic inflammation process includes leukocyte extraction from the blood stream into tissues that have been activated.[21] Neutrophils, a type of leukocytes, are recruited from the bloodstream by first adhering to the endothelium. This process is mediated by membrane bound proteins such as vascular adhesion molecules and selectins.[22,23] Once bound, the leukocytes then migrate into the tissue by moving between endothelial cells. While some leukocytes mature only upon migration into tissue, such as monocytes in the blood that become macrophages in tissues, others, such as neutrophils remain the same. Because ICAM-1 is a key participant of intercellular adhesion in the process of inflammation, the amount of its extracellular expression is believed to be a direct outcome of the regulation of the NF-κB pathway. As such it is an ideal target for immunological studies.

1.6 Immunocytochemistry

Immunocytochemistry is a method that is used to detect the location and/or quantity of a protein on or within a cell by labelling it with an antibody, which itself is labelled with a fluorescent tag. Immunocytochemistry involves a multiple step procedure, as depicted in figure 1.2. This method was used in this thesis to obtain a measure of the expression of ICAM-1.

At the end of any given experiment, the cell culture is fixed, such as through the use of a paraformaldehyde (PFA) solution, which kills the cells and fixes the locations of the proteins within the cell. After fixation, a blocking agent is added to the cell culture. This agent is typically serum. The role of the blocking agent is to minimize non-specific binding between the antibody and molecules other than its antigen. The primary antibody, which is specific to the protein of interest, is added next.

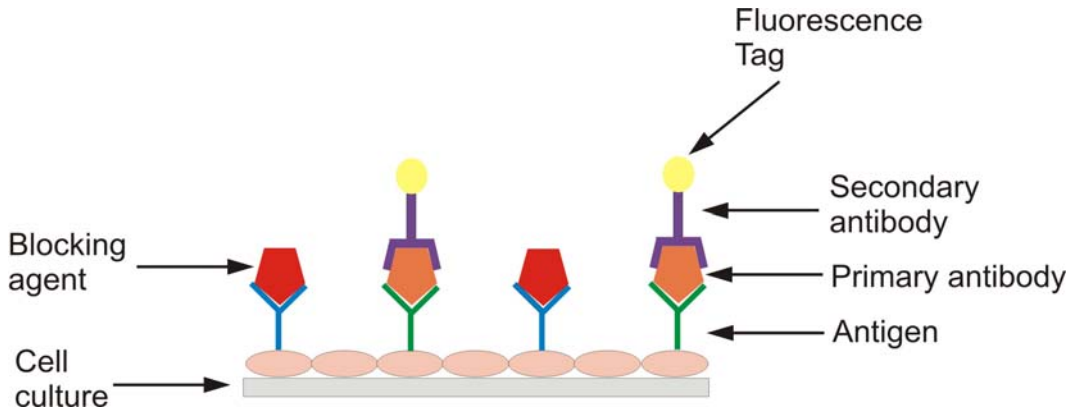

Figure 1.2 Graphical representation in which antibodies bind to the antigen protein of interest in an immunocytochemistry assay. The blocking agent ensures that only specific binding occurs. The primary antibody binds the antigen. Secondary antibodies then bind the primary antibody. The secondary antibodies are labelled with a fluorescent tag.

After incubation, the secondary antibody, which is specific for the primary antibody, is added. In order to ensure that no cross-reactivity will take place, the secondary antibody, which typically is an immunoglobulin G (IgG) protein, is raised in a different animal than that the primary antibody. The primary antibody used in the studies reported in this thesis was produced in mice (mouse anti-human ab), while the secondary antibody was produced in goat (goat anti-mouse ab), and it was labelled by covalently attaching a fluorophore.

In some instances, when signal amplification is desired, a labelled tertiary antibody may be used in addition. Each time a labelled-antibody is added in the labelling process, the likelihood of observing the protein of interest can be increased. This is simply a product of the structure of antibodies formed during the labelling process. Two antibodies bind to the previously bound antibody, which itself is bound to the protein of interest. In this way, the ability to detect a single protein molecule is increased as each target molecule of interest becomes bound to numerous labelled molecules (2^n, where n= number of sequential additions of labelled-antibody). Thus, the fluorescence signal that is proportional to the number of antigens expressed in the sample, can be amplified, making immunocytochemistry a sensitive, quantitative technique for determinations of membrane bound protein expression.

1.7 Mass Spectrometry based proteomics

Proteomics is the study of the proteome to identify, characterize, and quantify the complete set of proteins expressed by the entire genome in tissue or organisms including post-secondary modifications and protein-protein interactions.[24] Proteomics could be considered a subset of systems biology research, because knowledge of biological

expression, post-translational modifications, and sub-cellular localization provide valuable information needed to describe biological processes.[25]

Mass spectrometery is a sensitive tool that is used to measure the mass to charge ratio (m/z) of gas-phase ions. Because of soft ionization techniques, mass spectrometry has played an increasingly significant role in biological sciences. Today, mass spectrometry (MS) is considered a sensitive method for biomolecule characterization, and its already prominant role in proteomics, continues to grow.[26] MALDI (Matrix Assisted Laser Desorption Ionization) is a soft ionization technique that has become common place in biological studies due to its ability to transfer large, polar, thermally labile biomolecules into the gas phase for mass analysis without prior derivatization.

1.8 Research objectives

As described previously, ambient PM has many different sources, and therefore a sample of ambient PM is recognized as being a complex mixture of particles with different sizes and compositions. The extent and the nature of the injury caused by a dose of a specific composition of particle is not well characterized, but *in vivo* and *in vitro* dose response studies suggest that when particles are inhaled, those particles are deposited onto lung tissue and they induce cells to secrete pro-inflammatory mediators (cytokines). The hypothesis that this research was based upon was that different chemical compositions of a particle result in different down stream biological responses. The goal for this thesis was to develop a method that can simultaneously monitor downstream biological responses of lung cells by immunocytochemistry, and ideally by soft ionization mass spectrometry in a parallel and/or complementary manner, following incubation with different particles types having different sizes, ranging from coarse to fine. An objective

was to contribute new knowledge to the understanding as to how A549 lung cells respond dependent on the particle dose (particle number, size, and chemical composition).

CHAPTER 2
APPARATUS

2.1 The quadrupole ion trap

The quadrupole ion trap (QIT) was invented by physicist Wolfgang Paul, who was later awarded (1979) a Nobel prize.[27] A QIT is a device that can capture and store gaseous ions for a period of time. The QIT can also function as a mass spectrometer of considerable mass range and variable mass resolution.[27]

The QIT consists of at least three electrodes which are depicted in cross section in Figure 2.1. The two electrodes on each end have hyperbolic geometry on their inner surface. These electrodes are called end-cap electrodes. The third electrode positioned symmetrically between two end-cap electrodes also has a hyperbolic geometry on its inside surface, and it is referred to as the ring electrode.

Ions can be injected into the trap through an orifice in one of the end-caps, or the ring electrode, or along the asymptote between an end-cap and the ring electrode. Ions can also be created within the trap. Ions are stored by the electric field within the device that is created by applying a sinusoidal waveform, at a frequency of typically 1 Megahertz (MHz), to the ring electrode and, most commonly holding the endcap electrodes at 0 V. Depending on that electric field, ions having a mass to charge (m/z) within a certain range will have stable trajectories. Ions outside that m/z range will not be stable and will collide with the QIT electrodes and be neutralized.

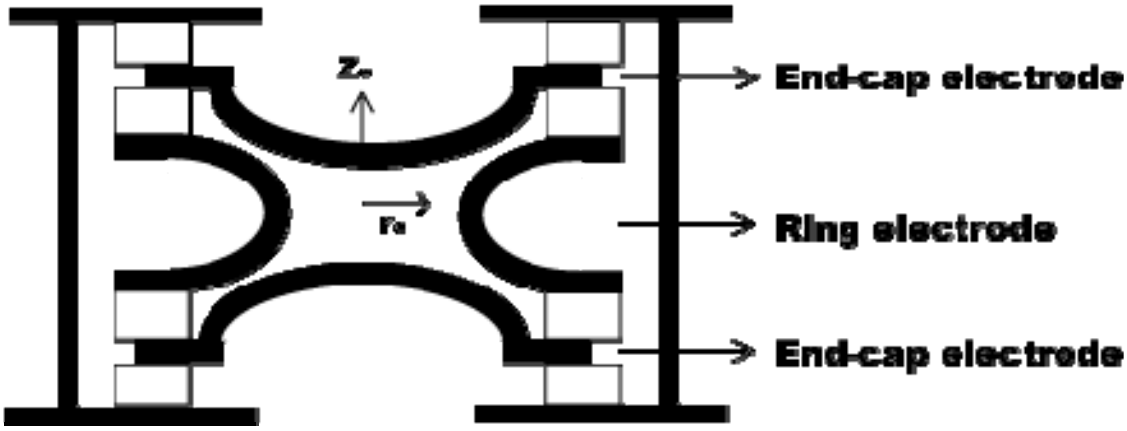

Figure 2.1 Schematic diagram of three electrodes of the quadrupole ion trap.

The ion trap when used as a quadrupole mass analyzer is described as a dynamic trap because ion trajectories in these instruments are influenced by a time-dependent force. An ion having appropriate m/z and kinetic energy to be trapped will experience a restoring force that increases in magnitude as the ion deviates further from the 3-dimensional mid-point of the device, driving the ion back towards the mid-point. The stability of ions in the quadrupole field can be described by a simple mathematical relationship from the solution to a second order linear differential equation relating the restoring force on a given ion by a given electric field, which was originally derived by Mathieu. Interestingly, the origin of this equation was from Mathieu's solution for the motion of stretched skins over a cylinder to form a drum. Mathieu was able to describe solutions in terms of regions of nodes and anti-nodes which have direct analogies to ion stability/instability. This is equation is now commonly referred as the Mathieu equation by investigators who use a QIT (equation 2.1) where $\phi_{r,z}$ is the potential at a given position r and z, in which r is the radial direction, z is the axial direction, and r_0 is half distance between the ring electrode, and ϕ_0 is the applied electric potential. When the

Mathieu equation is applied directly to the motion of trapped ions in a QIT, it describes regions of ion motion stability (eg. nodes) and instability (eg. anti-nodes).

Equation 2.1

$$\phi_{r,z} = \frac{\phi_0(r^2 - 2z^2)}{2r_0^2} + \frac{\phi_0}{2}$$

From the Mathieu equation, the stability of an ion within a QIT to be described as a function of two dimensionless parameters, a and q (equation 2.2 and 2.3). U is the DC voltage applied to the end-cap electrodes, V_{AC} is the amplitude of the time-dependent waveform applied to the ring electrode, ω is the angular frequency of the waveform applied to the ring electrode, which equal to $2\pi f$, with f being the frequency of the sinusoidal waveform, m_i is the mass of the ion, r_0 is half the diameter of the ring electrode, e is the electronic charge, and z is the number of net elementary charges on the ion.

Equation 2.2

$$a_z = -2a_r = -[(16ezU)/(m_i r_o^2 \omega^2)]$$

Equation 2.3

$$q_z = -2q_r = -[(8ezV_{ac})/(m_i r_o^2 \omega^2)]$$

The stability region of an ion can also be viewed graphically, in the axial direction through plotting a_z by q_z, and in the radial direction by plotting a_r by q_r (figure 2.2). By overlaying these two plots, areas of overlap are regions in which the ion is stable in both the radial and axial directions. Stability parameters β_r and β_z, which are both functions of a and q, are used to determine if an ion is stable within the QIT (equation 2.4 and 2.5).

Equation 2.4

$$\beta_r \cong \sqrt{a_r + \frac{q_r^2}{2}}$$

Equation 2.5

$$\beta_z \cong \sqrt{a_z + \frac{q_z^2}{2}}$$

Within these stability regions (figure 2.2c), ions must be stable in both the radial (r) and axial (z) directions to remain stored in a QIT. In Figure 2.2, the $\beta_z = 1$ stability boundary intersects with the q_z axis at $q_z = 0.908$ (for a_z and a_r). This working point is termed the low-mass cutoff, and it is of significance when the QIT is used as a mass spectrometer as it is the operating condition at which an ion can be moved from stability to instability, most commonly achieved by incrementally increasing the amplitude of the waveform applied to the ring electrode. In so doing, ions can be sequentially 'scanned out' of the QIT from lowest to highest m/z ratio. Detection of the ions scanned out of the QIT using an ion detector allows construction of a mass spectrum, that is, a plot of ion abundance versus m/z.

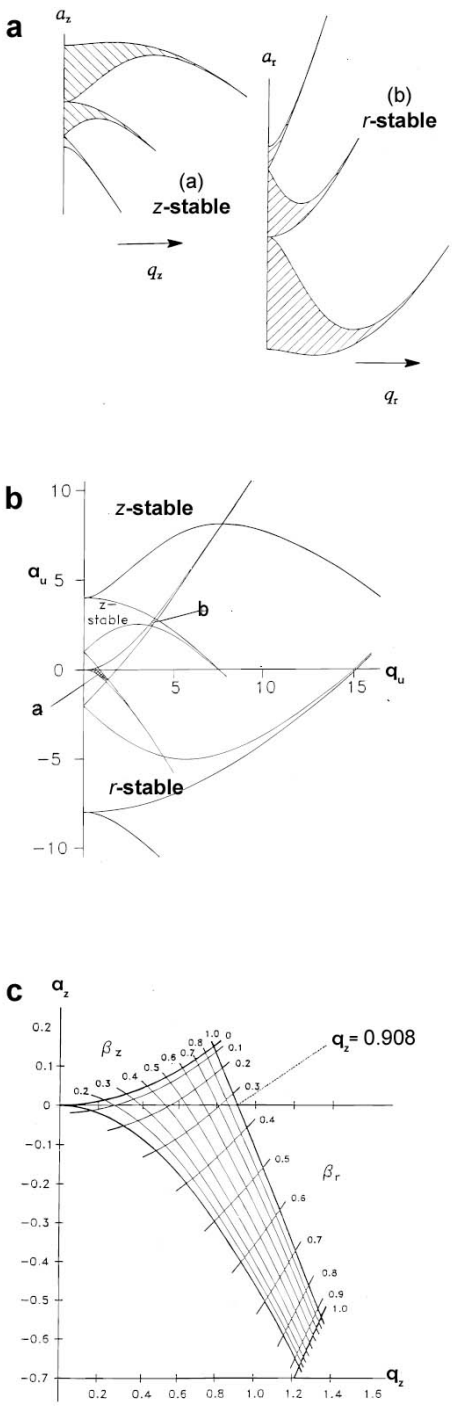

Figure 2.2 Graphical representation of the stability regions of a quadrupole ion trap determined by Mathieu equation. a) Diagrams for the z-direction of a_z and q_z space. b) Mathieu stability diagram in a_u and q_u space for both the r- and z- directions (eg. a_z and a_r, and q_z and q_r). Simultaneous overlap regions of a_z and q_z space are labelled a and b. c) Stability diagram for the first overlap region, identified in panel b) by the 'a'.

2.2 Electrodynamic Levitation Trap (EDLT)

Several applications of the electrodynamic levitation Trap (EDLT) have been developed in Agnes group.[28,29] An EDLT has been used to prepare MALDI-TOF-MS samples in a methodology termed wall-less sample preparation (WaSP)[29-32], to study ion induced nucleation[33,34], and to investigate the effect of ambient particle mimics on lung cells.[35,36] The configuration and operation of an EDLT has analogies to the QIT. However, because an EDLT is operated at atmospheric pressure, there is collisional damping of ion motion. An outcome of is that the shape and spacing of the electrodes can deviate significantly from hyperbolic geometry while still retaining the ability to levitate a droplet, and therefore the electric field also deviates from quadrupolar. For instance, in the EDLT used in this work, the end-cap electrodes were simply two flat conductive plates, and the ring electrode was in fact approximated as two wire rings of equal size mounted parallel. A diagram of an EDLT apparatus used in this work is presented in figure 2.3.

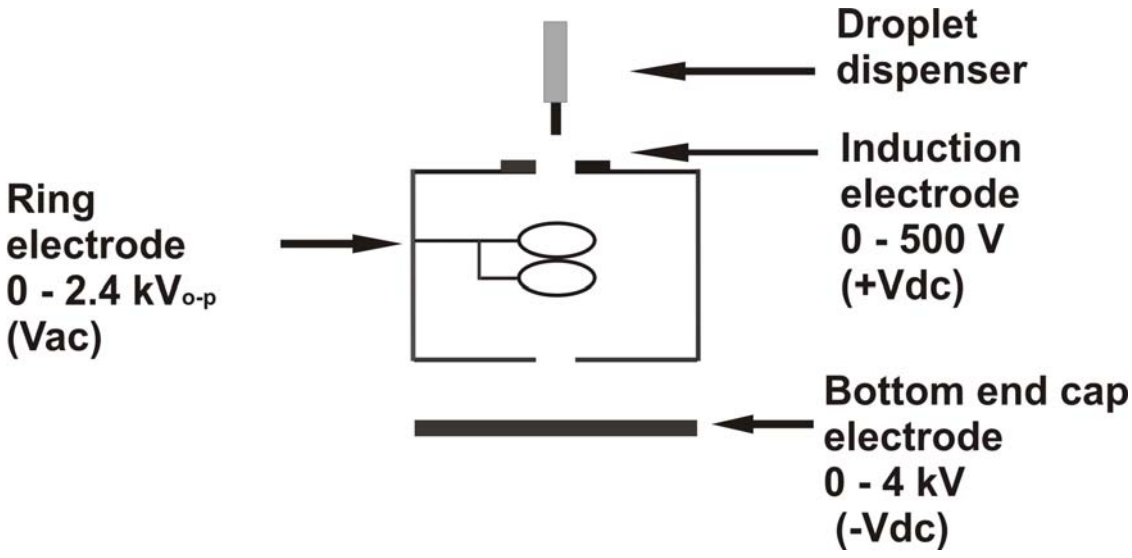

Figure 2.3 Diagram of an electrodynamic levitation trap (EDLT) used in the research described in this thesis.

2.2.1 Dispensing droplet with net charge

A droplet-on-demand droplet dispenser (MJ-AB-01-60, MicroFab Technologies Inc., Plano, TX, USA) was used to dispense a starting solution. An aliquot of a starting solution (~10 μL) is loaded into the reservoir of a droplet-on-demand dispenser using a hand held pipette. For starting solutions used in this work, there were volatile and non-volatile compounds and dispersed solids added to starting solution. The nozzle of the droplet dispenser was positioned ~1 mm above the induction electrode and centred over a 5 mm diameter hole cut into it. This induction electrode is situated directly above the ring electrodes.

A single droplet is created by applying a pulse waveform to the piezoceramic droplet dispenser. The shape of an example pulse waveform applied to the piezoceramic in shown in figure 2.4. The pressure wave thus created with the reservoir of the dispenser causes a jet of liquid to be ejected from the droplet dispenser nozzle. The induction electrode is biased with a DC potential within the range from 0 to ± 500 V. The electric field between induction electrode and the nozzle of the dispenser induces a net charge, by affecting the motion of charged species in the jet of solution, such that when the jet separates from the nozzle and collapses into a single droplet, that droplet carries a net charge. The repetition of this process is used to dispense a population of droplets, some of which are captured and levitated in the EDLT. Note that dust, lint, precipitation and coagulation of the solutes and dispersed particles from the starting solution, respectively, and imperfect activation of the piezoceramic, for example, can cause unwanted, multiple droplet production per pulse waveform.

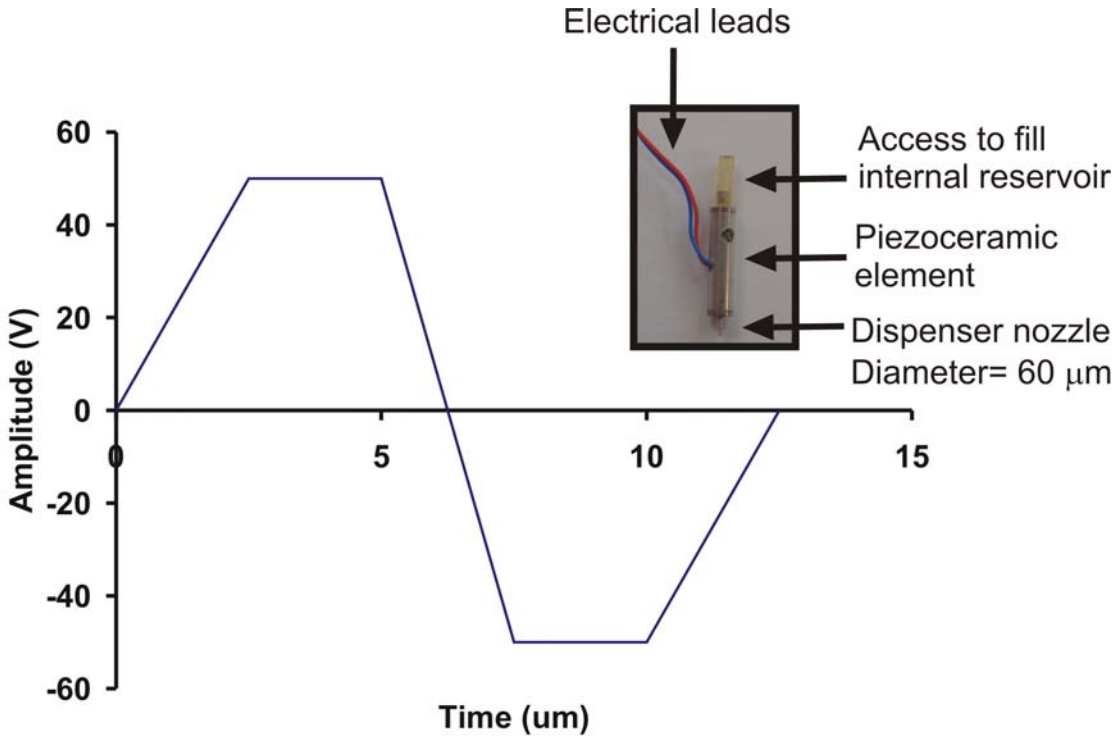

Figure 2.4 Shape of an example waveform applied to the piezoceramic within the MicroFab droplet dispenser employed to dispense a single droplet.

2.2.2 Levitation of droplet with net charge

While droplets are being dispensed, an AC waveform was applied to the two ring electrodes, typically a sine wave, 50 Hz and 2.4 $kV_{0\text{-}P}$. As soon as droplet dispensing ceased, the frequency of this waveform was manually ramped to 1,050 Hz over a period of 2 s. The reason for changing the AC frequency was that, as the volatile compounds evaporate from each droplet, the mass of the droplet decreases while the net charge did not change (unless there was a Coulomb explosion). When evaporation ceased (or reached steady-state), the remnant of the droplet was then a residue enriched with the low volatility compounds present in the starting solution. The resultant residue was either a liquid, solid, or a mixture of compounds in solid and liquid states. The mass of each

compound in a resultant residue was estimated based on the average initial volume of the dispensed droplets and the known concentration of each compound in the starting solution.

2.2.3 Particle delivery

Droplets levitated in the EDLT are removed from it by applying an attractive potential, in the range from 500 V to 4000 V, to the bottom end-cap electrode while reducing the trapping potential well depth, achieved by changing the trapping field through, for example, lowering the amplitude of the AC field. The residues can be deposited directly onto a substrate placed on the bottom end-cap electrode. Through out this work, the target was a culture of human lung cells (cell line A549, American Type Tissue Collection) grown on various supports such as, coverslips, tissue culture dishes, and center-well organ culture dishes.

2.3 Matrix Assisted Laser Desorption Ionization Time Of Mass Spectrometry (MALDI-TOF-MS)

MALDI was developed from the laser desorption ionization (LDI) technique. Since the late 1960's, LDI has been used as one of the many possible ion sources for mass spectrometry.[37] This technique is not suitable for analysis of molecules that have low volatility, such as peptides, proteins, or nucleic acids because the LDI technique causes fragmentation of such compounds, leading to spectra that are difficult to interpret. In 1988, Japanese scientist Tanaka *et al*., and German researchers Karas and Hillenkamp independently develop a new method in which a compound termed the matrix was used to absorb energy from a laser pulse and assist the delivery of low volatility, high molecular weight compounds into the gas phase without excess fragmentation.[38] This method was named matrix-assisted laser desorption ionization (MALDI).

MALDI uses a pulsed laser for ion formation of matrix and analyte.[39] The most common laser used is a N_2, with an output wavelength = 337 nm in the ultraviolet (UV), but there have been reports of the use of other lasers having ultraviolet outputs, such as the Nd:YAG, and the utility of infrared (IR) lasers has reported in research studies.[104]

Compounds used as matrices are typically organic acids with high absorptivity coefficients at the output frequency of the laser.[40-42] The mole ratio of analyte to matrix for solid matrices is optimized empirically, and the ratio is usually in the range of $1:10^2$ to $1:10^6$.[43] Matrices have three major contributions in MALDI. The matrix molecules isolate analyte molecules from each other in order to minimize their aggregation in a co-crystallized analyte matrix solid. The matrix molecules absorb energy from the laser, causing ablation of the co-crystallized solid matrix and analyte solid (figure 2.5).[44] The matrix molecules then participate further in the process of ionization the analyte in the gas phase, via proton transfer from an electronically excited matix molecule to an analyte molecule.

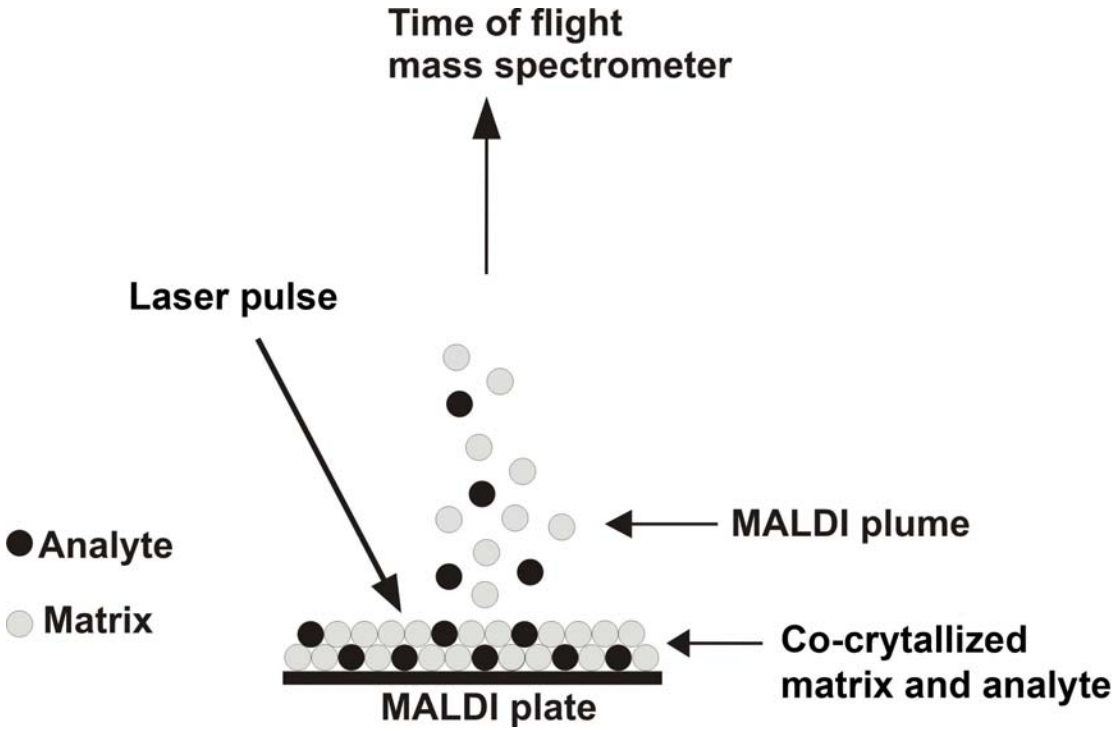

Figure 2.5 Illustration of sample ablation that forms a plume of material from the co-crystallized matrix and analyte solid, following pulsed laser irradiation.

All mass spectrometers have three main parts: the ion source, the mass analyzer and the detector. The function of the ion source is to generate ions from compounds in a sample, the mass analyzer then separates these ions based on their mass-to-charge ratio (m/z) and the relative abundance of the ions is measured by the ion detector.

2.3.1 Ionization

Ionization is the first required step in mass spectrometry. There are numerous mechanisms that have been developed to ionize a molecule in the gas phase such as chemical and electron impact ionization. Electron impact ionization is classified as hard ionization, because excess energy from the electron molecule collision is transferred into internal energy of the analyte in the process of ionizing it ($e + A \rightarrow A^{\bullet *} + 2e$), leading to

unavoidable fragmentation following the ionization. MALDI is a soft ionization technique in which the energy is transferred indirectly to the analyte through a collision with an organic compound (eg. the matrix), as described in simple terms in the following sections. MALDI ionization is believed to have two predominant pathways that are referred to as primary and secondary ionization.

2.3.1.1 Primary ionization

The primary ionization occurs during the laser pulse.[45] A matrix molecule (M) absorbs a photon, and is protonated to an excited state (M*). The excited matrix molecule can then transfer a labile proton in a collision to an analyte (A) before the excited molecule relaxes.

Equation 2.6 $\mathbf{M + h\upsilon \rightarrow M^*}$

Equation 2.7 $\mathbf{M^* + A \rightarrow (M\text{-}H)^- + AH^+}$

Equation 2.8 $\mathbf{M^* + M \rightarrow (M\text{-}H)^- + MH^+}$

2.3.1.2 Secondary ionization

Secondary ionizations are considered to be gas-phase reactions. These take place in the MALDI plume where explosive solid-to-gas transition occurs.[46,47] An example ionization process is comprised of two steps: gas-phase proton transfer and gas phase cationization.

In gas-phase proton transfer, matrix-matrix reactions occur, where matrix molecules are protonated.[37,39]

Equation 2.9 $\mathbf{M^{+\bullet} + M \rightarrow MH^+ + (M\text{-}H)^\bullet}$

Once the matrix molecules are protonated, MH^+, gas phase cationization occurs where matrix molecules protonate the analyte molecules.

Equation 2.10 $\mathbf{MH^+ + A \rightarrow M + AH^+}$

2.3.2 Time of flight (TOF) mass analyzer

Time of flight mass analyzer measures the time for an ion of a given kinetic energy to travel across a field-free drift region of known length, from which information the ion's mass and net charge can be deduced. An ion has an net charge equal to the number (z) of elementary electronic charges (e) and a mass of *m*. Upon ionization, the ion is imparted with energy (E) by the applied voltage (U):

Equation 2.11 $\mathbf{E = ezU}$

Equation 2.11 represents the potential energy that accelerates the ions prior to entering a field-free drift region. At the entrance to the drift region, the ions have a kinetic energy equal to its potential energy (equation 2.12).

Equation 2.12 $\mathbf{KE = ezU = \frac{1}{2}mv^2}$

The time of flight of an ion in the field free drift region is measured, and then using the length of this region, its velocity can be calculated. Using equation 2.12, the ion's mass to charge ratio (m/z) can be determined.[40] Presented in figure 2.6 is a diagram of analyte molecules being accelerated, drifting through the field-free region, and detected by the detector. The lighter ion will reach the detector first, before the heavier

ion (assuming z= +1 for all ions). A detector at the end of the field free region produces a signal as each ion strikes it.

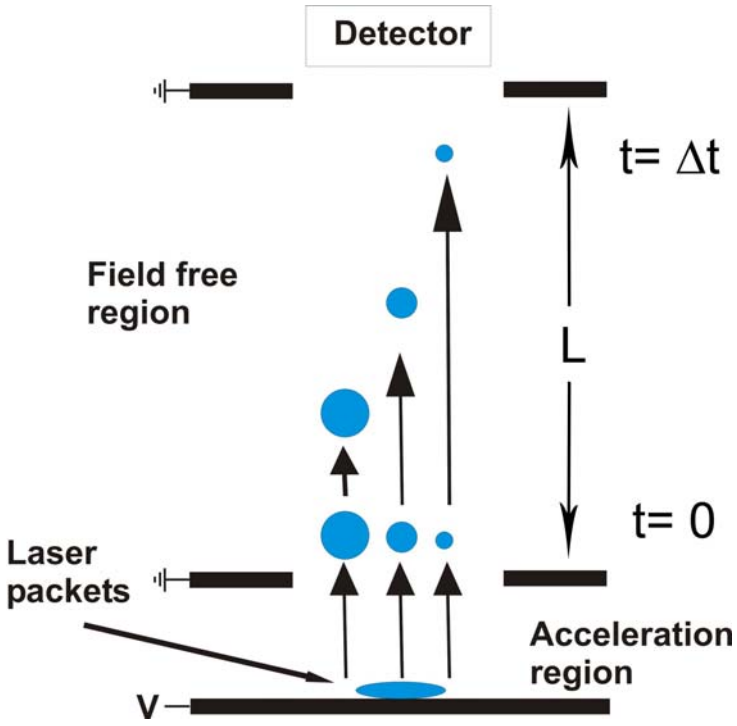

Figure 2.6 Diagram of a time of flight mass spectrometer used for MALDI. Depicted are ions having the same kinetic energy upon exiting the acceleration region, and thus having different velocities through the field-free region according to their mass and net charge. Arrows represent vectors that depict the velocity of each ion where lighter ions have higher velocity and travel through the field free region faster as compared to heavier ions that have lower velocity and reach the detector later.

2.4 Fluorescence microscopy

Fluorescence microscopy is simply a tool to view fluorescent species. The microscope used was fitted with a mercury lamp. Two filters were needed; the function of the first filter is to select a bandpass of light that is then directed to the sample (excitation frequencies), and the function of the second filter is to allow another bandpass

of light to reach the detector (fluorescence emission frequencies). The detector was a digital camera, allowing the ready archival and subsequent processing of the images. The principle components of a fluorescence microscope are shown in figure 2.7.

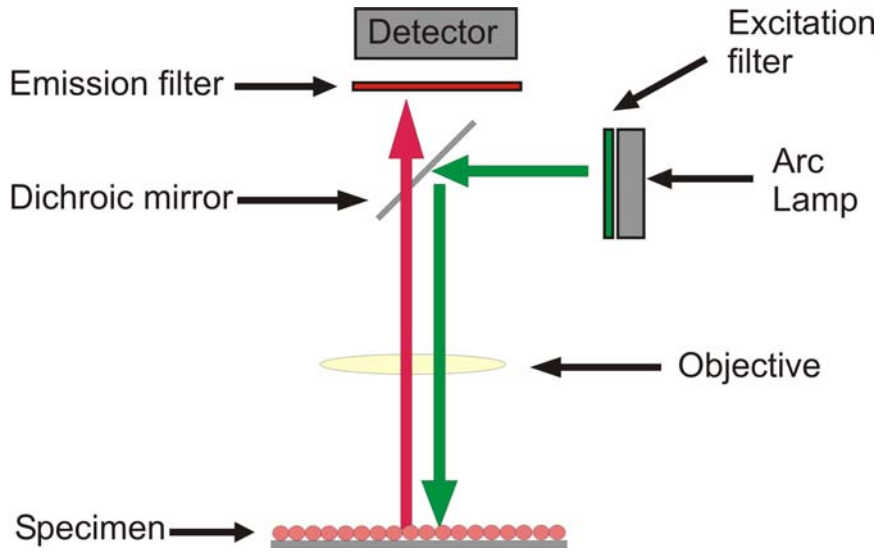

Figure 2.7 Physical setup of a fluorescence microscope.

CHAPTER 3
MALDI-TOF-MS MONITORING OF DIFFERENTIAL EXPRESSION OF BIOMOLECULES SECREATED FROM A549 CELLS IN RESPONSE TO INCUBATION WITH AMBIENT PARTICULATE MATTER (PM_{10}) MIMICS

3.1 Introduction

Technical innovations in proteomic based mass spectrometry (MS) techniques have resulted in a development of range of sensitive and versatile methods for high throughtput proteome-scale profiling.[39] The proteome is defined as all proteins in a given cell, tissue, or organism at any one instant. A proteome differs among cell types, organism and within the same cell depending on cell activity, stimuli, or disease. An objective of a proteomic study is to learn information about a proteome through the identification, characterization, and quantification of, ideally, the whole content of proteins present in challenged biological materials (tissues, cells in culture, organelles, or fluids) relative to controls. An objective of some proteomic studies is identification and characterization of compounds that could be biomarkers for a specific disease. A biomarker is a molecule whose presence, which can be detected, in a particular cell type depending on cell activity, stimuli, or disease that is indicative of a state of the cell/organ/organism.

The world health organization (WHO) predicts that in 2020, cardiovascular disease, already a predominant cause for premature death in developed nations, will likewise become a health burden of disease in developing and newly industrialized countries.[26] This prediction is the impetus to perform hypothesis driven research to identify factors in the pathogenesis of this disease, with the objective of identifying and validating biomarkers that could facilitate accurate diagnosis and lead to timely and appropriate treatment intervention strategies for individuals.

Inflammation is a process activated in response to injury, leading to the healing of affected tissues, in normal situations. However, when subjected to unusual injury, acute and chronic inflammation can lead to the development of disease. Two examples of diseases that are, possibly caused by, but certainly exacerbated by inflammation are cardiovascular disease and chronic obstructive pulmonary disease (COPD). Part of an inflammatory response includes the secretion of pro-inflammatory mediators such as cytokines, which are proteins that have mediate pro–inflammatory signal transduction. Many *in vivo* and *in vitro* particulate air pollution studies have correlated ambient particle exposure to elevated levels of pro-inflammatory mediators, such as tumor necrosis factor (TNF)-α, granulocyte macrophage colony stimulating factor (GM-CSF), interleukin (IL)-1β, IL-6, IL-8, leukaemia inhibitory factor (LIF), and oncostatin M (OSM).[48-53] An improved understanding of particulate air pollution may be learned with demonstration of an ability to monitor changes in a proteome.

Previously, graduate students in our laboratory, Michael Eleghasim and Allen Haddrell, demonstrated the ability to measure the downstream differential expression of a membrane bound pro-inflammatory mediator, intercellular adhesion molecule (ICAM)-1

as a function of dosing a cell culture with a known number of particles having known size and composition that had been formed in an electrodynamic levitation trap (EDLT).[35,36,54] ICAM-1 is a product of the activation of the pro-inflammatory pathway nuclear factor (NF)-κB, and as a result the measurement of the ICAM-1 protein expression has yielded valuable data in the study of particulate matter (PM) toxicity.[35,36,54] However, there are numerous other pro-inflammatory pathways each involving intercellular signalling molecules that may or may not be different.

Several techniques had been developed to identify and quantify secreted proteins prior to the emergence of MS based proteomic methods. The majority of these techniques are antibody based, such as ELISA and immunocytochemistry. These techniques are sensitive and selective because of the specificity of the antibody to the ligand.[49,55]

Proteomic studies for biomarker identification using matrix assisted laser desorption ionization (MALDI-MS) continues to attract interest.[25] MALDI is one of several prominent soft ionization techniques.[38] MALDI is a technique used to ionize compounds having low volatility, including proteins and peptides, and it offers detection limits as low as attmomoles.[45] This soft ionization technique is not selective; therefore, a technique such as MALDI-MS can be used to detect many of the biomolecules present in the sample.

In this study, the differential expression of secreted biomolecules from human lung cell cultures (A549 cells) dosed with a known number of ambient particulate mimics of known size and composition was monitored using MALDI-TOF-MS. In addition, two biomolecules that are members of the cytokine family present in the supernatants were measured by ELISA.

3.2 Experimental

3.2.1 Chemicals

Minimum essential medium (MEM), trifluoroacetic acid (TFA), acetonitrile (ACN), trypan blue solution (0.4 %), dodecan-1-al (nC_{11}-CHO), dodecan-1-oic acid (nC_{11}-COOH), dodecan-1-ol (nC_{12}-OH), minimum essential medium (MEM), fetal bovine serum (FBS), Trifluoroacetic acid (TFA), sinapic acid (SA) were purchased from Sigma-Aldrich Inc. India ink (Speedball, product #3338, Statesville, NC, USA) was used as the source for elemental carbon (C_s). Phosphate buffered saline (PBS) was purchased from Oxoid Ltd., Basingstoke, Hampshire, England.

3.2.2 Starting solutions

Stock solutions of india ink, dodecan-al (nC_{11}-CHO), and dodecan-ol (nC_{12}-OH) were prepared in distilled deionized water. A stock solution of 1.5 mM of dodecanoic acid (nC_{11}-COOH) was prepared in minimum volume of ethanol and diluted with distilled deionized water. Nine starting solutions were prepared by combining aliquots from single component stock solutions to yield the solute concentrations listed in table 3.1.

Table 3.1 Initial India Ink and organic compound concentrations in the starting solution.

starting solution	Particle type	India ink (mg/mL)	nC_{11}-CHO (M)	nC_{12}-OH (mM)	nC_{11}-COOH (mM)
a	C_s	2.5			
b	$[C_s + nC_{11}\text{-CHO}]_p$	2.5	0.1		
c	$[nC_{11}\text{-CHO}]_p$		0.1		
d	$[C_s + nC_{11}\text{-CHO}]_p$	2.5	1.5×10^{-3}		
e	$[nC_{11}\text{-CHO}]_p$		1.5×10^{-3}		
f	$[C_s + nC_{12}\text{-OH}]_p$	2.5		1.5	
g	$[nC_{12}\text{-OH}]_p$			1.5	
h	$[C_s + nC_{11}\text{-COOH}]_p$	2.5			1.5
i	$[nC_{11}\text{-COOH}]_p$				1.5

From these nine starting solutions, particles comprised of the compounds listed in table 3.2 were created using the apparatus described in section 2.2.

Table 3.2 Composition of each particle generated per droplet (eg. aliquot) from the respective starting solution

Starting solution	Particle type	C_s (pg)	nC_{11}-CHO (pg)	nC_{12}-OH (pg)	nC_{11}-COOH (pg)
a	C_s	127			
b	$[C_s + nC_{11}\text{-CHO}]_p$	127	6×10^3		
c	$[nC_{11}\text{-CHO}]_p$		6×10^3		
d	$[C_s + nC_{11}\text{-CHO}]_p$	127	94		
e	$[nC_{11}\text{-CHO}]_p$		94		
f	$[C_s + nC_{12}\text{-OH}]_p$	127		94	
g	$[nC_{12}\text{-OH}]_p$			94	
h	$[C_s + nC_{11}\text{-COOH}]_p$	127			94
i	$[nC_{11}\text{-COOH}]_p$				94

3.2.3 Cell culture

The alveolar type II epithelial cell line A549 (American Type Culture Collection (Manassas, VA, USA) was grown to >95% confluence on 18-mm glass cover slips placed in each of the wells of a 6-well plate (Corning). The cell cultures were grown in minimum essential medium (MEM) supplemented with 10 % heat-inactivated fetal bovine serum (FBS) under 5 % CO_2 at 37 $^{\circ}$C.

3.2.4 Negative control

The majority of the growth medium bathing the cell culture was drained of (~16 μL of growth medium remained on the culture).[35,36] The cover slip on which the culture had been grown was transferred to a sterile (35 mm x 10 mm) tissue culture dish that was placed in an incubation oven whose internal conditions were maintained at 100 % humidity, 37 $^{\circ}$C and 5 % CO_2. No growth medium was added to the culture during the incubation period.

3.2.5 Droplet dispensing and levitation for particle formation

Droplets were dispensed and levitated using the methodology described in section 2.2.1 and 2.2.2.

3.2.6 Particle delivery onto lung cells *in vitro*

With a population of particles levitated in the AC trap, all but ~16 μL of the growth medium bathing a cell culture was drained off. The coverslip supporting the culture was then positioned on the top of the bottom electrode of the AC trap. The levitated particle population was extracted from the AC trap by applying a 1000 V potential to the bottom electrode. Immediately following particle deposition, the culture was transferred to a sterile (35 mm x 10 mm) tissue culture dish and incubated at 100 % humidity, 37 $^{\circ}$C and 5 % CO_2 with no medium added. The total time elapsed between the draining of the growth medium and placing the culture onto which the particles had been deposited back into the incubation oven was <60 s. No growth medium was added to the culture during the incubation period.

3.2.7 Supernatant collection and MALDI-TOF-MS sample preparation

Following a 22 hrs incubation period for the culture, 200 μL of serum free growth medium was added onto the center well, and the culture incubated for an additional 2 h (in order for the fresh serum free medium to equilibrate with the supernatant) bringing the total incubation period to 24 h. Following the 24 hrs incubation period, 50 μL of supernatant was collected and a fresh 50 μL aliquot of serum free medium (SFM) was added into the center well in order to maintain the volume of the medium bathing the cell culture constant.

The biomoleucles in the supernatant were prepared for MALDI-MS as follows. A 10 μL aliquot of the supernatant was diluted and conditioned by adding 2.0 μL of 2.5 % trifluoroacetic acid (TFA) in order to acidify the aliquot, and then 50 μL of 0.1 % TFA was added to dilute the aliquot of supernatant.

3.2.8 MALDI-TOF-MS preparation and analysis of the supernatant

A matrix solution was prepared by dissolving 5.0 mg of Sinapic Acid (SA) in 100 μL of acetonitrile (ACN) and 100 μL of 0.1 % TFA. A 4 μL aliquot of matrix solution was spotted onto a well of the MALDI plate and air dried.

A C_{18} ZipTip (Millipore) was conditioned by wetting the ZipTip C_{18} bed with two washings of 10 μL reagent grade acetonitrile (ACN) followed by two washings of 10 μL of 0.1 % TFA. ~10 μL of the conditioned supernatant solution was aspirated into a C_{18} ZipTip (Millipore) and dispensed back into the vial holding the supernatant. This was repeated 10 times. The ZipTip was then washed with two 10 μL aliquots of 0.1 % TFA. Biomolecules retained in the ZipTip were then eluted and spotted onto the same well of the MALDI-plate to which the matrix had been delivered and air dried using a 4.0 μL of solution containing an equal volume of ACN and 0.1 % TFA.

The supernatant was also collected using the method described following the 48 h and 72 h incubation time points.

Mass spectrometric analysis was performed using MALDI-TOF-MS (Waters Corporation, Milford, MA, USA) equipped with a nitrogen UV laser (337 nm, pulse width 2 ns) and 1.2 m flight path in the linear mode, and controlled by MassLynx software (version 3.5, Waters Technologies Inc). The standard operation conditions for biomolecule detection includes an accelerating voltage of 15 kV and the ion extraction

pulse voltage of 2450 V. All data were acquired using a positive ion linear mode. The mass spectra were acquired in the mass range from 3 to 25 kDa.

3.2.9 Supernatant Analysis by Enzyme-Linked Immunosorbent Assay

Following particle deposition and a 30 minute incubation period, the cell culture supernatant was collected as described in the manufacturer's protocol. The concentration of each cytokine in the supernatant was measured by enzyme-linked immunosorbent assay (ELISA).

3.2.10 Measurement of time required for the particles to adhere onto the cell culture

A population of elemental carbon particles (C_s) were delivered onto a cell culture. Immediately after the delivery of the particles, the position where the particles landed was viewed using a calibrated optical microscope (Motic, AE31). Particle adherence versus movement was observed by monitoring the position of the particle following the particle deposition at selected time points during the incubation period.

3.2.11 Viability assay

The viability of the cells was analyzed by trypan blue assay throughout this work.

3.3 Results

3.3.1 Characterization of particle diameter

Droplets of initial volume 326 ± 194 pL were dispensed. Droplets were levitated and deposited onto a clean glass slide. Representative images of $[C_s]_p$, $[nC_{11}\text{-CHO}]_p$ and $[nC_{11}\text{-CHO} + C_s]_p$ were viewed using an optical microscope and representative images are presented in figure 3.1. Figure 3.1b and e are images of $[C_s]_p$ formed from starting solution a in Table 3.1. Figure 3.1a and d are images of $[nC_{11}\text{-CHO}]_p$ formed from

starting solutions c and e, respectively, as defined in Table 3.1. Figure 3.1bc and f are images of $[nC_{11}\text{-CHO} + C_s]_p$ formed from starting solutions b and d respectively, also as defined in Table 3.1.

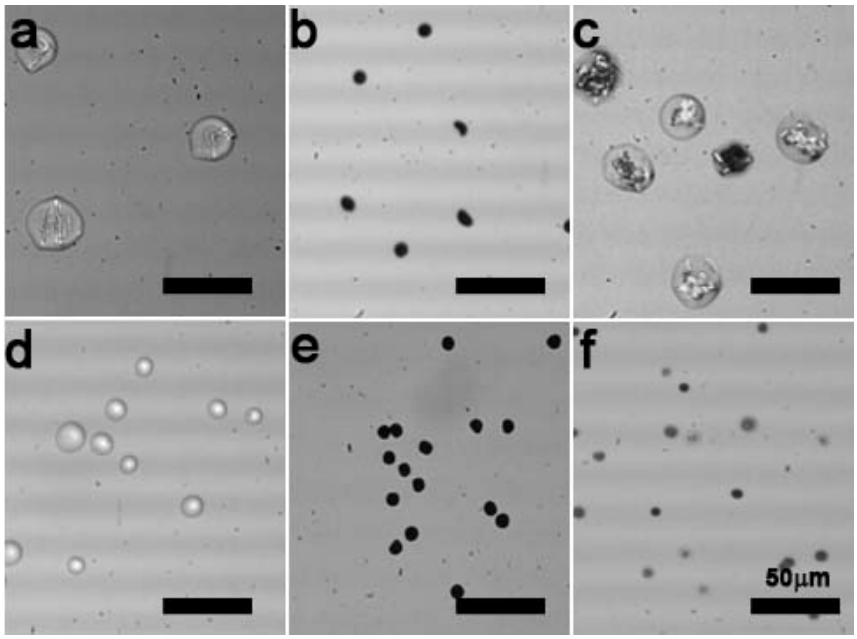

Figure 3.1 Representative image of a) 6 ng of dodecan-al of $[nC_{11}\text{-CHO}]_p$, b) 127 pg of carbon $[C_s]_p$, c) 6 ng of dodecan-11 and 127 pg of carbon particles $[nC_{11}\text{-CHO} + C_s]_p$, d) 94 pg of $[nC_{11}\text{-CHO}]_p$, e) 127 pg of carbon $[C_s]_p$, and f) 94 pg of dodecan-al and 127 pg of carbon particles $[nC_{11}\text{-CHO} + C_s]_p$.

3.3.2 Viability assay

To determine the maximum time for the cells to stay viable, various negative controls were incubated for 1 h, 4 h, 6 h, and 18 h at which time the viability of these cell cultures were determined. Representative images of this cell viability assay of different cell cultures following different incubation period are presented in figure 3.2. It was observed that the cell culture is not viable following an 18 h incubation period.

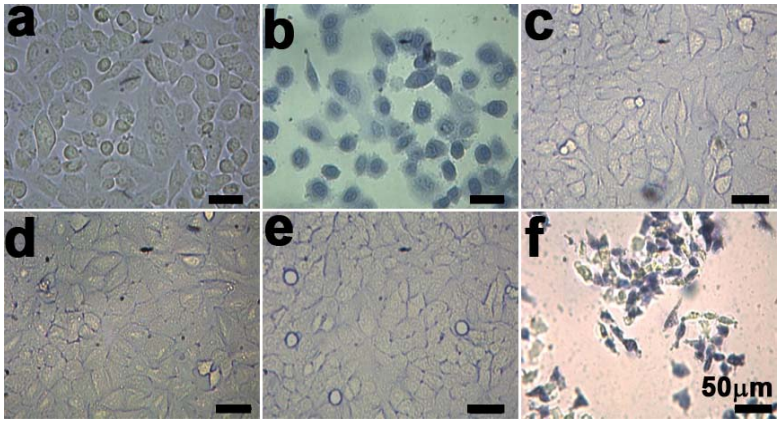

Figure 3.2 Viability assay of the A549 cell culture following different incubation period. a) negative control, b) positive control., c) 1 h, d) 4 h, e) 6 h, and f) 18 h

3.3.3 Particle movement

Movement of particles deposited onto a culture, to learn the time required for the particles to adhere onto the cells, was monitored by tracing the movement of the particles from the site of delivery to the site where the particles settled. Representative images of the movement of the particles are shown in figure 3.3.It was observed that particles were moved following the deposition onto a cell culture (figure 3.3a-b) and were settling down following a 10 minute incubation period (figure 3.3c-d).

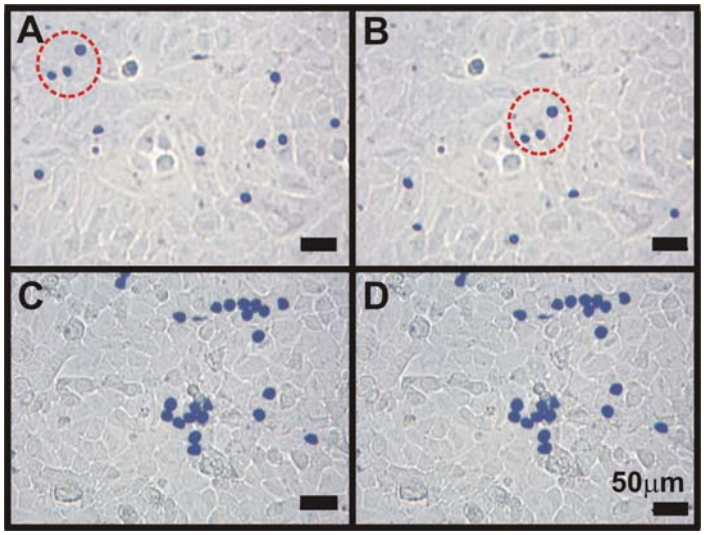

Figure 3.3 Representative images of moving particles. A) Initial position of particles following the particle delivery, B) Position of particles 20 seconds after particle delivery, C) Positions of particles after 10 minutes after particle delivery, D) Positions of particles after 10 minutes and 10 seconds after particle delivery.

3.3.4 MALDI-TOF-MS from the supernatant of cell culture dosed with particles following a 30 min incubation period.

Three representative mass spectra from a supernatant sample of a cell culture dosed with 6 ng of $[nC_{11}\text{-}CHO]_p$, and [6 ng of nC_{11}-CHO + 127 pg of $C_s]_p$ particles are shown in figure 3.4. Each mass spectrum shown is the cumulative average of >50 individual mass spectra collected from an individual sample.

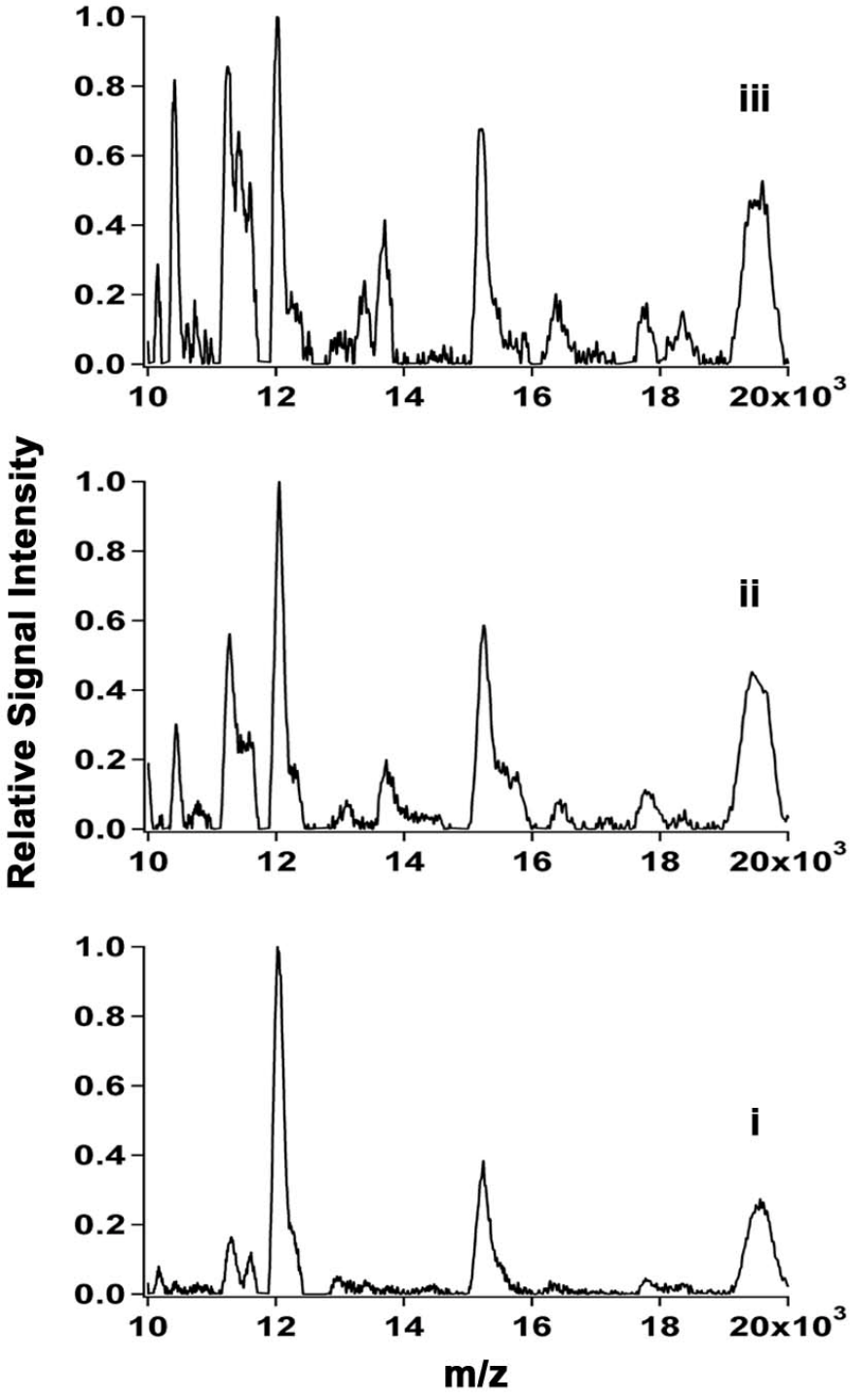

Figure 3.4 Representative MALDI mass spectra from the supernatant A549 cell cultures dosed with a) 127 pg of dodecanal $[nC_{11}\text{-CHO})]_p$, b) 6 ng of carbon $[C_s]_p$, and c) 127 pg of dodecanal and 6 ng of carbon particles $[nC_{11}\text{-CHO} + C_s]_p$ following a 30 minute incubation period.

The relative signal intensity of every ion peak in each mass spectrum was calculated using equation 3.1 where the difference between signal intensity of an ion, S, and the signal intensity of background, S_b, is divided by the difference between signal intensity of the reference peaks S_{ref} with signal intensity of background, S_b. The background signal intensity, S_b was determined by taking the signal intensity average of the last 50 data points in each spectrum. The reference peak signal intensity, S_{ref} was obtained from the signal intensity of the peak that has constant intensity in either negative control or test sample. The assumption was made that the reference peak signal intensity was not dependent on the experimental factors. In this case, S_{ref} was the peak intensity at m/z= 8500 Da for mass spectra using a mass window from 3 to 10 kDa, S_{ref} at m/z= 12,300 Da for mass spectra using a mass window from 10 to 25 kDa. The relative signal intensity of these ion peaks are plotted in figure 3.6.

Equation 3.1 **Relative Ion Intensity= $(S-S_b)/(S_{ref}-S_b)$**

Representative mass spectra collected from supernatant of the cell culture dosed with less than 100 particles per experiment, with any one experiment involving particles having the following compositions, [127 pg of C_s]$_p$, [94 pg of nC_{11}-CHO]$_p$, [127 pg of C_s + 94 pg of nC_{11}-CHO]$_p$, [94 pg of nC_{11}-COOH]$_p$, [127 pg of C_s + nC_{11}-COOH]$_p$, [nC_{12}-OH]$_p$, or [127 pg of C_s+nC_{12}-OH]$_p$ are shown in figure 3.5. Each mass spectrum shown is the cumulative average of >50 individual mass spectra collected from an individual sample.

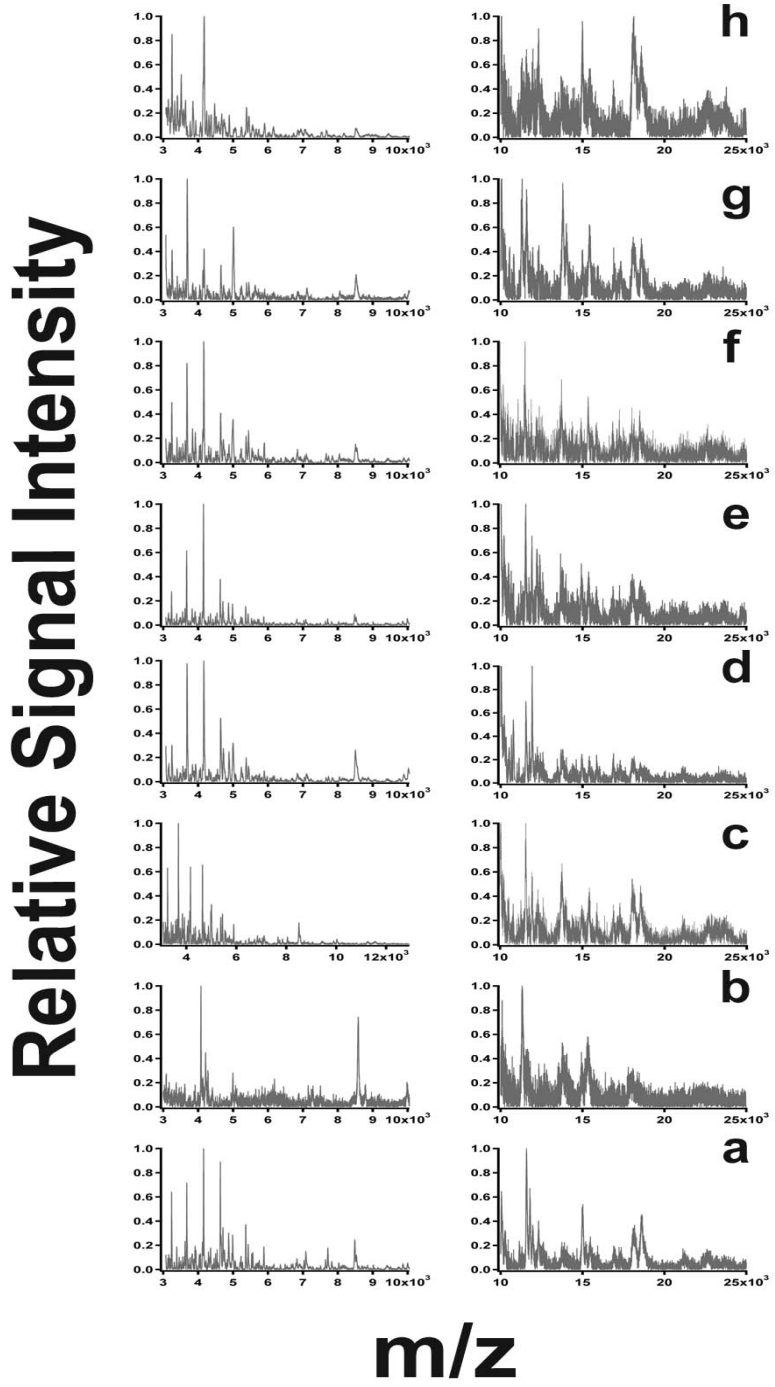

Figure 3.5 Representative MALDI mass spectra from the supernatant A549 cell cultures dosed with a) negative control b) 127 pg of carbon particle $[C_s]_p$, c) 94 pg of dodecanal particle $[nC_{11}\text{-}CHO]_p$, d) 94 pg of dodecanal containing 127 pg of carbon particles $[nC_{11}\text{-}CHO + C_s]_p$, e) 94 pg of dodecanoic acid particle $[nC_{11}\text{-}COOH]_p$, f) 94 pg of dodecanoic acid containing 127 pg of carbon particle $[nC_{11}\text{-}COOH + C_s]_p$, g) 94 pg of dodecanol $[nC_{12}\text{-}OH]_p$, h) 94 pg of dodecanol containing 127 pg of carbon particles $[nC_{12}\text{-}OH + C_s]_p$ following a 30 minute incubation period.

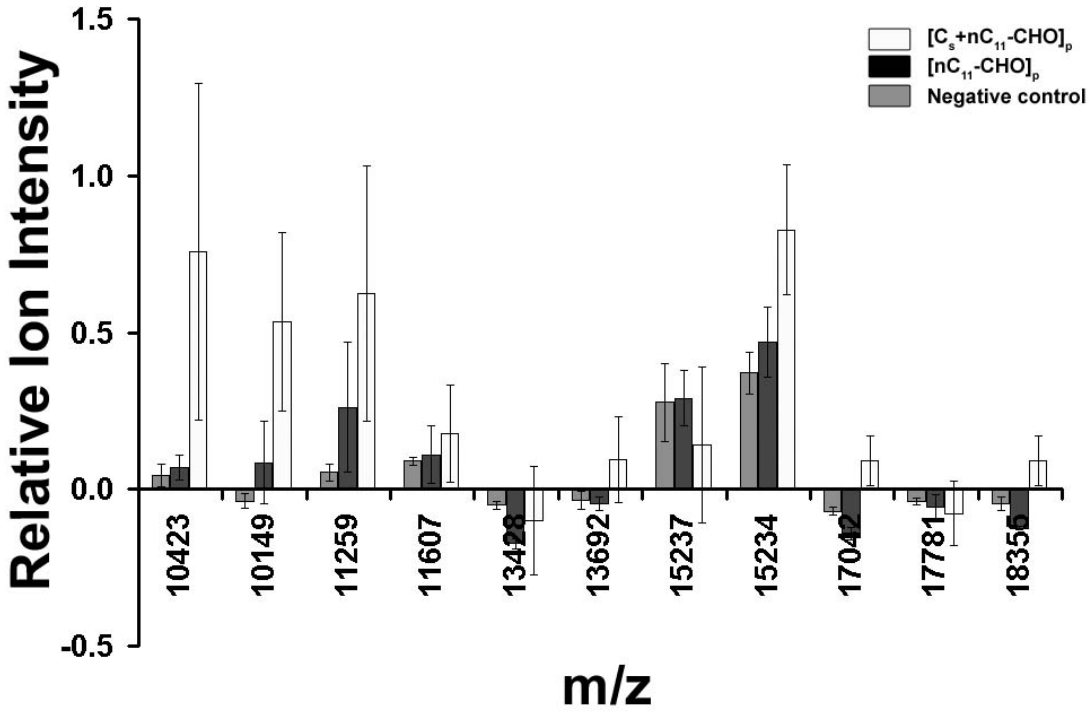

Figure 3.6 Relative abundance of ions observed in the MALDI-TOF-MS of the supernatant collected from an A549 cell culture dosed with a population of 6 ng of dodecanal $[nC_{11}\text{-CHO}]_p$, and 6 ng of dodecanal containing 127 pg of carbon particles $[nC_{11}\text{-CHO} + C_s]_p$ following a 30 minute incubation period

The relative ion intensity of every ion peak in each mass spectrum was calculated using equation 3.1. The relative signal intensity of differentially expressed biomolecules from cell cultures dosed with either 0 or 127 pg of $[C_s]_p$ containing 94 pg of $[nC_{11}\text{-CHO}]_p$, $[nC_{11}\text{-COOH}]_p$, or $[nC_{12}\text{-OH}]_p$ particles are shown in figure 3.7 to 3.9 respectively.

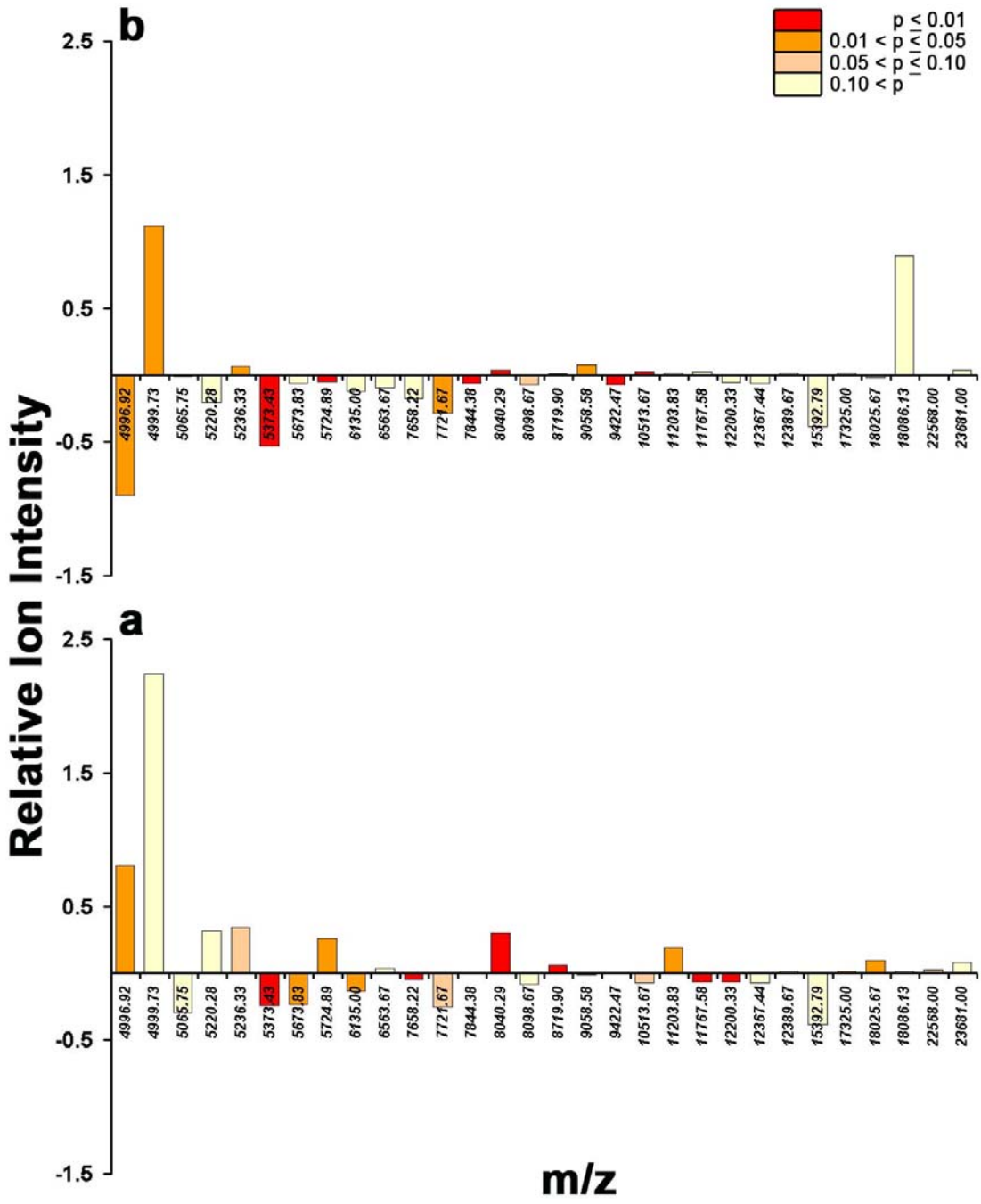

Figure 3.7 Relative abundance of ions observed in the MALDI-TOF-MS of the supernatant collected from an A549 cell culture dosed with a population of a) 94 pg of dodecanal $[nC_{11}\text{-}CHO]_p$ and b) 94 pg of dodecanal containing 127 pg carbon particles $[nC_{11}\text{-}CHO + C_s]_p$ following a 30 minute incubation period

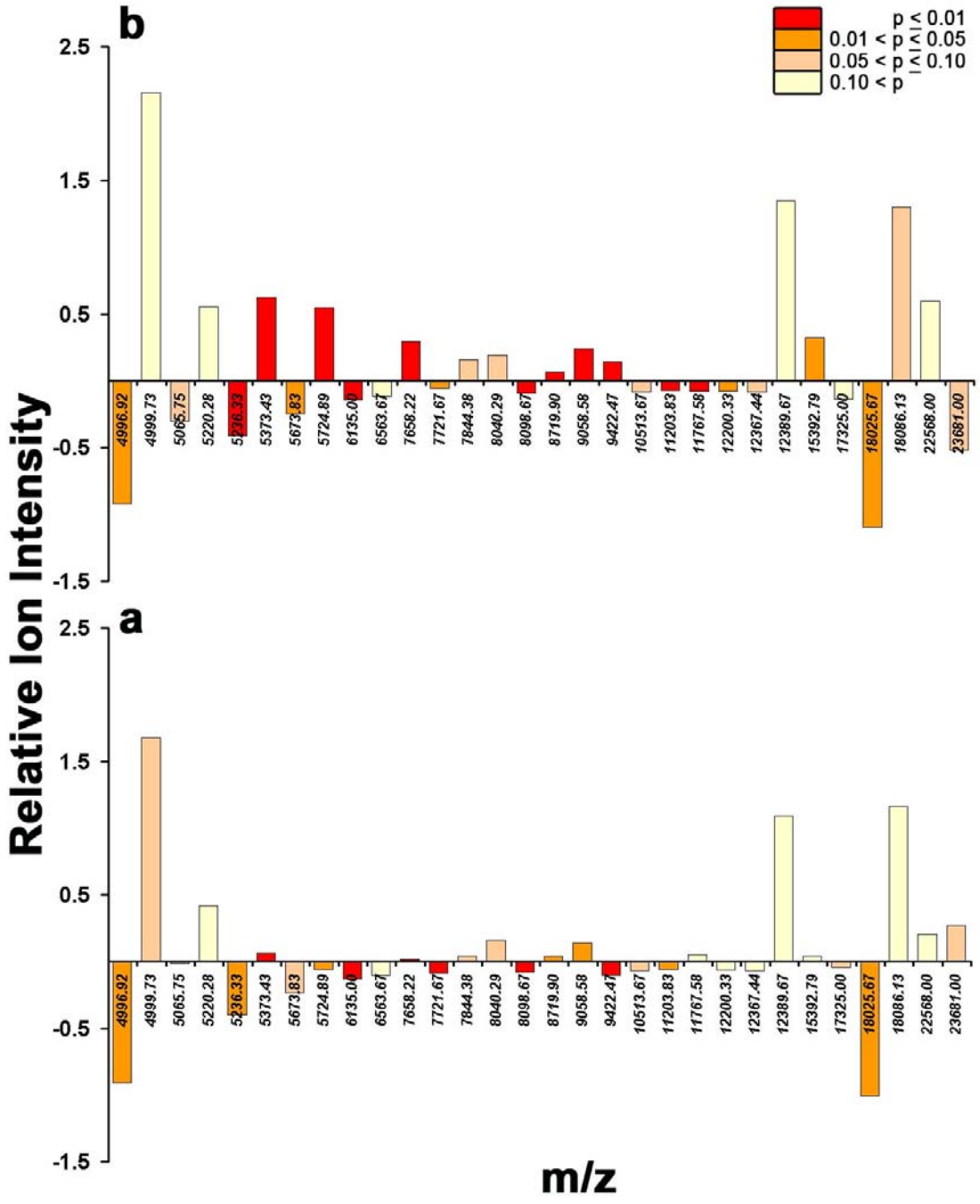

Figure 3.8 Relative abundance of ions observed in the MALDI-TOF-MS of the supernatant collected from an A549 cell culture dosed with a population of a) 94 pg of dodecanoic acid $[nC_{11}\text{-}COOH]_p$ and b) 94 pg of dodecanoic acid containing 127 pg of carbon particles $[nC_{11}\text{-}COOH + C_s]_p$ following a 30 minute incubation period

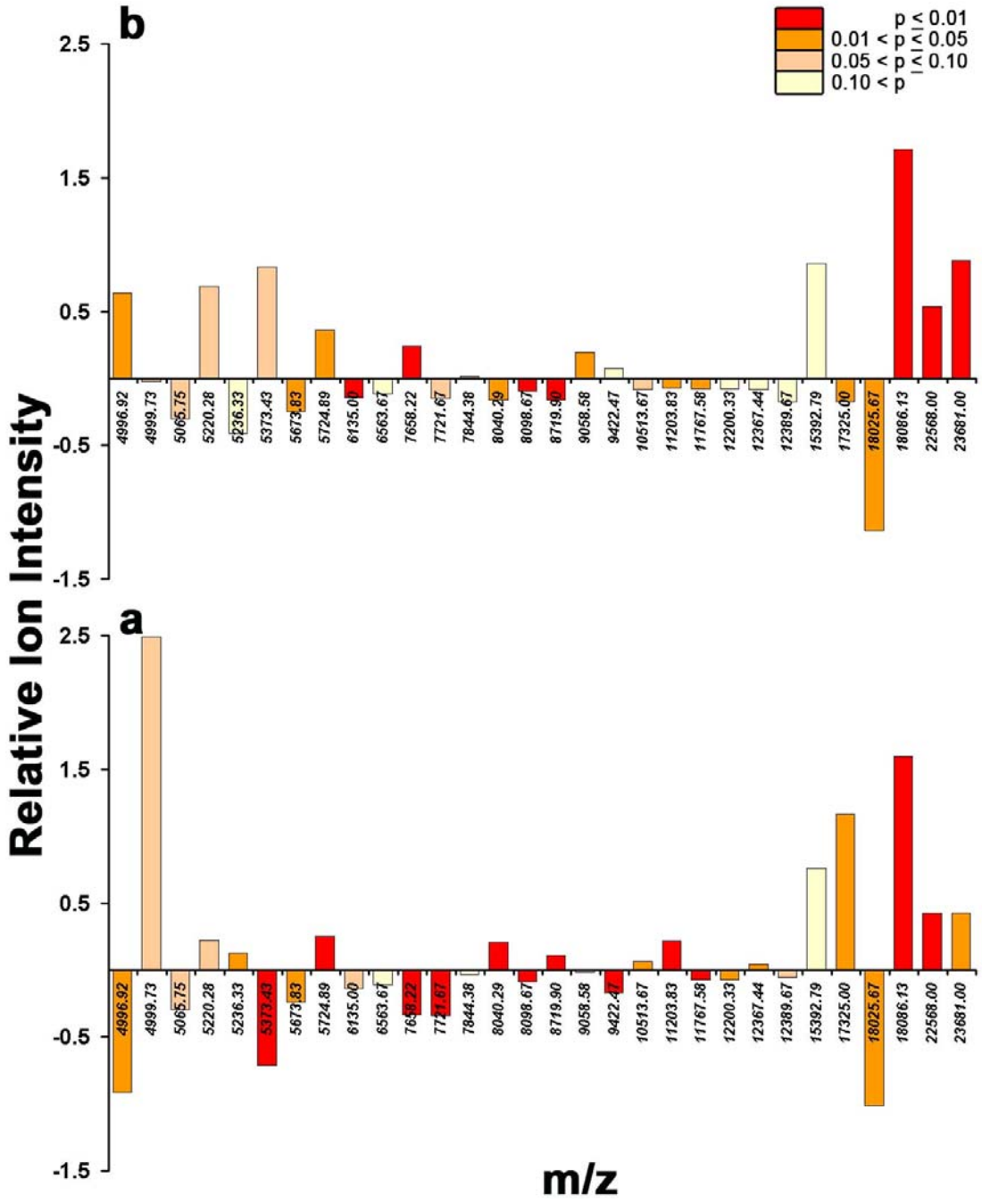

.Figure 3.9 Relative abundance of ions observed in the MALDI-TOF-MS of the supernatant collected from an A549 cell culture dosed with a population of a) 94 pg of dodecanol $[nC_{12}\text{-}OH]_p$ and b) 94 pg of dodecanol containing 127 pg of carbon particles $[nC_{12}\text{-}OH + C_s]_p$ following a 30 minute incubation period

3.3.5 Identification of biomolecules with ELISA

Following the deposition of a population of [nC_{11}-CHO + C_s] particles and a 30 minute incubation period, the concentration of CCL 24 and CCL 16 in A549 supernatant was measured by ELISA (figure 3.10). It was found that CCL 24 was upregulated from the cell culture dosed with [nC_{11}-CHO + C_s] particles

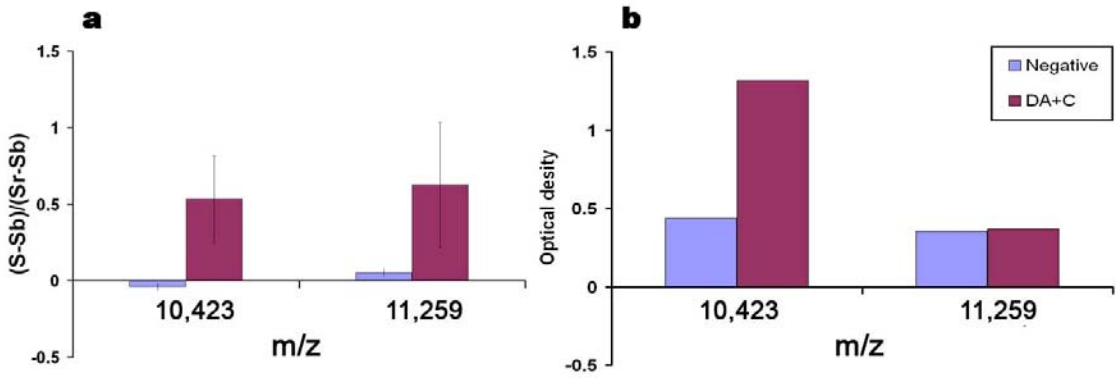

Figure 3.10 a) Relative signal intensity of ion peaks at m/z = x and m/z = y measured by MALDI-TOF-MS, b) Optical density of CCL 24 and CCL 16 measured by ELISA.

3.4 Discussion

Particles with known size and compositions were created from volatile and non-volatile compounds using a levitation apparatus. The compounds used were compounds those are commonly present in the atmosphere as a result of anthropogenic activities. Though ambient particles are expected to be comprised of numerous compounds, this study investigated the cell response due to the presence of one organic compound on the particle. Particles as prepared in the ac trap were observed prior to their use in dose-response studies by delivering them onto a clean glass slide and measured using an optical microscope (figure 3.1). Note that a particle population viewed using an optical

microscope was a different population than that delivered to a cell culture, though both populations were prepared similarly.

The viability of different cell cultures following different incubation periods (1 h, 4 h, 6 h, and 18 h) were ascertained using a trypan blue assay (figure 3.2). The cell cultures were viable up to a 6 h incubation period. Following 18 h incubation period, the cell culture was not viable. In addition to the cell staining, cells also dislodged from the coverslip. The dislodgement of the cells is speculated to be due to dehydration of the cell culture.

The adherence of particles onto the cell cultures was monitored immediately following particle delivery using an optical microscope. The particles were observed to be moving following the particle delivery. The particles were observed to not move on the cells after 10 minutes. This observation provided an important piece of information regarding the time at which the population of particles could be considered to be in close contact with the cells.

Following a 30 minute incubation period, exposure of cell cultures to 16.5±12.2 μm diameter particles either $[nC_{11}\text{-CHO}]_p$ or $[nC_{11}\text{-CHO}+C_s]_p$, resulted in observable differential expression of twelve different biomolecules in the mass spectra (figure 3.4). Similarly, mass spectra of cell cultures exposed to 6.3 ±0.4 μm diameter particles containing 127 pg of carbon $[C_s]_p$, 94 pg of dodecanal $[nC_{11}\text{-CHO}]_p$, 94 pg of dodecanoic acid $[nC_{11}\text{-COOH}]_p$, 94 pg of dodecanol $[nC_{12}\text{-OH}]_p$, 94 pg of dodecanal containing 127 pg of carbon particle $[C_{11}\text{-CHO} + C_s]_p$, 94 pg of dodecanoic acid containing 127 pg of carbon particle $[nC_{11}\text{-COOH} + C_s]_p$, or 94 pg of dodecanol containing 127 pg of carbon particle $[nC_{12}\text{-OH} + C_s]_p$ resulted in differential expression of at least thirty different

biomolecules (figure 3.5). Thus, these are further evidence that size and compositions of particles resulted in differential secretion of biomolecules.

Based on the molecular mass of the detected biomolecules, we speculate that the identity of these molecules may belong to the following classes of secreted proteins, β-defensins, cytokines, and chemokines. The mass of some of these compounds are compared to the m/z of the compounds observed to have been differentially expressed using MALDI-MS are presented in following tables.

Table 3.3 Known signalling proteins that may being observed differentially expressed from the mass spectra collected from the supernatants of A549 cells dosed with either 0 or 127 pg of $[C_s]_p$ particles containing 6.0 ng of $[nC_{11}\text{-}CHO]_p$

Secreted Biomolecule	Cytokines
CCL 24	Unknown b
CCL 27	Unknown c
CCL 16	Unknown d
IL 5	Unknown e
IL 19	Unknown f
Unknown a	

Table 3.4 Known signalling proteins that may being observed differentially expressed from the mass spectra collected from the supernatants of A549 cells dosed with 0 or 127 pg of $[C_s]_p$ containing 94 pg pf $[nC_{11}\text{-}CHO]_p$. $[nC_{11}\text{-}COOH + C_s]_p$, or $[nC_{12}\text{-}OH + C_s]_p$

No	Tentative Biomolecule	No	Tentative Biomolecules
1	BD-7	16	MCP-1/CCL 2
2	BD-6	17	BD-16
3	BD-27	18	CXCL 14
4	BD-3	19	CCL 24
5	BD-14	20	CCL 16
6	BD-34	21	CXCL 9
7	BD-11	22	CCL 21
8	BD-24	23	PF-4/Oncostatin A
9	BD-35	24	IL-13
10	BD-36	25	IL-2
11	MIP-1b	26	TNF-a
12	CCL 3	27	BD-29
13	CCL 4	28	IL-18
14	CCL 20	29	IL-12a
15	CCL 22	30	OSM

The biomolecules that were observed to be upregulated in this short of a time frame are believed to have been pre-made and stored in vesicles within the cell, ready to be released upon stimulation of the cell. The species that are down regulated are possibly those mediators that are taken up by the cell once the culture is stimulated; significant down regulation in this short of a period of time suggests that numerous receptors for these molecules must also have been pre-made by the cell and readily expressed.

Following exposure of the cell culture to 127 pg of $[C_s]_p$ particles containing 6.0 ng of $[nC_{11}\text{-}CHO]_p$ particle, the MALDI-MS ion intensity of the ion at m/z= 10,423 Da correlated with the optical density of CCL 24 as measured by ELISA from the same supernatant samples.

3.5 Conclusion

The use of technology and methodology described has demonstrated its ability to provide results that are able to address issues regarding the effect of ambient PM and lung inflammations. EDLT technology allows the formation of particle types with known size and compositions and the delivery of the particles directly onto an air-liquid interface culture. In principle, methodologies developed to identify proteins using mass spectrometry can be applied to identify the compounds detected in this work. In practice, the abundance of these compounds in these samples may prove a limiting factor in their identification.

CHAPTER 4
DEVELOPMENT OF METHODOLOGY TO DEPOSIT $PM_{2.5}$ ONTO LUNG CELLS *IN VITRO*

4.1 Introduction

The impact of ambient air pollution such as particulate matter (PM) on health effects has been extensively reported.[2,56-58] PM are suspended particles <10 μm in diameter having complex chemical composition including mineral dusts, soots, sea spray, biologic materials and additional compounds formed by atmospheric chemistry.[59-61] *In vitro* studies with human and rat alveolar macrophages exposed to urban particulate matter exhibit cytotoxicity, production of oxygen radicals and release of various cytokines, suggesting that these cells are key players in events that lead to lung injury and inflammatory responses following exposures to ambient particles.[62,63] The characterization of how components within PM are involved in causing these effects is the subject of many studies worldwide.[64]

Numerous strategies to study PM toxicity have been developed. A common *in vivo* and *in vitro* strategy is to use a size-segregated collection of ambient particles from filters, separation of the soluble and insoluble fractions followed by instillation of these fractions to an animal model or incubation with lung cells.[65-67] Another strategy involves incubation of lung cells with compounds, or individual compounds, that have been

identified as existing on ambient particles so as to characterize the lung cell injury caused by those compounds.[68-70]

Allen Haddrell, a prior graduate student, developed an *in vitro* methodology to the study inflammation potential of ambient PM that utilized a particle levitation trap apparatus to generate PM_{10} particles ($\varnothing$ = 6 μm) of known composition. The capability was then demonstrated the capability to deliver the particles directly onto a cell culture.[35,36] The primary goal of the method development described in this chapter was to mimic ambient $PM_{2.5}$ exposure *in vivo* and elucidate the individual compounds most significant in causing response, such as expression of adhesion molecules and of cytokine secretion.

I started by adopting the Haddrell PM_{10} methodology to generate ambient $PM_{2.5}$ with the intention of also delivering the particles onto cell cultures. It was soon observed that this method was not performing well for carbon particles with diameter of 2.4±0.1 μm. Carbon particles could be caused to make contact with the cells, but they did not adhere to the cells. As a consequence, an investigation of methodology to enable direct delivery of $PM_{2.5}$ onto cell cultures, with the establishment of cell-particle interaction leading to the particles remaining in contact with the cells was initiated.

As will be described, many variations to this methodology were investigated and it was generally observed that cell cultures were not viable but that carbon particles did adhere to the cells, or vice versa. Throughout this study, the viability of the cell culture was determined using a trypan blue assay. Ironically, because carbon particles were used extensively in this phase of the project, only in the end was it evident that clear progress was made in developing a robust methodology. This can now be attributed to the fact

that, in these experiments, there was repeated observation of carbon particles not adhering tightly to viable A549 cells regardless of the method. It turns out that the interaction between black carbon particles and A549 cells do not favour their adherence, even after centrifugation. The inadvertent outcome, in retrospect could be argued as not surprising, was in fact responsible for the successful development of a method for creating and dosing A549 cells with carbon particles < 2.5 μm in diameter, such that ~>80 % of the particles per population do adhere to A549 cells that remain viable for incubation periods at least as long as 72 hours.

4.2 Chemicals

Lippopolysaccharide from E. Coli (Serotype 0.111:B4, L-2630) (LPS), tumor necrosis factor alpha (T6674-10UG) (TNFα), minimum essential medium (MEM), trifluoroacetic acid (TFA), sinapic acid (SA), acetonitrile (ACN), trypan blue solution (0.4%) were purchased from Sigma-Aldrich Inc. Phosphate buffered saline (PBS) was purchased from Oxoid Ltd., Basingstoke, Hampshire, England. 20 nm diameter fluospheres were purchased from Molecular Probes, Invitrogen Inc., Burlington, ON, Canada. These fluospheres are polystyrene-based spheres (density = 1.05 g/ml) that encapsulated ~180 fluorescein molecules per fluosphere. India ink (Speedball, product #3338, Statesville, NC, USA) was used as the source for elemental carbon (C_s). L-glutamine, MEM Vitamin, and fetal bovine serum (FBS) were purchased from Invitrogen Corporation, Burlington, Ontario, Canada.

4.2.1 Growth medium

Minimum essential medium (MEM) solution was prepared from MEM powder according to instructions provided by the supplier of this material. 9.4 g MEM powder

was added to 1 L of distilled deionised water. While this solution was stirred, 2.2 g of sodium bicarbonate ($NaHCO_3$) powder was added. The pH of the resulting solution was adjusted to 7.6 with 1 N sodium hydroxide solution. With dissolution of the solids added, this solution was filtered in a biological safety cabinet (Forma scientific Inc. # 14567-386, Marietta, OH, USA) using a sterilized cellulose acetate membrane filter having a mean pore size of 0.2 μm. Following filtration, 10 mL of L-glutamine, 10 mL of MEM vitamin, and 100 mL of fetal bovine serum (FBS) were added into the 1 L of MEM solution:

According to the manufacturer, L-glutamine has pH in the range of 4.7 - 6.0 and contains 29.8 mg L-glutamine per mL in 0.85 % sodium chloride. It is required for nucleic acid synthesis, and is a source of energy for the cells.[71]

MEM Vitamin according to the manufacturer has pH (7.0 - 7.4) and contained vitamin B-complex in 0.85 % saline. These vitamins are required mostly for cell growth, energy production, and synthesis of genetic materials and phospholipids.[71-73]

FBS solution contains proteins, growth factors, hormones, amino acids, and minerals.[71] Albumin in FBS serves as a carrier for lipids and minerals. Transferrin detoxifies the medium by binding metals.[35,36,51,74-77] Fetuin in FBS promotes cell attachment and spreading.[71]

Growth factors stimulate cell proliferation.[78,79] The hormones are required for cellular uptake of glucose and amino acids.[80-82] Amino acids are precursors for the synthesis of phospholipids.[(13)] Metals including iron, copper and zinc are cofactors for enzymes.[(32)]

4.2.2 Serum free medium (SFM)

SFM solution was prepared similarly to MEM solution (section 4.2.1) except, it did not contain FBS.

4.2.3 Phosphate buffered saline (PBS)

This solution was prepared according to the manufacture's directions as follows. A tablet of PBS salt was dissolved in 100 mL distilled deionised water, and the resulting solution autoclaved at 115 ^{o}C for 10 minutes. The resulting concentrations of the different salts in PBS were 1.4×10^{-1} M NaCl, 2.7×10^{-3} M KCl, 6.5×10^{-3}M $Na_2HPO_4.2H_2O$, and 1.5×10^{-3} M KH_2PO_4.

4.3 Starting solutions

An example of a starting solution from which carbon particles (C_s) were prepared, is as follows. 1.5×10^{-3} g/mL of india ink and 1.3×10^{-6} g/mL of fluospheres in distilled deionized water were prepared. From this solution, carbon particles with 2.4 ± 0.1 μm in diameter (~76.7 pg carbon) were created using the apparatus described below. The fluospheres were added to the starting solution simply to assist with visualizing particles after delivery to the culture, to count how many particles adhered after an incubation period, and monitoring the breakdown of the particles (eg. break up of the aggregate of carbon black nanoparticles). The concentration of fluospheres in starting solution was held constant.

4.4 Droplet dispensing and levitation for particle formation

An AC trap was employed to trap, levitate, and deposit a population of particles on a bare glass slide or cell culture (figure 4.1). 10 μL of a starting solution was used to fill the reservoir of a droplet-on-demand dispenser (MJ-AB-01-60, MicroFab

Technologies Inc., TX, USA). A 120 Hz pulsed waveform of amplitude 50 V was applied to activate the piezoceramic element of the dispenser (figure 4.2). With each activation of the piezoceramic, an acoustic pressure wave within the cavity of the dispenser caused a volume of the starting solution to be forced through the dispenser nozzle. This volume of solution formed a jet of liquid that because of its momentum, separated from the nozzle and collapsed to form an individual droplet. These droplets were estimated as being 326 ± 194 pL at the instance of their formation.

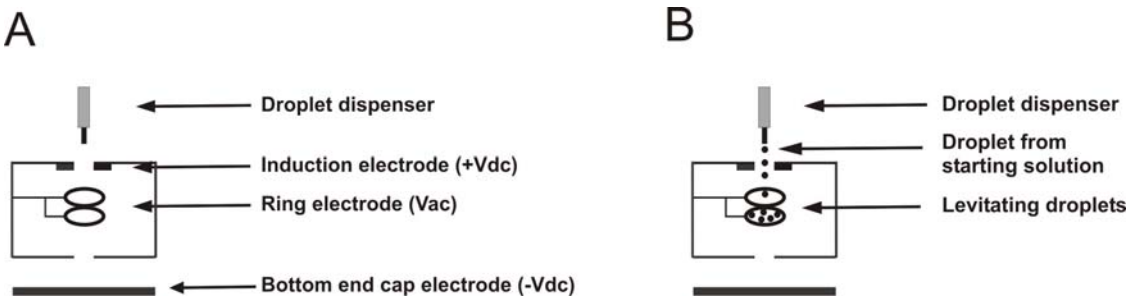

Figure 4.1 A) Schematic diagram of the AC trap apparatus. B) Schematic diagram depicting picoliter aliquots of a starting solution being dispensed from the droplet dispenser, with each aliquot forming a single droplet, some of which were captured in the AC trap and levitated.

A DC potential of 500 V was applied to the induction electrode, which was a flat plate having a 5 mm diameter hole cut into it during droplet dispensing. That hole was centered under the nozzle of the dispenser. The induction electrode was positioned 2 mm from the tip of the nozzle. The electric field created between the plate and the nozzle induced differential ion mobility in the jet of solution prior to it separating from the nozzle to form a droplet with net elementary charge.

While dispensing droplets, the AC waveform applied to the two ring electrodes of the AC trap was a sinusoidal waveform 50 Hz and 2.4 $kV_{0\text{-}P}$. The frequency of this waveform was then manually ramped to 1,050 Hz over a period of ~2 s. The loss of mass

from the droplets due to the evaporation of solvent, water or ethanol, necessitated tracking the electric field in the AC trap to prevent the remnant of each droplet from being ejected from the AC trap. The remnant of each droplet is hereafter referred to as a particle.

4.5 Cell culture

The alveolar type II epithelial cell line A549 (American Type Culture Collection (Manassas, VA, USA) was derived from a human lung carcinoma in a 58 year old Caucasian male.[83] This cell line exhibits many features of alveolar type type II cells. These cells have been used extensively in studies of particulate matter-induced responses via ICAM-1 expression.[35,84,85] This cell line has also been used as a model to study alveolar reactivity to micro-organisms and macromolecules.[86]

4.5.1 Cell passaging

Cell passaging was performed in a biological safety cabinet. Growth medium bathing the cell culture grown on a tissue culture dish (100 mm × 20 mm) was aspirated and the culture rinsed with PBS solution. 1 mL of trypsin-ethylenediaminetetraacetic acid (Trypsin-EDTA) solution was added and incubated for 5 min. The purpose of adding Trypsin-EDTA solution was to detach the cells from their support. After incubation, trypsinized cells were collected using 5 mL of minimal essential medium (MEM) and placed in a 15 mL test tube. This test tube was centrifuged at 1000 revolutions per minute (rpm) for 5 min enabling cell pellet formation. The MEM was aspirated after centrifugation. Pelleted cells were resuspended with 10 mL of fresh aliquots of fresh MEM. 0.5 mL of the solution containing the resuspended A549 cells was dispensed onto an 18 mm × 18 mm cover slip placed in each well of a six-well plate

(corning) containing 2 mL of MEM. Cells were grown to 95 % confluence in an incubator at conditions of 37 ^{o}C, 5 % CO_2, and 100 % relative humidity before use. The average incubation time for the cells to grow to 95 % confluence was 24 h.

Cell cultures were also grown on other supports, including 60 mm × 15 mm tissue culture dishes (BD Falcon # 353004), and 60 mm × 15 mm center well organ culture dishes (BD Falcon # 355037) (figure 4.3). To grow a cell culture on a tissue culture dish, 1 mL of the solution containing the resuspended A549 cells was dispensed onto a 60 mm × 15 mm tissue culture dish containing 2 mL of MEM. To grow a cell culture on the center well of an organ cell culture dish, 1 mL of the solution containing the resuspended A549 cells was dispensed into the center well of 60 mm × 15 mm center-well organ culture dish.

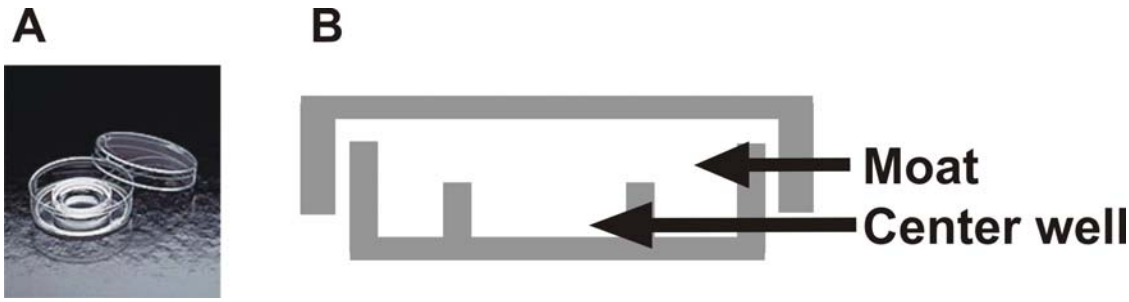

Figure 4.2 (A) Photgraph and (B) sketch of a center-well organ culture dish.

4.6 Negative control for dose-response experiments using particles formed in an AC trap.

The majority of the growth medium bathing the cell culture was drained. The cover slip on which the culture had been grown was transferred to a sterile (35 mm x 10 mm)

tissue culture dish that was placed in an incubation oven whose internal conditions were maintained at 100 % humidity, 37 °C and 5 % CO_2.

Depending on the particle delivery method and support used, the negative control was treated the same as the test sample except there were no particles delivered from the levitation trap.

4.7 Particle delivery onto lung cells *in vitro*

4.7.1 Existing methodology

A methodology that enabled to deposition of PM_{10} particles had been developed, and it was shown that dose response studies involving particles of 6 μm in diameter could be reproducibly performed. [35,36] My studies began with the use of this method to deposit particles of 2.4 ± 0.1 μm. A schematic diagram illustrating the particle delivery onto a cell culture grown on a coverslip is shown in figure 4.4. With a population of carbon particles levitated in the AC trap, some but not all growth medium bathing a cell culture was drained off by gently, but quickly touching one side of the coverslip on a kimwipe. In doing so, an estimated 85 μL of the 100 μL of growth medium bathing the cells was removed from the coverslip. The residual 15 μL was intended to keep the cells moist. The coverslip supporting the culture was then placed on the top of the bottom electrode of the AC trap. The levitated particle population was extracted from the AC trap by applying a 1000 V DC potential to the bottom electrode. Immediately following particle delivery, the culture was transferred to a sterile tissue culture dish (35 mm × 10 mm) and incubated at 100 % humidity, 37 °C and 5 % CO_2 for 30 min with no medium added. The total time elapsed between the draining of the growth medium, delivering the population of particles, and placing the culture back into the incubation oven was <60 s. No growth

medium was added to the culture during the incubation period. Following the incubation period, the cell viability was tested using trypan blue assay. In general, it was observed that the cells were viable but the particles did not adhere, or vise versa.

With this outcome, the method was clearly not satisfactory with respect to the dosing A549 cultures with $PM_{2.5}$ particles. Modification of this method for use with $PM_{2.5}$ was required.

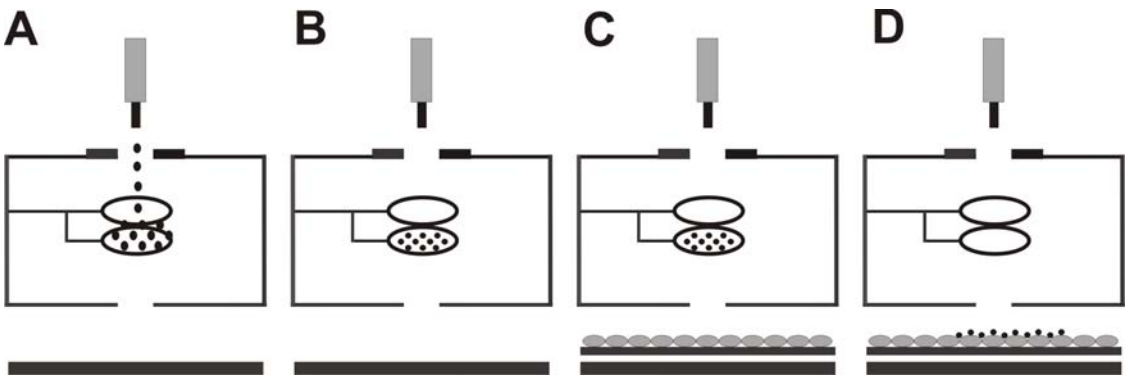

Figure 4.3 Schematic diagram of particle delivery onto a cell culture supported on a coverslip A) an aliquot of a starting solution was dispensed from a droplet dispenser and the resulting droplet per aliquot levitated, B) solvents from each levitating droplet evaporate, causing the non-volatile compounds from the droplet to precipitate and coagulate forming particles, C) a cell culture positioned underneath the levitation chamber, D) a potential was applied to the bottom end cap electrode to extract the population from the trap, depositing the particles onto the cell culture.

4.7.2 Removal of a majority (estimated > 90%) of the growth medium

This method is similar to that described in the previous section. The difference from the previous section is that a lot more growth medium was removed by touching all the coverslip sides onto a kimwipe. It is estimated that approximately 90% of the 100 μL of media bathing the cell culture was removed.

With a population of carbon particles levitated in the AC trap, the growth medium bathing a cell culture was drained off by quickly touching all sides of the coverslip on a kimwipe, <16 μL of growth medium was left on the coveslip supporting the cell culture. The coverslip supporting the culture was then placed on the top of the bottom electrode of the AC trap. The levitated particle population was extracted from the AC trap by applying 1000 V DC potential to the bottom electrode. Immediately following particle delivery, the culture was transferred to a sterile tissue culture dish (35 mm x 10 mm) and incubated at 100 % humidity, 37 $^{\circ}$C and 5 % CO_2 for 30 min with no medium added. Following the incubation period, it was observed that the cell cultures were not viable, but the particles were observed to not move when viewed using the camera on the microscope.

4.7.3 Without removal of the growth medium

In this section, the coverslip was placed directly onto the bottom end-cap electrode without touching a kimwipe to any edge of the coverslip.

With a population of carbon particles levitated in the AC trap, the coverslip supporting the culture was then placed on the top of the bottom electrode of the AC trap without draining any of the media, estimated to be ~100 μL. The levitated particle population was extracted from the AC trap by applying a 1000 V DC potential to the bottom electrode. Immediately following particle delivery, the culture was transferred to a sterile tissue culture dish (35 mm × 10 mm) and incubated at 100 % humidity, 37 $^{\circ}$C and 5 % CO_2 for 1 h with no additional medium added.

Following the incubation period, the viability of the cell culture was analyzed by trypan blue assay. It was observed that the cells in the culture were viable, but particles

were observed to move when viewed using sequential images acquired using the camera on the microscope.

4.7.4 Addition of a fresh aliquot of serum free medium (SFM)

This method is similar to method 4.7.1, with only the following additional step. Immediately following carbon particle delivery, the culture was transferred to a sterile tissue culture dish (35 mm × 10 mm) and incubated at 100 % humidity, 37 $^{\circ}$C and 5 % CO_2 with no medium added for 30 min. Following this incubation time, 100 μL of SFM were added onto the cell culture and re-incubated for 18 h.

Following the incubation period, it was observed that cells were viable but the particles again did not adhere. The same method was also repeated, by adding 4 × 25 μL of SFM medium at the corners of the coverslip after 30 min. Using this method, the outcome was observed to be same, cells were viable, but the particles did not adhere to any cell.

4.7.5 Serum Free Medium (SFM) aerosol exposure

In this section, a nebulizer and spray chamber were employed in order to create fine SFM aerosol. A schematic diagram of the nebulizer and the spray chamber is shown in figure 4.4. Compressed air was connected to the inlet of the nebulizer. SFM was aspirated through the capillary tube. The air flow around the capillary tip ruptures the solution being drawn from the capillary tube into droplets that are then carried into the spray chamber. In the spray chamber, large droplets impact on the spray chamber walls with that liquid flowing to the waste outlet. Emerging from the spray chamber was an aerosol having droplets < 10 μm in size and vapour that was directed to the cell culture.

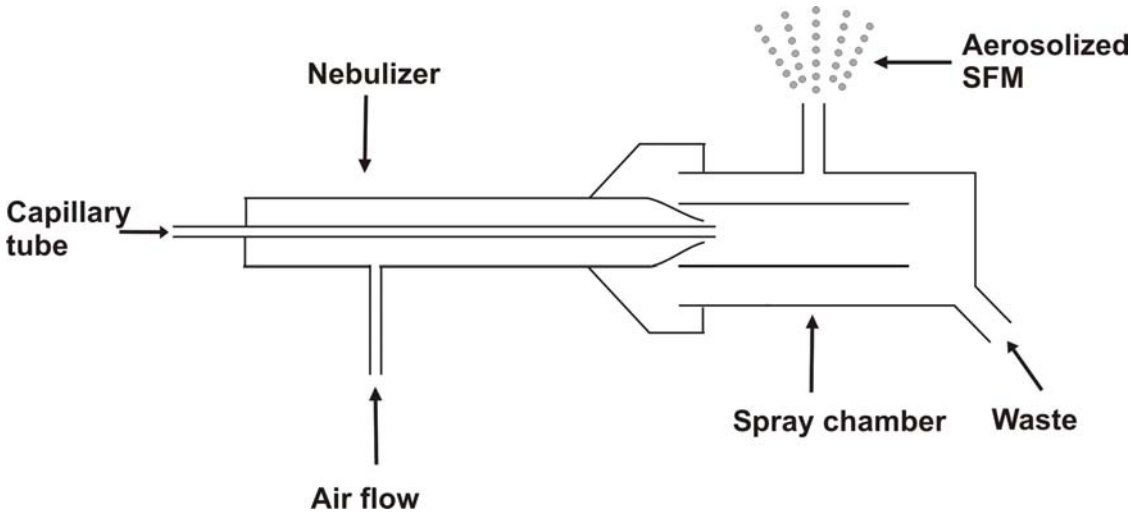

Figure 4.4 Schematic diagram of the nebulizer and spray chamber. Diagram is not drawn to scale.

Similar to method 4.7.2, immediately following particle delivery, the culture was transferred to a sterile tissue culture dish (35 mm × 10 mm) and exposed to aerosolized SFM for 10 s. The cell culture was then incubated at 100 % humidity, 37 $^{\circ}$C and 5 % CO_2 for 30 min, and these steps then repeated bringing the total incubation time to 1 h. Following the incubation time, the cell culture was observed to be not viable however, the particles adhered.

Because this method was not able to keep the cell culture viable, a variety of aerosolized SFM exposure times and additions of fresh aliquots of SFM were performed. Following variation of this procedure, each cell culture was placed in the incubator for a total incubation time of 4 h. The permutations of SFM exposure time, incubation period, and volume of SFM added are summarized in table 4.1. From these permutations, it was observed that the cell cultures were not viable, but the particles adhered.

Table 4.1 Variation of the SFM exposure time, the incubation period and the volume of SFM added

SFM aerosol exposure (sec)	Incubation period (Min)	SFM aerosol added (sec)	Incubation period (Min)	SFM added (μl)	Incubation period (Hrs)	Cell viability	Particle adherence
10	30	10	30	100	4	No	Yes
10	15	10	15	100	4	No	Yes
10	15	10	15	4x25	4	No	Yes
20	15	20	15	4x25	4	No	Yes
60	15	60	15	4x25	4	No	Yes
0	15	30	15	4x25	4	No	Yes

4.7.6 Variation of the DC potential at the bottom end-cap electrode

The variations of the methodology described were evaluated based only on whether the cells were viable and if the carbon particles adhered. It was observed that when 'all' of the growth medium on the cell cultures was removed, the cells were not viable yet the particles adhered. When 'some but not all' of the growth medium was removed, the opposite outcome was observed. From these observations, it was abundantly clear that there should be sufficient enough growth medium on the coverslip supporting cell culture in order to keep the cell culture viable for a 24 h incubation period (time required to stimulate cells and measure resulting maximum ICAM-1 expression per dose), while observing particles adherence, the trick was readily attaining this optimum and then being able to reproduce the conditions.

In the sections described below, not only was the amount of the growth medium varied, but also the DC potential at the bottom end-cap electrode was varied. A rationale for increasing the DC potential was to generate a stronger electric field for extracting the levitated particles, so as to allow them to break the surface tension of the growth medium on the air-liquid surfaces and liquid-cell, assuming this is a factor in achieving dose-response with the particle levitation platform.

4.7.6.1 The Haddrell Methodology

Similar to the method described in section 4.7.1, the levitated carbon particle population was extracted from the AC trap by applying 2000, 3000, or 4000 V DC potential to the bottom electrode. Immediately following particle delivery, the culture was transferred to a sterile tissue culture dish (35 mm × 10 mm) incubated at 100 % humidity, 37 °C and 5 % CO_2 for 1 h. Following the incubation period, the cell culture was observed to be not viable, however the particles adhered.

4.7.6.2 Removal of a majority of the growth medium

Using the same method described in section 4.7.2, in preparing the cell culture for particle delivery, the levitated carbon particle population was extracted from the AC trap by applying a 2000 V potential to the bottom electrode. Immediately following particle delivery, the culture was transferred to a sterile tissue culture dish (35 mm × 10 mm) and exposed to aerosolized SFM for 20 s. The cell culture was then incubated at 100 % humidity, 37 °C and 5 % CO_2 for 15 min and repeated for a total incubation time of 30 min. Following the incubation time, 4×25 μL of SFM was added onto the cell culture and re-incubated for 30 min. Following the incubation period, though the particles were observed to not move when viewed using the camera on the microscope, but the cell culture was not viable.

This method was also performed by applying 3000 and 4000 V DC potentials to the bottom end cap electrode. The outcome was observed to be the same.

4.7.6.3 Without removal of the growth medium

Using the same method described on section 4.7.3, the levitated carbon particle population was extracted from the AC trap by applying a 2000 V potential to the bottom

electrode. Immediately following particle delivery, the culture was transferred to a sterile tissue culture dish (35 mm × 10 mm) and exposed to aerosolized SFM for 20 s. The cell culture was then incubated at 100 % humidity, 37 °C and 5 % CO_2 for 1 h. Following the incubation period, the cell culture was viable, but the particles were not adhered to cells when viewed using the camera on the microscope.

This method was also performed by applying 3000 and 4000 V DC potential to the bottom end cap electrode. The result was observed to be the same.

4.7.7 Centrifugation of the cell culture

In this section, centrifugation of the cell culture following the particle delivery was employed to realize particle-cell contact.

4.7.7.1 Cell culture grown on coverslip

Using method described in section 4.7.1, the levitated carbon particle population was extracted from the AC trap by applying a 4000 V DC potential to the bottom electrode. The culture was transferred to a sterile tissue culture dish (35 mm × 10 mm) and centrifuged at 1000 revolutions per minute (rpm) for 1 min. Following the centrifugation, the cell culture was incubated at 100 % humidity, 37 °C and 5 % CO_2 for 30 min. Following the incubation time, the cell culture was observed to be not viable and particles were not able to located.

4.7.7.2 Cell culture grown on a tissue culture dish

A cell culture was grown on a tissue culture dish. With a population of carbon particles levitated in the AC trap, ~80% of the 100 μL of the growth medium bathing a cell culture was removed by aspiration. The cell culture was then placed on the top of the bottom electrode of the AC trap. The levitated particle population was extracted from the

AC trap by applying a 4000 V DC potential to the bottom electrode. Following delivery of the particles, the cell culture was centrifuged at 1000 rpm for 1 min. Following the centrifugation, 100 μL of SFM was added onto the cell culture and incubated at 100 % humidity, 37 °C and 5 % CO_2 for 18 h. Following the incubation time, the cell culture was observed to be viable and particles (> 80%) were observed to not move when viewed using the camera on the microscope.

The speed of centrifugation was also performed at 1100, 1200, 1300, 1500 and 2000 rpm for 1 and 2 minute periods. At these higher centrifugation speeds and longer times, the cell culture was observed to be viable, and though the particles were in contact with cells and observed to not move, the particles had left "trench-like" tracks across the cell culture.

Another issue when using a tissue culture dish (60 mm × 15 mm) as the support, was the difficulty in locating the particles following the centrifugation due to the large area of the dish and therefore it required considerable time to locate the positions of the particles. This had an additional negative effect of leaving the cell culture out at room temperature too long and hence cell culture viability was a concern.

4.7.7.3 Cell culture grown on a center-well organ culture dish

A cell culture was grown on a center-well organ culture dish. With a population of carbon particles levitated in the AC trap, 3 mL of distilled deionized water was added into the moat of the dish. The growth medium bathing the cell culture was aspirated using a 1000 μL pipette as follows. The dish was tilted at ~45° followed by aspiration of ~500 μL of the growth medium. This step was repeated by tilting the culture dish in the opposite direction until no more growth medium was pooled and able to be aspirated. The

reason for using this method to aspirate the growth medium was to distribute the remaining growth medium in the center-well where the cells were. With the growth medium was aspirated as described, 50 μL of fresh aliquot of SFM was added into the cell culture. The cell culture was then placed on the top of the bottom electrode of the AC trap. The levitated particle population was extracted from the AC trap by applying 4000 V potential to the bottom electrode. Following delivery of the particles, the cell culture was centrifuged at 1000 rpm for 1 min and incubated at 100 % humidity, 37 $^{\circ}$C and 5 % CO_2 for 18 h. After the incubation period, the cell culture was found to be viable, and 52±7% particles were observed to adhere when viewed using the camera on the microscope.

In a subsequent experiment, following the 24 h incubation of the cell culture with LPS containing carbon particles (65 pg of LPS per particle), the culture was found to be viable, and 92±3% particles were observed to adhere when viewed using the camera on the microscope.

4.8 Summary

Delivery of $PM_{2.5}$ particles onto cell cultures using the Haddrell PM_{10} methodology was observed to be not suitable for depositing 2.4 μm particles. Growing the cell culture on a center well organ culture dish and centrifugation of the delivered particles, was found to be the one procedure out of all outlined where the cell culture remained viable following an 18 h incubation period, and > 50 % particle adherence (Carbon particles). Additionally, particles compositions is also the factor for particle adheranence.

CHAPTER 5
INCUBATION OF 2.4±0.1 μM LIPOPOLYSACCHARIDE PARTICLES CONTAINING CARBON WITH HUMAN LUNG CELLS (A549) AND MEASUREMENT OF SELECTED CYTOKINE EXPRESSION

5.1 Introduction

The lung is constantly exposed through inhalation to ambient particles and potentials pathogens. To cope with this pressure, the lung has evolved a sophisticated defence mechanism designed to clear offending agents while inducing a minimum amount of concomitant inflammation. At first, mechanical defences constituted by the "mucociliary escalator" in the upper respiratory tract participate in the removal of solid material from the tracheobronchial tree.[1] Augmenting this path of removal are resident and recruited phagocytes in the lower respiratory tract and alveoli ingest particulate matter and pathogens that circumvent the first line of defence. Pulmonary epithelial cells maintain integrity by modulating local immune responses. These cells respond to a range of stimuli by producing pro-inflammatory mediators, that influence airway inflammation.[13-15,87]

Lipopolysaccharide (LPS) is a soluble component of endotoxin, found on the outer cell wall of gram-negative bacteria.[88] LPS is present in many different air borne

particle types, such as tobacco smoke, windblown mineral dust, and a variety of occupational and residential indoor dusts. *In vivo* and *in vitro* exposure to LPS has been measured to result in the upregulation of pro-inflammatory mediators such as interleukin (IL)-8, tumor necrosis factor (TNF)-α, interferon (IFN)-γ, granulocyte colony-stimulating factor (G-CSF) and intercellular adhesion molecule (ICAM)-1.[53,89] A number of studies have correlated the presence of elevated levels of these pro-inflammatory mediators in the blood and in tissues with the pathogenesis of the majority of the adverse effects on human health that result from particulate air pollution.

Haddrell *et al*., measured differential expression of ICAM-1 from previous studies as a result from dosing an A549 cell culture with up to 150 particles of known size and composition.[36,54,90] Herein, we describe a levitation apparatus and a methodology to generate particles of known size whose composition is of relevance in the troposphere and then deliver those particles directly onto cells *in vitro*. The particles used in this study were comprised of elemental carbon plus LPS. LPS is used in this experiment because studies have found significant concentrations of endotoxin in ambient PM, with daytime average concentration as high as 100 endotoxin units (EU)/mg ambient particles.[91-93] Furthermore, many investigators have suggested that endotoxins play a substantial role in determining the overall toxicity of PM.[94-96] ICAM-1 is a product of the major pro-inflammatory pathway nuclear factor (NF)-κB's activation and as a result the measurement of the ICAM-1 protein has yielded valuable data with regards to the association of the chemical composition of particulate matter (PM) with its overall toxicity. [36,54,90] Following an incubation period, differential expression of multiple

biomolecules and the differential expression of ICAM-1 from cells at different locations across the cell culture were measured.

5.2 Experimental

5.2.1 Chemicals

Lippopolysaccharide from E. Coli (Serotype 0.111:B4, L-2630) (LPS), tumor necrosis factor alpha (T6674-10UG) (TNFα), minimum essential medium (MEM), fetal bovine serum (FBS), trifluoroacetic acid (TFA), sinapic acid (SA), acetonitrile (ACN), trypan blue were purchased from Sigma-Aldrich Inc. 20 nm diameter fluospheres was purchased from Molecular Probes, Invitrogen Inc., Burlington, ON, Canada. These fluospheres are polystyrene-based spheres (density = 1.05 g/ml) that encapsulated ~180 fluorescein molecules per fluosphere. India ink (Speedball, product #3338, Statesville, NC, USA) was used as the source for elemental carbon (C_s). L-glutamine, MEM Vitamin, and fetal bovine serum (FBS) were purchased from Invitrogen Corporation, Burlington, Ontario, Canada. Primary antibody, mouse anti human ICAM-1 monoclonal antibody was purchase from Immunotech, Marseille, France. Scondary antibody, fluorescently labelled goat anti-mouse IgG (Alexa Fluor 546) was purchased from Molecular probes, Eugene, OR, USA.

5.2.2 Starting solutions

Starting solution containing 1.5 mg/mL of india ink with either 0, 0.02 mg/mL, or 0.2 mg/mL of LPS, and 1.3×10^{-6} g/mL of fluospheres in distilled deionized water were prepared. From these solutions, carbon particles with 2.4 ± 0.1 μm in diameter containing 0, 6.5, or 65 pg of LPS, plus fluospheres were created using the apparatus described below.

5.2.3 Droplet dispensing and levitation for particle formation

Droplets were dispensed and levitated using methodology described in section 4.4.

5.2.4 Cell culture

The alveolar type II epithelial cell line A549 (American Type Culture Collection (Manassas, VA, USA) was grown to ~95% confluence on a center-well organ culture dish (BD Falcon, 353653). The cell cultures were grown in minimum essential medium (MEM) supplemented with 10 % heat-inactivated fetal bovine serum (FBS) under 5 % CO_2 at 37 $^{\circ}$C.

5.2.5 Negative control

3 mL of autoclaved distilled deionized water was added into the moat of a center-well organ culture dish. The growth medium bathing the cell culture was removed, and 50 μL of fresh serum free growth medium was added to the cell culture. The cell culture was then placed on the bottom electrode for 5 s, and the dish was removed and then centrifuged at 1,200 relative centrifugal forces (rcf) for 1 min. The cell culture was then placed in an incubation oven for 22 hrs whose internal conditions were maintained at 100 % humidity, 37 $^{\circ}$C and 5 % CO_2.

5.2.6 Positive control

3 mL of autoclaved distilled deionized water was added into the moat of a center-well organ culture dish and the growth medium bathing the cell culture was removed. Following the removal of the growth medium from the culture in the center well as described previously, 10 μL of a solution having 10 mg/mL of TNF-α in water was diluted into 200 μL of serum free medium, and then the resulting solution added to the

cell culture. The dish supporting the cell culture was placed in an incubation oven for 22 hrs whose internal conditions were maintained at 100 % humidity, 37 $^{\circ}$C and 5 % CO_2.

5.2.7 Particle delivery onto lung cells in vitro

With a population of particles levitated in the AC trap, the growth medium bathing the cell culture was removed using a hand-held pipette as described previously. 50 μL of fresh serum free growth medium was then delivered onto the cells in the center-well. The dish supporting the culture was then placed on the bottom electrode of the AC trap. The levitated particle population was extracted from the AC trap by applying a 4,000 V potential to the bottom electrode. Immediately following particle deposition, the culture was centrifuged at 1,200 rcf (relative centrifuge force) for 1 min and incubated for 22 hrs at 100 % humidity, 37 $^{\circ}$C and 5 % CO_2.

5.2.8 Supernatant collection

Following a 22 hrs incubation period for the culture, 200 μL of serum free growth medium was added onto the center well, and the culture incubated for an additional 2 h (in order for the fresh serum free medium to equilibrate with the supernatant) bringing the total incubation period to 24 h. Following the 24 hrs incubation period, 50 μL of supernatant was collected and a fresh 50 μL aliquot of serum free medium (SFM) was added into the center well in order to maintain the volume of the medium bathing the cell culture constant.

The biomoleucles in the supernatant were prepared for MALDI-MS as follows. A 10 μL aliquot of the supernatant was diluted and conditioned by adding 2.0 μL of 2.5 % trifluoroacetic acid (TFA) in order to acidify the aliquot, and then 50 μL of 0.1 % TFA was added to dilute the aliquot of supernatant.

5.2.9 MALDI-TOF-MS preparation and analysis of the supernatant

A matrix solution was prepared by dissolving 5.0 mg of Sinapic Acid (SA) in 100 µL of acetonitrile (ACN) and 100 µL of 0.1 % TFA. A 4 µL aliquot of matrix solution was spotted onto a well of the MALDI plate and air dried.

A C_{18} ZipTip (Millipore) was conditioned by wetting the ZipTip C_{18} bed with two washings of 10 µL reagent grade acetonitrile (ACN) followed by two washings of 10 µL of 0.1 % TFA. ~10 µL of the conditioned supernatant solution was aspirated into a C_{18} ZipTip (Millipore) and dispensed back into the vial holding the supernatant. This was repeated 10 times. The ZipTip was then washed with two 10 µL aliquots of 0.1 % TFA. Biomolecules retained in the ZipTip were then eluted and spotted onto the same well of the MALDI-plate to which the matrix had been delivered and air dried using a 4.0 µL of solution containing an equal volume of ACN and 0.1 % TFA.

The supernatant was also collected using the method described following the 48 h and 72 h incubation time points.

Mass spectrometric analysis was performed using MALDI-TOF-MS (Waters Corporation, Milford, MA, USA) equipped with a nitrogen UV laser (337 nm, pulse width 2 ns) and 1.2 m flight path in the linear mode, and controlled by MassLynx software (version 3.5, Waters Technologies Inc). The standard operation conditions for biomolecule detection includes an accelerating voltage of 15 kV and the ion extraction pulse voltage of 2450 V. All data were acquired using a positive ion linear mode. The mass spectra were acquired in the mass range from 3 to 13 kDa.

5.2.10 Antibody Assay

Following the incubation period and collection of the supernatant, the cells were fixed using a solution of paraformaldehyde at pH 7.4 for 20 min. The primary antibody

was mouse anti-human ICAM-1 monoclonal antibody (Immunotech, Marseille, France) and secondary antibody was labeled goat anti-mouse IgG (Alexa Fluor 546, Molecular Probes, Eugene, OR, USA)

5.3 Results

Droplets of initial volume 326 ± 194 nL were dispensed from a starting solution that contained 1.5 mg/mL of India ink by volume, 0.2 mg/mL of LPS, and 1.3 x 10^{-3} mg/mL of fluospheres. A population of particles, each particle containing 76.7 pg of carbon, 65 pg of LPS per particle, and 4.23 x 10^{-4} pg of fluospheres, was generated and deposited onto cell cultures grown on center-well organ culture dish. Representative images of $[C_s$+ 65 pg of LPS$]_p$ particles deposited on different cell cultures and monitored following 0 h, 24 h, 48 h, and 72 h incubation periods are presented in figure 5.1. The top images (figure 5.1a-d) and the bottom images (figure 5.1a'-d') are images captured using bright field and fluorescence microscope respectively. The appearance of the particles, most readily observed from the fluorescence images, were observed to change over the incubation periods (figure 5.1a'-d'). The region from which emission from the fluospheres was observed to become larger as the time of incubation increases. We interpret this to mean that the particles were being broken down, releasing the fluospheres so that they were able to diffuse away from the site at which the particle became adhered to a cell.

Populations of $[C_s$+ 65 pg of LPS$]_p$ particles were deposited onto center well organ dish with no cells and incubated for 72 h in the presence of SFM (figure 5.1e and e'). The region from which emission from the fluosphere was observed to be the same following the incubation period; it was interpreted that the particles were not broken down.

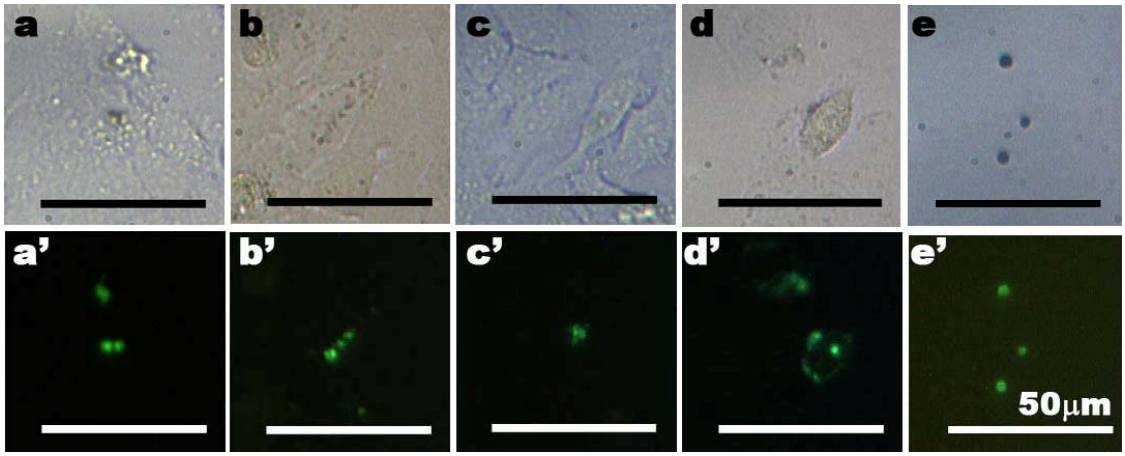

Figure 5.1 $[C_s+ 65 \text{ pg of LPS}]_p$ particles on different cell cultures that were incubated at a) t= 0 h, b) t= 24 h, c) t= 48 h, and d) t= 72 h. e) $[C_s+ 65 \text{ pg of LPS}]_p$ particles on center well dish with no cells and incubated for 72 h. Top images are viewed using bright field microscope and bottom images are viewed using fluorescence microscope. The scale bars of each image are equivalent.

Secreted biomolecules were harvested from the supernatant following a 72 h incubation period and analyzed using MALDI-TOF-MS. It was observed from the spectra (figure 5.2), that the peak at m/z = 8,300 Da was present in the supernatant of the positive control as well as in the supernatant of the cell culture dosed with a population of particles (x= 168, $[C_s+65 \text{ pg of LPS}]_p$) where x is number of particles deposited. This indicates that this biomolecule is being up-regulated in response to exposure to TNF-α, and a population of 168 $[C_s+65 \text{ pg of LPS}]_p$.

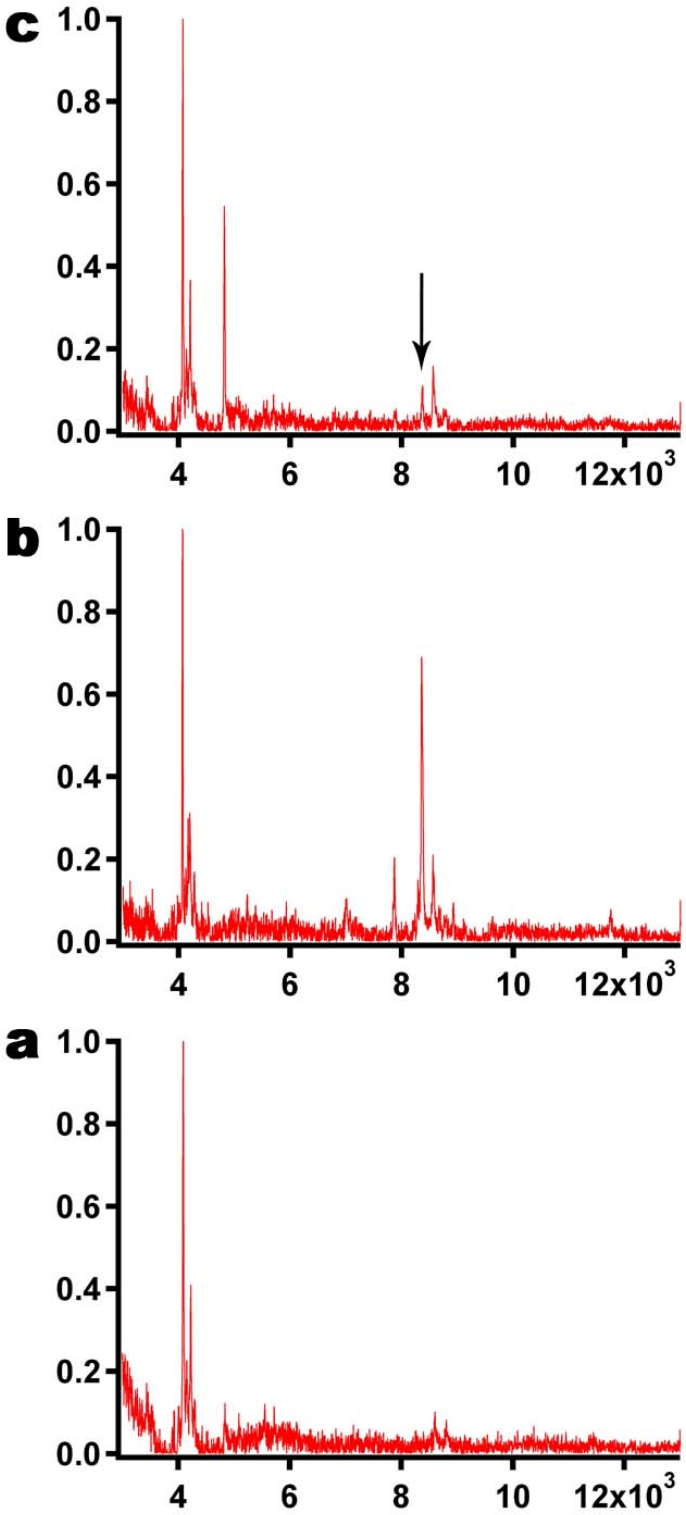

Figure 5.2 Representative spectra from the supernatant of cell cultures using MALDI-MS (a) negative controls, (b) TNFα (positive controls), and (c) a population of 168 particles of $[C_s$+ 65 pg of LPS$]_p$. Arrow indicates ion signal at m/z= 8.3 kDa.

Fluorescence emission images indicating ICAM-1 upregulation on the cell culture surface resulting from the deposition of $[C_s+65 \text{ pg of LPS}]_p$ is shown in figure 5.3. It was observed that ICAM-1 expression was being upregulated across the entire cell culture (figure 5.3c). Additionally, at the site of deposition, ICAM-1 upregulation was more commonly observed one or two cells away from the cell that was in contact with the particle, than was observed from the cells in direct contact with a particle.

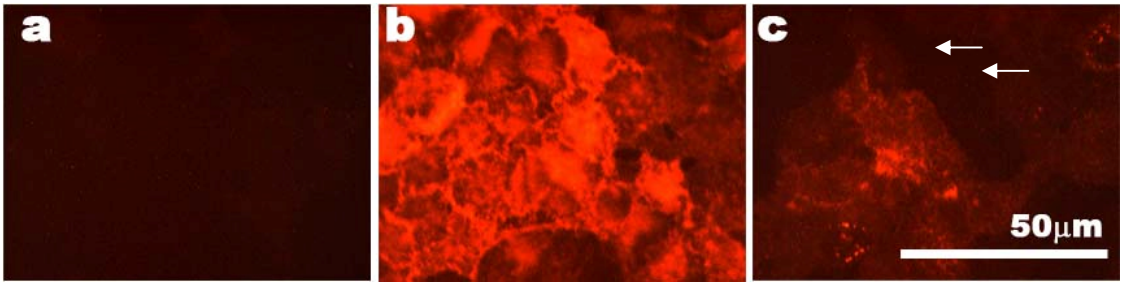

Figure 5.3 Differential ICAM-1 expression following a 72 h incubation period. a) Negative control, b) positive control, c) a population of LPS containing carbon particles (65 pg of LPS per particle). Arrows indicate the position where the particles deposited and adhered.

The differential expression of ICAM-1 was determined based on the signal intensity of fluorescence emission. Differential ICAM-1 expression was calculated based on the fluorescence emission signal intensity at each pixel in each scan of a cell culture using Image J software (Research Services branch, National Institute of Health, Bethesda, MD, USA) and the numerical values of the pixel signals were summed using Microsoft Excel. The summed ICAM-1 expression is reported as a percent of total signal intensity relative to A549 cell cultures treated with TNF-α as the positive control.

Data plotted in figure 5.4 are the fluorescence intensity of ICAM-1 as a function of number of particles deposited on cell cultures and were incubated for 24 h, 48, and 72 h. From emission data plotted in figure 5.4 it was observed that there are two distinct regions of the data that can each be fitted with a linear least square fit. Therefore, particle dose response (ICAM-1) relationship was calculated as the slope of a linear least square fit for cell cultures dosed with < 50 particles, and also for > 50 particles (table 5.1). Observed in figure 5.4, the fluorescence intensity of ICAM-1 is depend on the number of deposited particles for the cell culture dosed with < 50 particles where the fluorescence intensity of the cell culture dosed with > 50 particles is independent on the number of deposited particles. This suggests that when the cell culture is dosed with > 50 particles, the cells reach its maximum upregulation of ICAM-1, which is an interpretation of the fluorescence intensity indicative of ICAM-1 expression remaining at a constant level (eg. plateauing, or levelling off).

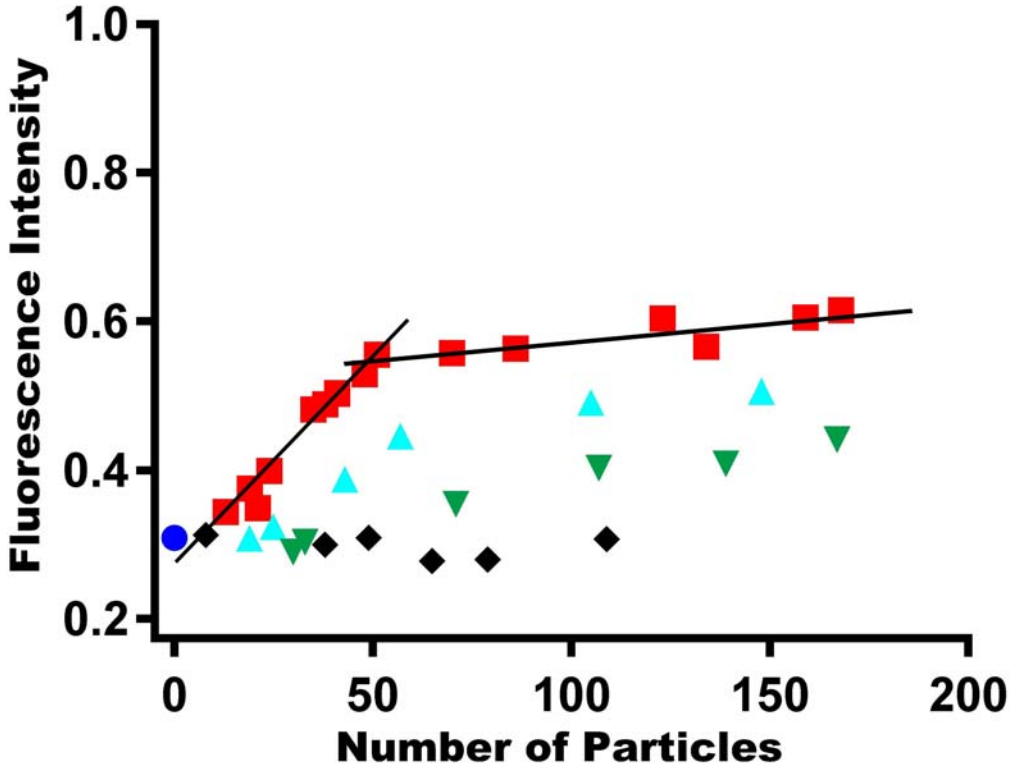

Figure 5.4 Differential expression of ICAM-1 as a function of particle dosage, $[C_s$+ 65 pg of LPS$]_p$, measured at different incubation periods. (•) Negative control, (■) t= 72 h, (▲) t= 48 h, and (▼) t= 24 h.

Table 5.1 ICAM-1 Dose response relationship of the cell cultures dosed with 65 pg LPS containing carbon and were incubated for 24 h, 48 h, and 72 h.

Incubation Period (h)	Slope of a least squares linear fit for < 50 particles (fluorescence per number of particles deposited)	Slope of a least squares linear fit for > 50 particles (fluorescence per number of particles deposited)
24	4.4×10^{-3}	5.0×10^{-4}
48	3.4×10^{-3}	7.0×10^{-4}
72	5.9×10^{-3}	8.0×10^{-4}

Fluorescence intensity of ICAM-1 as a function of number of particles for the cell cultures dosed with 6.5 or 65 pg of LPS particle containing carbon is plotted in figure 5.5. The linear least square fits were evaluated for cell cultures dosed with < 50 particles, and for > 50 particles (table 5.2).

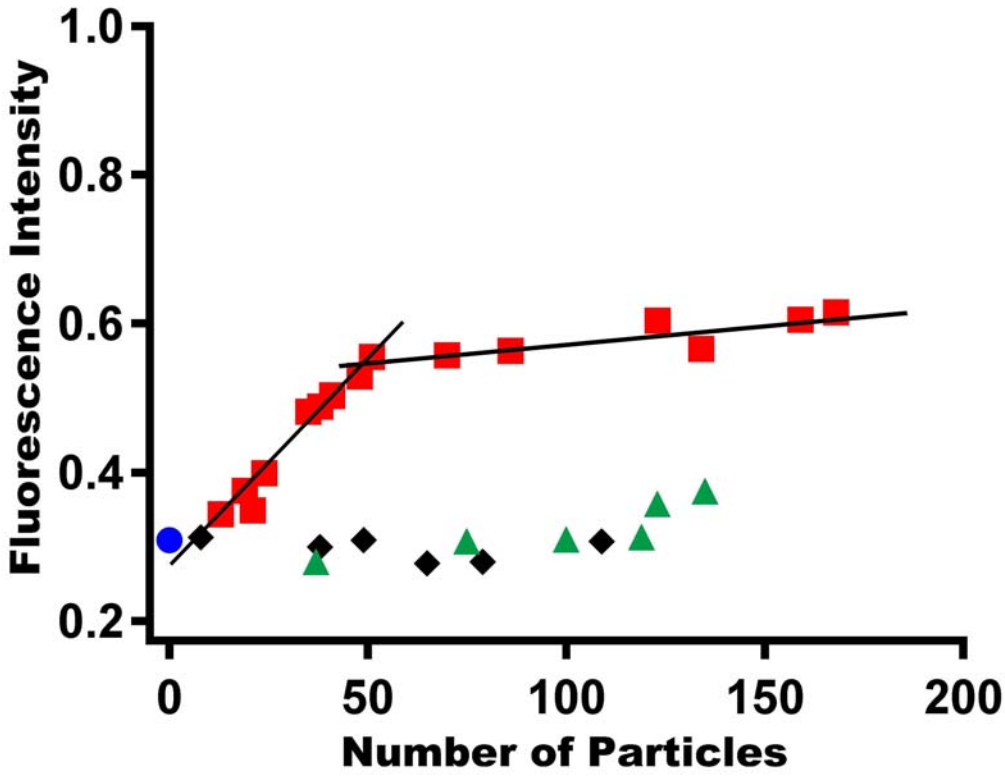

Figure 5.5 Differential expression of ICAM-1 as a function of particle dosage. Cell cultures incubated for 72 h. (●) negative control, (◆) carbon particles, (■) $[C_s$+65 pg of LPS$]_p$ containing carbon particles, (▲) $[C_s$+6.5 pg of LPS$]_p$

Table 5.2 Particle dose ICAM-1 response relationship of the cell cultures dosed with 6.5 pg or 65 pg LPS containing carbon and were incubated for 72 h.

	Mass (pg)	Slope of a least squares linear fit for 50 particles (fluorescence per number of particles deposited)	Slope of a least squares linear fit for > 50 particles (fluorescence per number of particles deposited)
LPS	6.5	7.0×10^{-4}	1.9×10^{-3}
	65	5.9×10^{-3}	8.0×10^{-4}
C_s	76	2.0×10^{-4}	7.0×10^{-4}

5.4 Discussion

Droplets of initial volume 326 ± 194 pL were dispensed from the starting solution that contained 1.5 mg/mL of India ink, 0.2 mg/mL of LPS, and 1.3×10^{-3} mg/mL of fluospheres. As described, these droplets evaporated to form a population of particles each containing 76.7 pg of C_s, 65 pg of LPS, and 4.23 x 10^{-4} pg of fluospheres. Populations of these particles were deposited onto center well culture dish with no cells and also onto cell cultures grown on center well organ culture dishes and incubated for 24 h, 48 h, and 72 h.

The fluorescence emission of fluosphere from these particles (figure 5.1) shows that particles that were deposited onto a center well culture dish with no cells (figure 5.1e') were observed to not change following a 72 h incubation period. The fluorescence emission of fluosphere from particles that were deposited onto cell culture grown on a center well culture dishes (figure 5.1a' to d') were observed to change ,with the area of the fluorescence emission of fluospheres from these particles observed to become larger as the incubation period increased. From experiments described in section (4.7.7.3), the area of the fluorescence emission from the carbon particle was observed to not change.

From these observations, the 65 pg of LPS containing carbon particles on a cell cultures were interpreted to break down, but the Carbon particles did not. As the consequence of the diffusion of fluospheres away from the site of LPS containing carbon particle deposition, there was the potential for more LPS, had it been contained within the particle, to be released and interact with other cells.

Cell cultures dosed with 65 pg of LPS containing carbon particles ($[C_s$ + 65 pg of LPS$]_p$) were found to cause ICAM-1 expression (figure 5.3). From emission data plotted in figure 5.4, there are two distinct regions of the data that can each be fitted with a linear least square fit for cell cultures incubated for 48 and 72 h whereas cell cultures incubated for 24 h is not. These regions shows that the expression of ICAM-1 was upregulated when the cell cultures dosed with < 50 particles in a dose-dependent manner at low particle doses, but those cells cease to respond in a dose-dependent manner when dosed with > 50 particles, because the data plotted suggest that the ICAM-1 expression reached a maximum.

In addition to different incubation periods, the ICAM-1 expression of the cell cultures dosed with 6.5 pg of LPS containing carbon particles ($[C_s$ + 65 pg of LPS$]_p$) is plotted in figure 5.5. The emission data (figure 5.5) shows that there is not two distinct regions of the data that can each be fitted with a linear least square however, when the cell culture dosed with 120 of 6.5 pg of LPS containing carbon particles, there was an observable expression of ICAM-1. For the purpose of treating this data set similarly to that plotted in Figure 5.4, the slope of the dose-response linear least squares fit for <50 particles deposited, was less than the slope of dose-response linear least squares fit for >50 particles deposited (table 5.2). This suggests that the dose of 120 particles comprised

of 6.5 pg LPS + carbon was possibly just beginning to cause a response that could be differentiated form the negative control (cell culture dosed with C_s only).

Following a 72 h incubation period the supernatant from the cell culture was analyzed using MALDI-TOF-MS. Differential expression of one biomolecule was observed relative to the negative control (figure 5.2). A biomolecule detected at m/z= 8.3 kDa, was observed to be up regulated from the supernatants of positive controls and the cell cultures dosed with $[C_s + 65 \text{ pg of LPS}]_p$.

5.5 Summary

Deposition of 65 pg of LPS particles containing carbon onto the cell cultures was interpreted to be broken down following incubation periods ranging from 24 to 72 hours, causing differential expression of ICAM-1. When the incubation period of the cell culture increases, the fluorescence intensity of ICAM-1 of cell cultures dosed with 65 pg of LPS containing carbon increases, but there was a change in the ICAM-1 upregulation at the 72 incubation period for cell cultures dosed with <50 particles or >50 particles. For doses >50 particles, the data indicated that the ICAM-1 upregulation has reached a maximum. When the cell culture was incubated for 72 with 6.5 pg of LPS particles containing carbon, the fluorescence intensiy of ICAM-1 was not slightly upregulated. Using MALDI-TOF-MS, one biomolecule, detected at m/z= 8.3 kDa, was observed to be upregulated when the cell culture dosed with 65 pg LPS containing carbon particles.

CHAPTER 6
INCUBATION OF 2.4±0.1 μM OF METAL SALT CONTAINING CARBON PARTICLES WITH HUMAN LUNG CELLS (A549) AND MEASUREMENT OF SELECTED CYTOKINE EXPRESSION

6.1 Introduction

The adverse effects of ambient PM on human health have been a concern for decades, but only in the past 15 years have epidemiology studies demonstrated linkages between PM_{10} and cardiovascular disease.[97] Example classes of compounds known to be present on ambient particulate matter (PM) are metals, salts, carbonaceous materials, volatile organic compounds (VOC), polycyclic aromatic hydrocarbons (PAH), and endotoxins and other biological compounds. The role that each component of PM_{10} plays in this linkage is being investigated in laboratories worldwide using different methods.

In locations with metallurgic industries such as Utah Valley, metals are detected in the ambient PM. One study demonstrated that during a closure of a steel mill, the rates of hospital visits decreased for patient exhibiting increased morbidity.[98,99] Experimental determination of metal content in PM filter extracts sampled in the Utah Valley track the epidemiological findings. For instance, *in vivo* instillation studies and *in vitro* studies have shown that PM collected while the steel mill was open induced pulmonary injury

and inflammation, whereas PM sampled during the period of closure did not induce pulmonary injury or inflammation.[98]

Many toxicological studies have been conducted on PM toxicity using complex mixtures of ambient particles sampled from the troposphere, including a chemically well characterized sample of ambient particles collected from an Ottawa building's air intake filters, referred as Environmental Health Centre-93 (EHC-93). EHC-93 is an example of a heterogeneous population of ambient particles being used in toxicology studies in which the whole particle, and its soluble and insoluble fractions have been characterized (table 6.1).[67,100,101] EHC-93 is comprised of metals, inorganic compounds[67,102] and organic compounds. 99 % of EHC-93 particles are <3 μm in diameter.[49]

Table 6.1 The concentration of compounds that have been characterized in EHC-93.

Metals			
Metal	Concentration (μg/g)	Metal	Concentration (μg/g)
Aluminum	$9.8x10^3$	Manganese	483
Ammonium	104	Nickel	69.6
Arsenic	-	Sodium	$20.6x10^3$
Barium	295	Strontium	272
Boron	81.2	Tin	$1.2x10^3$
Cadmium	7.3	Titanium	929
Calcium	$109x10^3$	Vanadium	90.4
Chromium	42.3	Zinc	$10.4x10^3$
Cobalt	5.9	Lead	$6.7x10^3$
Copper	845	Magnesium	$7.2x10^3$
Iron	$14.9x10^3$	Molybdenum	4.6
Non-metals			
Non-metal	Concentration (μg/g)	Mon-metal	Concentration (μg/g)
Nitrate	1.93	Sulphate	15.6
Chloride	8.72		
Polycyclic aromatic hydrocarbons (PAH)			
PAH	Concentration (μg/g)	PAH	Concentration (μg/g)
Dibenz(a,c&a,h)anthracene	-	Chrysene	1.66
Anthracene	0.54	Perylene	0.28
Benzo (a) anthracene	1.10	Prylene	2.11
Benzo (b) fluoranthracene	2.78	Benzo (e) pyrene	1.09
Benzo (k) fluoranthracene	Not detectable	Fluoranthene	2.47
Benzo (a&b) fluorene	0.23	Phenanthrene	1.83
Benzo (ghi) perylene	1.52	Benzo (a) pyrene	0.95
Indeno(1,2,3-cd) pyrene	1.19	Acenaphthene	0.20

In toxicological studies that involved EHC-93 introduction to cell cultures, the mass of particulate matter introduced to a culture was known, but not known was the actual size, number, and composition of particles delivered to the culture.[100] In these studies, the particulate matter had been dispersed in solution, often with the assistance of ultrasonication, and then an aliquot introduced to a cell culture. Consequently, the number of particles interacting with any given cell was not known. Because the chemical composition of each individual particle in EHC-93 is not characterized, it is difficult to

extrapolate from those studies what individual particle compositions are most significant with respect to their role in causing tissue inflammation. For instance, metals in PM have been hypothesized to cause lung injury, because studies have shown that, the soluble metal component of ambient PM may be responsible for the pulmonary injury.[65,67,69] Moreover, Zinc, for example, is a commonly measured metal in PM_{10} samples, notably near industrial sources or roadways, and zinc in the water soluble fraction of PM_{10} samples have been postulated to be a causative agent in PM induced injury. [65,69] However, another investigation has shown that the insoluble fraction of EHC-93 also has the ability to cause response from lung cells.

Hence, to improve knowledge of which component of ambient PM induced toxicity, we have employed an apparatus that enables creation of ambient PM mimics and then those mimics are directly onto human lung cells, *in vitro*. In this study, 0 to 200 particulate matter mimics were deposited onto center-well culture dishes in which A549 cells had been cultured, and the differential expression of biomolecules was monitored using MALDI-TOF-MS and immunocytochemistry (ICAM-1) in response to their exposure to different ambient PM mimics. The particles used in this study contained black carbon (from india ink) and/or polyethylene glycol (PEG) plus varied quantities of zinc nitrate [$Zn(NO_3)_2 \cdot 6H_2O$], sodium chloride [NaCl], ammonium nitrate [NH_4NO_3], nickel nitrate [$Ni(NO_3)_2 \cdot 6H_2O$], and in one series of experiments, EDTA. The cations of these metal salts used are known to be present in EHC-93. The purpose of adding EDTA to a starting solution was to complex zinc in these solutions (and in the carbon particles) because the pH was neutral. The rationale for incorporation of PEG, which is not expected to be present in PM_{10}, into some of the particle mimics will be described.

6.2 Experimental

6.2.1 Chemicals

Zinc nitrate [$Zn(NO_3)_2 \cdot 6H_2O$], sodium chloride [NaCl], ammonium nitrate [NH_4NO_3], nickel nitrate [$Ni(NO_3)_2 \cdot 6H_2O$], polyethyleneglycol (PEG, mw= 2,000 g/mol), tumor necrosis factor alpha (T6674-10UG) (TNFα), minimum essential medium (MEM), fetal bovine serum (FBS), trifluoroacetic acid (TFA), sinapic acid (SA), acetonitrile (ACN), trypan blue were purchased from Sigma-Aldrich Inc. 20 nm diameter fluospheres was purchased from Molecular Probes, Invitrogen Inc., Burlington, ON, Canada. These fluospheres are polystyrene-based spheres (density= 1.05 g/ml) that encapsulated ~180 fluorescein molecules per fluosphere. India ink (Speedball, product #3338, Statesville, NC, USA) was used as the source for elemental carbon (C_s). L-glutamine, MEM vitamin, and fetal bovine serum (FBS) were purchased from Invitrogen Corporation, Burlington, Ontario, Canada. Primary antibody, mouse anti human ICAM-1 monoclonal antibody was purchase from Immunotech, Marseille, France. The secondary antibody, fluorescently labelled goat anti-mouse IgG (Alexa Fluor 546), was purchased from Molecular probes, Eugene, OR, USA.

6.2.2 Starting solutions

Stock solutions of india ink, PEG, $Zn(NO_3)_2 \cdot 6H_2O$, NaCl, NH_4NO_3, $Ni(NO_3)_2 \cdot 6H_2O$, and EDTA were prepared in distilled deionized water. Numerous starting solutions were prepared, many of which contained 1.5 mg/mL of India ink plus aliquots from single component stock solutions (Table 6.1). All starting solutions contained 1.3×10^{-3} mg/mL of fluospheres. The reason for inclusion of the fluospheres in each of the starting solutions at a constant concentration was thee fluospheres greatly

facilitated visualization of the particles on the A549 cultures when viewed using a fluorescence microscope.

Table 6.2 Initial concentration of the inorganic compounds in the starting solution.

	Particle type	C_s (mM)	PEG (mM)	$Zn(NO_3)_2.6H_2O$ (mM)	NaCl (mM)	NH_4NO_3 (mM)	$Ni(NO_3)_2.6H_2O$ (mM)	EDTA (mM)
a	PEG	0	1.0×10^{-2}					
b	$[C_s+PEG]_p$	1.5	1.0×10^{-2}					
c	$[C_s+Zn+PEG]_p$	1.5	1.0×10^{-2}	5.0×10^{-3}				
d	$[C_s+Zn+PEG]_p$	1.5	1.0×10^{-2}	2.0×10^{-2}				
e	$[C_s+Zn+PEG]_p$	1.5	1.0×10^{-2}	2.0×10^{-1}				
f	$[C_s+Na+PEG]_p$	1.5	1.0×10^{-2}		3.0×10^{-3}			
g	$[C_s+Na+PEG]_p$	1.5	1.0×10^{-2}		3.0×10^{-2}			
h	$[C_s+Na+PEG]_p$	1.5	1.0×10^{-2}		10			
i	$[C_s+NH4+PEG]_p$	1.5	1.0×10^{-2}			1.3×10^{-4}		
j	$[C_s+NH4+PEG]_p$	1.5	1.0×10^{-2}			8.1×10^{-3}		
k	$[C_s+Ni+PEG]_p$	1.5	1.0×10^{-2}				3.7×10^{-5}	
l	$[C_s+Ni+PEG]_p$	1.5	1.0×10^{-2}				3.7×10^{-4}	
m	$[C_s+Zn+PEG]_p$	1.5	0.1	2.0×10^{-2}				
n	$[C_s+PEG+EDTA]_p$	1.5	0.1					2.1×10^{-1}
0	$[Zn+PEG+EDTA]_p$	0	0.1	2.0×10^{-2}				2.1×10^{-1}
p	$[C_s+Zn+PEG+EDTA$	1.5	0.1	2.0×10^{-2}				2.1×10^{-1}

The compounds and their calculated abundance in the particles created using the solutions indicated in Table 6.2 and the apparatus described in section 6.2.3. For the starting solutions identified in Table 6.2 that included Carbon, particles with 2.4 ± 0.1 μm in diameter were prepared, with each particle containing 76.7 pg of C_s and 4.23×10^{-4} pg of fluospheres. The formation coefficient calculation for Zn particle containing EDTA is shown in the appendix.

Table 6.3 Composition of each particle type generated per starting solution

	Particle type	C_s (pg)	PEG (pg)	$Zn(NO_3)_2.6H_2O$ (pg)	NaCl (pg)	NH_4NO_3 (pg)	$Ni(NO_3)_2.6H_2O$ (pg)	EDTA (pg)
a	PEG	0	6.5					
b	$[C_s+PEG]_p$	76.7	6.5					
c	$[C_s+Zn+PEG]_p$	76.7	6.5	1.1×10^{-1}				
d	$[C_s+Zn+PEG]_p$	76.7	6.5	4.3×10^{-1}				
e	$[C_s+Zn+PEG]_p$	76.7	6.5	4.3				
f	$[C_s+Na+PEG]_p$	76.7	6.5		2.2×10^{-2}			
g	$[C_s+Na+PEG]_p$	76.7	6.5		7.7			
h	$[C_s+Na+PEG]_p$	76.7	6.5		77			
i	$[C_s+NH_4+PEG]_p$	76.7	6.5			8.1×10^{-4}		
j	$[C_s+NH_4+PEG]_p$	76.7	6.5			8.1×10^{-3}		
k	$[C_s+Ni+PEG]_p$	76.7	6.5				3.6×10^{-3}	
l	$[C_s+Ni+PEG]_p$	76.7	6.5				3.6×10^{-2}	
m	$[C_s+Zn+PEG]_p$	76.7	65	4.3×10^{-1}				
n	$[C_s+PEG+EDTA]_p$	76.7	65					2.3
0	$[Zn+PEG+EDTA]_p$	0	65	4.3×10^{-1}				2.3
p	$[C_s+Zn+PEG+EDTA_p$	76.7	65	4.3×10^{-1}				2.3

6.2.3 Droplet dispensing and levitation for particle formation

Droplets were dispensed and levitated using methodology described in section 4.4.

6.2.4 Cell culture

The alveolar type II epithelial cell line A549 (American Type Culture Collection (Manassas, VA, USA) was grown on the same support and in the same condition as described in section 5.2.4.

6.2.5 Negative control

The negative control was treated using methodology described in section 5.2.5.

6.2.6 Positive control

The positive control was treated using methodology described in section 5.2.6

6.2.7 Particle delivery onto lung cells in vitro

Particles were delivered onto lung cells using method described in section 5.2.7.

6.2.8 Antibody Assay

Following the incubation period and collection of the supernatant, the cells were fixed and assayed using method described in section 5.2.8.

6.2.9 Fluorescence Microscopy and Image Analysis

A Zeiss Axioplan 2 (North York, Ont., Canada) fitted with an excitation filter (BP-546/12) and emission filter (LP-590) was used to collect all of the fluorescence emission images of the samples fluorescently tagged with antibodies for ICAM-1. For each fluorescently labelled sample, the fluorescence emission was collected from nine different sites, each 1.00 mm X 1.25 mm, from across the cell culture; The signal intensity of fluorescence emission for each sample, indicative of ICAM-1 expression, was determined using Image J software (Research Services Branch, National Institute of Mental Health, Bethesda, MD, USA) and integrated using Excel (Microsoft, Seattle, Washington, USA). The degree of ICAM-1 upregulation was reported as a percentage of the total signal relative to the positive control.

6.2.10 Fluorescein

A stock solution having 15 μM of fluorescein solution was prepared in distilled deionized water. Fluospheres were not added to this starting solution. A series of standard solutions of 1.5×10^{-10} μM, 3.0×10^{-10} μM, 1.5×10^{-9} μM, and 3.0×10^{-9} μM, was prepared from the stock solution.

A starting solution containing 76.7 pg of C_s, 4.3×10^{-1} pg of Zn, 6.5 pg of PEG, and 5.0×10^{-4} pg of fluorescein were loaded onto a droplet dispenser. 200, and 50,

droplets of this starting solution were dispensed into separate 5 mL volumetric flasks and diluted with serum free medium.

Using the same starting solution, droplets were dispensed, levitated, and deposited onto a center-well organ culture dish containing 1 mL of SFM. Following the deposition of the resultant particles, the SFM solution was transferred into a 5 mL volumetric flask and diluted with serum free medium.

The fluorescence intensity of these solutions was measured using a spectrofluorimeter (Photon Technology International, mode: 1258-MP1)). The spectrofluorimeter was operated using an excitation wavelength of 350 nm, and and emission wavelength of 440 nm.

6.3 Results

6.3.1 The effect of metal salts particles on A549 cell culture

Droplets of initial volume 326 ± 194 pL were dispensed from one of the starting solutions listed in table 6.1. The droplets were dispensed into an ac trap, captured and levitated. The resultant population of particles thus produced were deposited onto cell cultures and incubated for 72 h in the presence of SFM.

A representative image of one particle type (76.7 pg of C_s, 4.3×10^{-1} pg of Zn, 6.5 pg of PEG, and 4.23 x 10^{-4} pg of fluospheres per particle, $[C_s+Zn+PEG]_p$) that had deposited onto a cell culture (no cells present) and incubated for 72 h in the presence of SFM is presented in figure 6.1. Figure 6.1a and b are image of the particles aquired using bright field microscope and fluorescence microscope respectively. The shape of the particles in these images that were acquired using a bright field microscope suggested that the particles were round in shape. Based on the images aquired using fluorescence

microscopy, the region from which fluorescence (eg. fluospheres) was observed to be in round shape as well. These results suggested that the particles were not caused to fragment by the deposition step that included their impact into the center well of a center-well tissue culture dish nor the 72 hour incubation period in SFM .

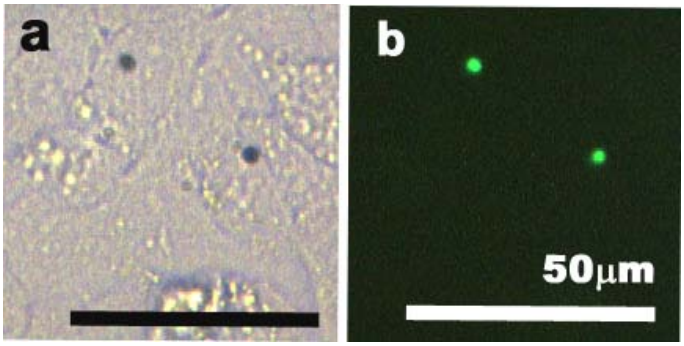

Figure 6.1 Images of particles ([76.7 pg of C_s + 4.3×10^{-1} pg of Zn+ 6.5 pg of PEG]$_p$) on A549 cell culture that had been incubated for 72 h. a) image is acquired using bright field microscope, b) image is acquired using fluorescence microscope.

Representative fluorescence emission images indicating ICAM-1 upregulation on the cell culture surface are shown in figure 6.2. In figure 6.2c, ICAM-1 upregulation of a cell culture dosed with particles (76.7 pg of C_s, 4.3×10^{-1} pg of Zn, 6.5 pg of PEG, and 4.23×10^{-4} pg of fluospheres per particle, [C_s+Zn+PEG]$_p$) was observed from isolated cells distributed across the entire cell culture. This expression pattern has been observed repeatedly over experiments spanning several months. In addition, at the site of deposition, the brightest fluorescence emission signals, indicative of ICAM-1 expression, was typically observed one or two cells away from the site of particle adherence. The fluosphere emission image was separately acquired (emission in green), and overlaid with the ICAM-1 emission using image processing software. The appearance of the green

emission signal suggests that these particles did not get broken down by the cells during the incubation period.

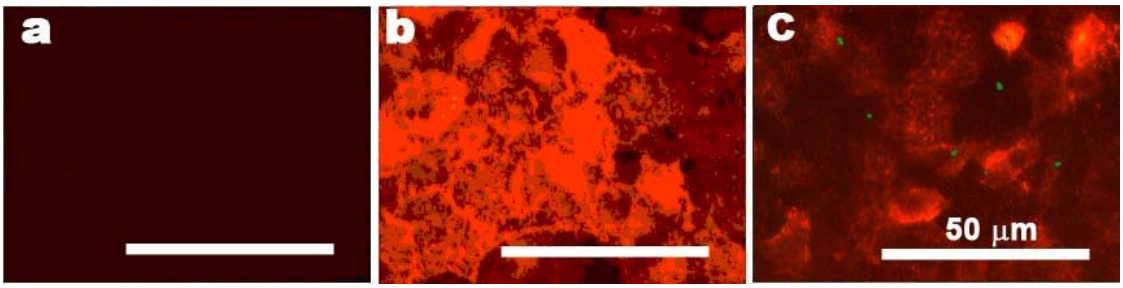

Figure 6.2 Representative fluorescence emission of fluorescently labeled antibodies bound ICAM-1 from A549 cell culture following the deposition of a) negative control, b) positive control, c) ([76.7 pg of C_s + 4.3×10^{-1} pg of Zn+ 6.5 pg of PEG]$_p$). Green dots are from an overlay of the fluorescence emission from fluospheres, and this signal indicates the position of particles that in this experiment.

The differential expression of ICAM-1 was determined based on the signal intensity of fluorescence emission versus number of particle deposited per population. Data plotted in figure 6.3 are the fluorescence intensity of ICAM-1 as a function of number of particles deposited on cell cultures that had been incubated from 72 h.The relative ICAM-1 expression was determined by deviding the slopes by the number of mole of the metal salts (Table

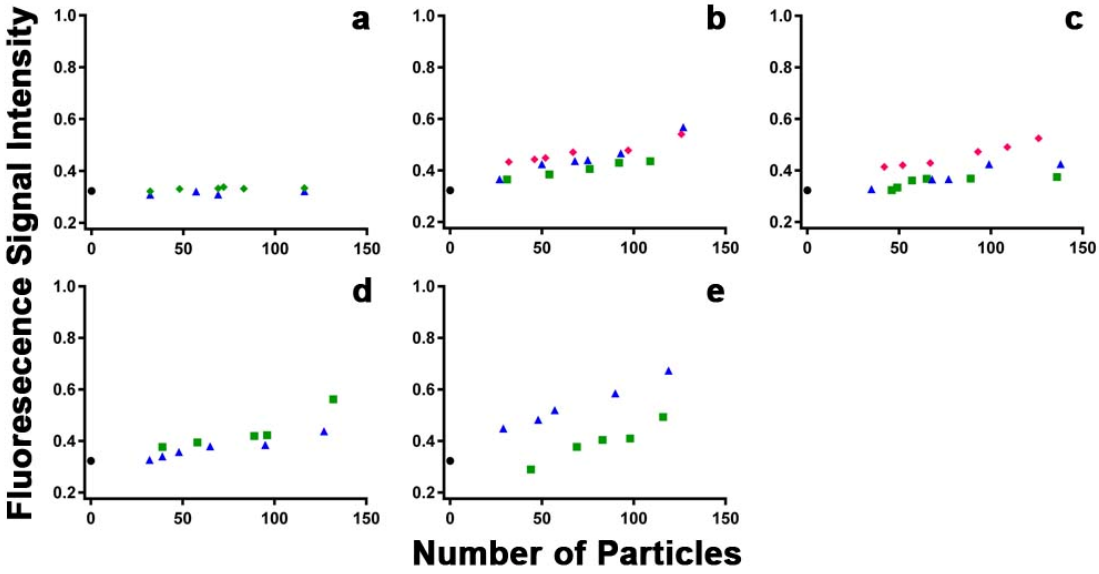

Figure 6.3 Differential expression of ICAM-1 as a function of particle dosage following a 72 h incubation period. (●) negative control, **a)** (▲) [76.7 pg of C_s + 6.5 pg of PEG]$_p$, (◆) [6.5 pg of PEG]$_p$. **b)** (■) [76.7 pg of C_s + 1.1×10^{-1} pg of Zn + 6.5 pg of PEG]$_p$, (▲)[76.7 pg of C_s + 4.3×10^{-1} pg of Zn + 6.5 pg of PEG]$_p$ (◆)[76.7 pg of C_s + 4.3 pg of Zn + 6.5 pg of PEG]$_p$, **c)** (■) [76.7 pg of C_s + 2.2×10^{-2} pg of Na + 6.5 pg of PEG]$_p$, (▲)[76.7 pg of C_s + 7.7 pg of Na + 6.5 pg of PEG]$_p$, (◆)[76.7 pg of C_s + 77 pg of Na + 6.5 pg of PEG]$_p$ **d)** (■)[76.7 pg of C_s + 8.1×10^{-4} pg of NH_4 + 6.5 pg of PEG]$_p$, (■)[76.7 pg of C_s + 8.1×10^{3} pg of NH_4 + 6.5 pg of PEG]$_p$. **e)** (■)[76.7 pg of C_s + 3.6×10^{-3} pg of Ni + 6.5 pg of PEG]$_p$, (▲)[76.7 pg of C_s + 3.6×10^{-2} pg of Ni + 6.5 pg of PEG]$_p$.

Table 6.4 Relative signal intensity of different metal salts.

Particle Type	Relative ICAM-1 Expression
PEG	No response
C_s+PEG	No response
Zn+C_s+PEG	$1.5\times^{+11}$
Na+C_s+PEG	$2.9\times^{+09}$
NH_4+C_s+PEG	$2.1\times^{+12}$
Ni+C_s+PEG	$4.1\times^{+12}$

6.3.2 The Effects of $[C_s+Zn]_p$ Particles containing different quantity of PEG on Cell Cultures

Populations of particles containing 76.7 pg of C_s, 4.3×10^{-1} pg of Zn, and 65 pg of PEG particle were deposited onto cell cultures grown on center-well organ culture dish. Representative images of [76.7 pg of C_s+ 4.3×10^{-1} pg of Zn+ 65 pg of PEG]$_p$ particles

deposited on cell cultures monitored following 72 h incubation periods are presented in figure 6.4. The top images (figure 6.4a-c) and the bottom images (figure 6.4a'-c') are images acquired using bright field and fluorescence microscope respectively.

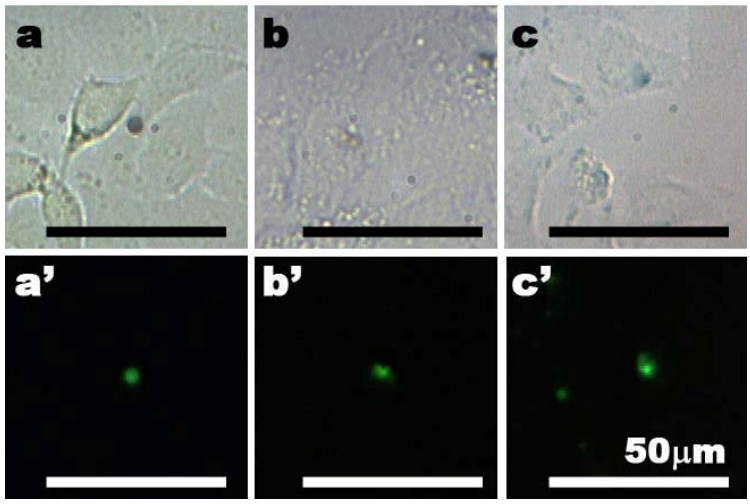

Figure 6.4 Image of [76.7 pg of C_s+ 4.3×10^{-1} pg of Zn+ 65 pg of PEG]$_p$ particles on different cell cultures that were incubated at a) t= 0 h, b) t= 24 h, and c) t= 72 h. a to c are images are viewed using bright field microscope and a' to c' are images viewed using fluorescence microscope. The scale bars of each image are equivalent.

The appearances of the particles, most readily observed from the fluorescence images, were observed to change over the incubation periods (figure 6.4a'-c'). The region from which fluorescence emission (eg. fluospheres) was observed to increase in size as the time of incubation increased. In contrast, the fluorescence emission (eg. fluosphere) of the particle (76.7 pg of C_s, 4.3×10^{-1} pg of Zn, 6.5 pg of PEG, and 4.23 x 10^{-4} pg of fluospheres per particle, [C_s+Zn+PEG]$_p$) on a cell culture was observed to not change (figure 6.1b). Therefore, particles containing 76.7 pg of C_s, 4.3×10^{-1} pg of Zn, and 65 pg of PEG was interpreted being broken down, releasing fluospheres to diffuse from the particle.

The expression of ICAM-1 upregulation on the cell culture dosed with different [76.7 pg of C_s+ 4.3×10^{-1} pg of Zn+ 6.5 pg of PEG]$_p$ or [76.7 pg of C_s+ 4.3×10^{-1} pg of Zn+ 65 pg of PEG]$_p$ following a 24 and 72 h incubation period are shown in figure 6.5a and b respectively.

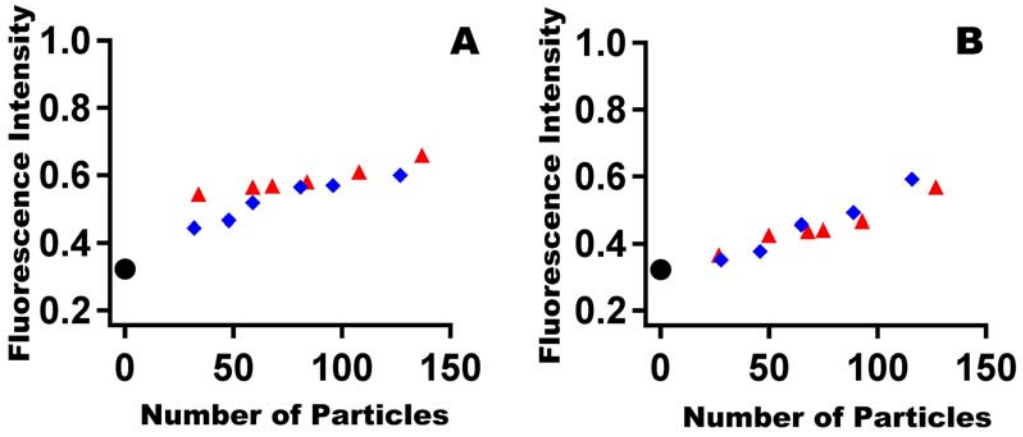

Figure 6.5 Differential expression of ICAM-1 as a function of particle dosage. Cell cultures incubated for A) 24h and B) 72h. (•) negative control, (◆)[76.7 pg C_s + 4.3×10^{-1} pg of Zn + 65 pg of PEG]$_p$, (▲)[76.7 pg C_s + 4.3×10^{-1} pg of Zn + 6.5 pg of PEG]$_p$

6.3.3 Detection of fluorescein fluorescence emission in supernatant samples to which fluorescein containing carbon particles were delivered

A series of fluorescein standard solutions were prepared and the fluorescence signal from each standard was measured. Additionally, 50 and 200 droplets of fluorescein containing carbon particles were prepared and the fluorescence emission from a solution into which those particles had been delivered was also measured. The results are plotted in figure 6.6 as a method calibration response curve.

To address whether or not the soluble component (ie. metal salt) leaches out of the particles that were observed to not break down after 72 h incubation period,

fluorescein containing particles was deposited onto a center-well containing serum free medium and incubated for 5 minutes. The solution was aspirated using a pipette and transferred to a cuvette, and the fluorescence signal measured. The fluorescence emission from the 50 and 200 droplet samples was used to bracket the emission signal measured for the sample solution retrieved from the center-well organ dish into which 200 particles had been deposited into water. Based on this calibration, it was interpreted that approximately 50 % of the fluorescein leached out of the particles within a 5 minute incubation period. By extrapolation to the analogous particle types containing $ZnNO_3$, a more soluble compound than fluorescein, at least 50 % of the Zn^{2+} may also leach from the particle within a period of 5 minutes.

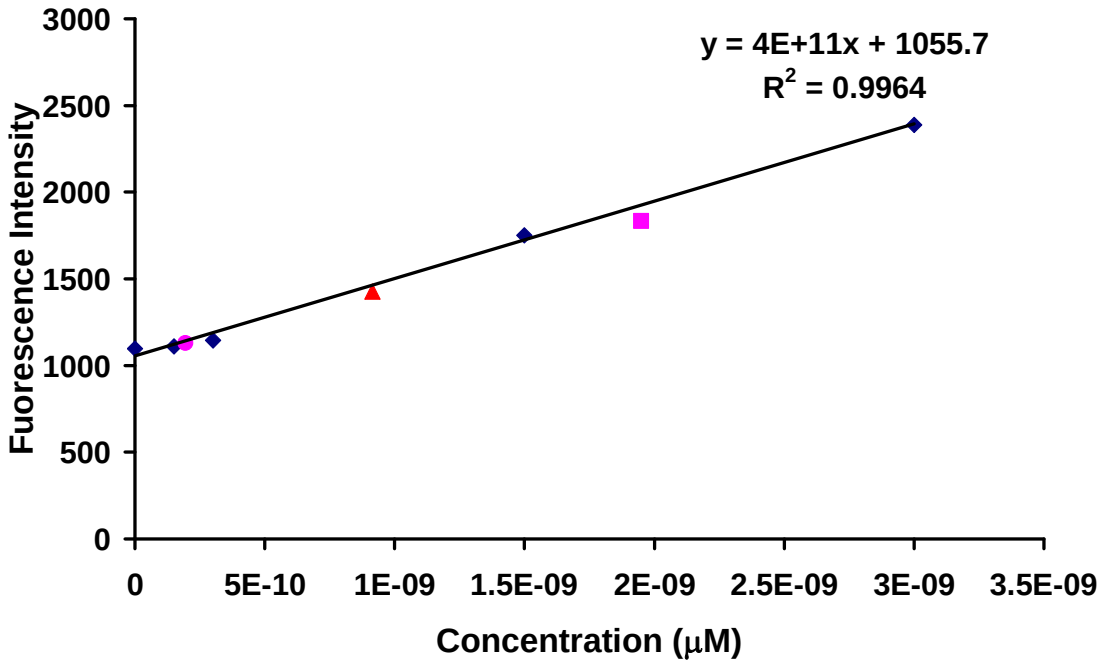

Figure 6.6 Calibration curve of the fluorescein standard solution and fluorescence intensity of (■) 200 droplets, (●) 50 droplets, and (▲) 200 particles of starting solutions

containing 76.7 pg of C_s, 4.3×10^{-1} pg of Zn, 6.5 pg of PEG, and 5.0 x 10^{-4} pg of fluorescein.

6.3.4 The Effects of $[Cs+Zn]_p$ Particles containing EDTA on Cell Cultures

ICAM-1 expression across the cell culture was measured in nine different sites as illustrated in figure 6.7a. When the cell culture was dosed with [76.7 pg of C_s+ 4.3×10^{-1} pg of Zn + EDTA + 65 pg of PEG]$_p$, ICAM-1 was observed to be upregulated only at the site of particle deposition, where the particles also adhered to cells. Representative fluorescence image indicating ICAM-1 upregulation on the cell culture dosed with [76.7 pg of C_s+ 4.3×10^{-1} pg of Zn + EDTA + 65 pg of PEG]$_p$ at the site of deposition and ~5 mm away from the site of deposition are shown in figure 6.7b and c respectively.

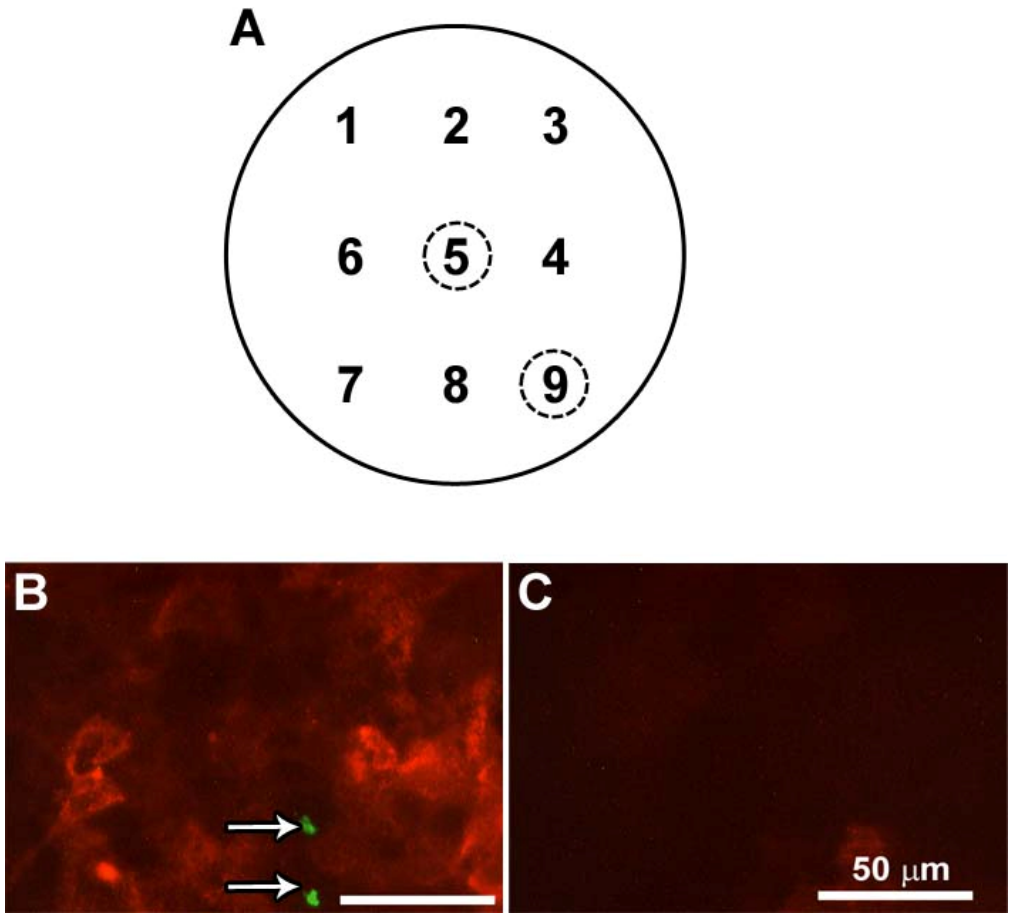

Figure 6.7 a) Illustration of the measured ICAM-1 at nine different sites across the cell culture, b) Expression of ICAM-1at the site of deposition., c) Expression of ICAM-1 ~5 mm away from the site of deposition

Differential expression of ICAM-1 upregulation on the cell culture, as indicated by the fluorescence emissions intensity of fluorescently labelled antibodies bound to ICAM-1 are plotted as a function of particle dosage (figure 6.8). Differential expression of ICAM-1 relative to negative controls was not observed on the cell cultures dosed with $[76.7\text{ pg of } C_s + 2.3\text{ pg of EDTA} + 65\text{ pg of PEG}]_p$ or $[4.3\times10^{-1}\text{ pg of Zn} + \text{pg of EDTA} + 65\text{ pg of PEG}]_p$. In contrast, cell cultures dosed with $[76.7\text{ pg of } C_s + 4.3\times10^{-1}\text{ pg of Zn} + \text{EDTA} + 65\text{ pg of PEG}]_p$ were measured to have undergone ICAM-1 upregulation relative to negative control.

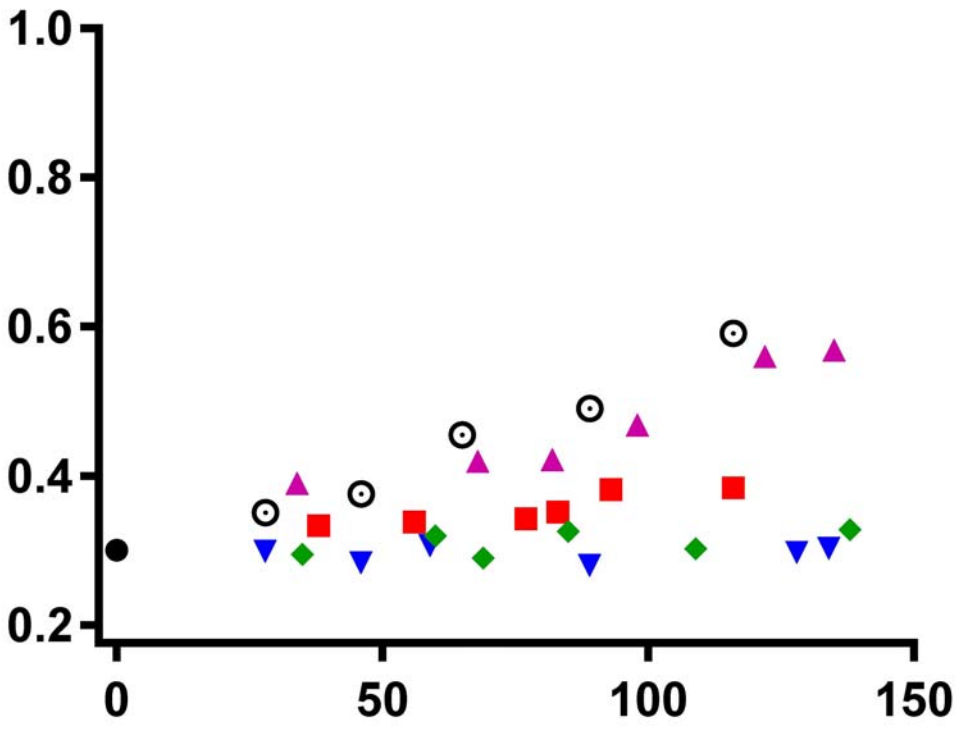

Figure 6.8 Differential expression of ICAM-1 as a function of particle dosage. Cell cultures were incubated for 24 h. (●) negative control, (▲) $[76.7\text{ pg of } C_s + 4.3\times10^{-1}\text{ pg of Zn} + \text{EDTA} + 65\text{ pg of PEG}]_p$, (▼) $[4.3\times10^{-1}\text{ pg of Zn} + \text{pg of EDTA} + 65\text{ pg of PEG}]_p$, (◆)

[76.7 pg of C_s+ 2.3 pg of EDTA+ 65 pg of PEG]$_p$, (■) [76.7 pg Cs + 4.3×10^{-1} pg of Zn + 65 pg of PEG]$_p$. Fluorescence intensity of ICAM-1 for cell cultures dosed with particles containing EDTA was measured at the site of deposition where cell culture dosed with particles not containing EDTA was measured at nice different site across the cell culture. (⊙) [76.7 pg of C_s+ 4.3×10^{-1} pg of Zn + EDTA + 65 pg of PEG]$_p$

6.4 Discussion.

Droplets of initial volume of 326±194 pL were dispensed from one of the starting solutions that contained 1.5×10^{-3} g/mL of India ink, 1.3×10^{-6} g/mL of fluospheres and 4.3×10^{-4} g/mL of PEG. The emission region of fluospheres in ambient particulate mimics containing 76.7 pg of C_s, 4.3×10^{-1} pg of Zn, 6.5 pg of PEG, and 4.23×10^{-4} pg of fluospheres incubated for 72 h was observed (figure 6.1) to be the same. It was speculated that the fluosphere from the particles were starting to difuse away andparticle have not been broken down following the 72 h incubation period.

Several studies have indicated that exposure of EHC-93 to lung cells result in upregulation of pro-inflammatory mediators.[66, 100, 101] With regard to which specific component results in inflammation is not well understood. Through the use of particulate matter mimics, we were able to independently study the *in vitro* injury caused by C_s particles containing a different quantity of the metal salts $Zn(NO_3)_2{\cdot}6H_2O$, NaCl, NH_4NO_3, and $Ni(NO_3)_2{\cdot}6H_2O$. The downstream biological response of the A549 cell culture following the interaction with these particle types was measured immunocytochemistry (ICAM-1). Differential expression of ICAM-1 of the cell culture dosed with carbon particle containing PEG and fluosphere plus different quantity of $[C_s+Zn+PEG]_p$, $[C_s+Na+PEG]_p$, $[C_s+NH_4+PEG]_p$, or $[C_s+Ni+PEG]_p$ were presented in figures 6.3a to e. Dosing the cell culture with either $[PEG]_p$ or $[C_s+PEG]_p$ alonewas found no ICAM-1 upregulation. These results indicate that neither poly-ethyleneglycol nor carbon particles give any effect to the cells. When the cell culture was dosed with

different metal salts it was observed that the expression of ICAM-1 was similar, but note that, the quantity of the specific metal salt per particle type was different. Of note is that prior studies also show ICAM-1 is upregulated when the cells were dosed with samples of whole or fractionated ambient particles, typically at doses of 0.1-1 mg/mL of particles.[51,103,104] However, in this study cell cultures were dosed with up to 150 particles, with a total dose between 2.3×10^{3} to 5.0×10^{3} pg of material. Though different particle chemical compositions result in different ICAM-1 expression, based on the number moles of salt per particle, the mechanism of the ICAM-1 upregulation may have been the same, rupture of lysozomes by osmotic stress. Since the ICAM-1 expression was similar, the relative ICAM-1 expression for the cell cultures was determined by dividing the slope of the ICAM-1 expression with the number of moles of the metal salts per particle. From this, it was found that cell culture dosed with ammonium or nickel containing particles was observed to have high relative ICAM-1 expression.

Based on the observation of particles containing 76.7 pg of C_s, 4.3×10^{-1} pg of Zn, 6.5 pg of PEG, and 4.23×10^{-4} pg of fluospheres, the fluosphere were observed not diffused away following a 72 h incubation period (figure 6.1), whereas increasing only the quantity of PEG to 65 pg in this particle type (figure 6.4) did result in the diffusion away of the fluospheres. Interestingly, differential expression of ICAM-1 of the cell culture dosed with $[C_s+Zn+PEG]_p$ containing 6.5 pg or 65 pg of PEG was observed to be similar (figure 6.5). This observation suggests again suggest that PEG does not affect the

cells however it was not clear whether the soluble or insoluble component of the particles result in ICAM-1 upregulation.

To further examine whether the soluble component leaches out of the insoluble component of the particle, fluorescein containing carbon particles was examined using spectrofluormeter. luorescein fluorescence emission, from the fluorescein containing carbon particles, was detected in serum free medium following a 5 min incubation period (figure 6.6). This suggests that ~50% of soluble components in the particles may leach out of the particle following 5 min incubation period.

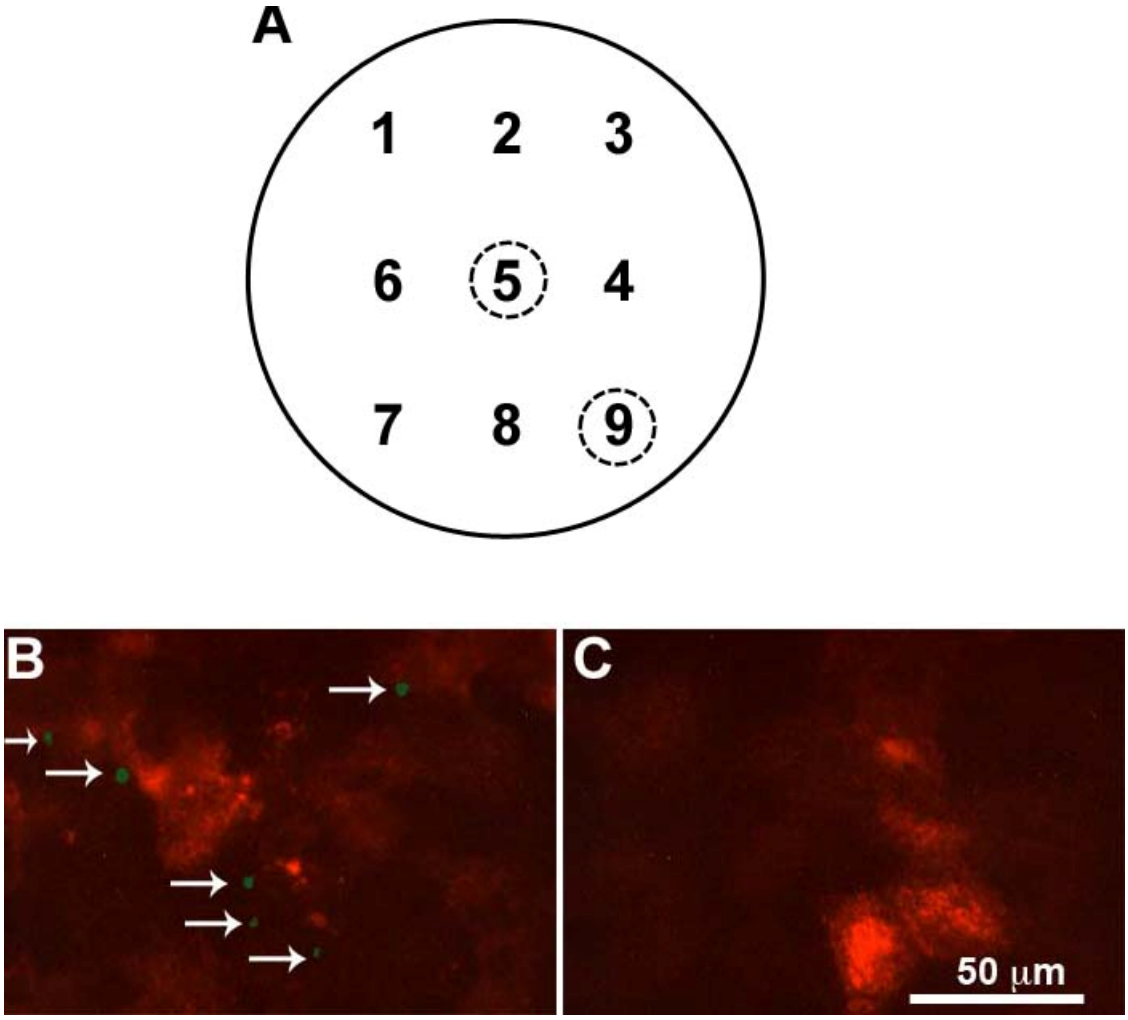

Figure 6.9 a) Illustration of the measured ICAM-1 at nine different sites across the cell culture dosed with[76.7 pg of C_s + 4.3×10^{-1} pg Zn + 6.5 pg of PEG]$_p$ with out EDTA , b) Expression of ICAM-1at the site of deposition., c) Expression of ICAM-1 ~5 mm away from the site of deposition. Arrows indicated where the particles adhered.

EDTA is known as a metal chelator. It was observed that cell cultures dosed with either 76.7 pg of C_s, or 4.3×10^{-1} pg of Zn alone containing EDTA was observed to not express ICAM-1. In contrast, cell cultures dosed with particles containing [76.7 pg of C_s + 4.3×10^{-1} pg of Zn + 6.5 pg of PEG + 2.3 pg of EDTA]$_p$ express ICAM-1 only at the site of deposition. ICAM-1 expression of cell culture dosed with [76.7 pg of C_s + 4.3×10^{-1} pg

of Zn + 6.5 pg of PEG + 2.3 pg of EDTA]$_p$ at the site of deposition was observed to be similar with the cell culture dosed with [76.7 pg of C_s + 4.3×10^{-1} pg Zn + 6.5 pg of PEG]$_p$ with out EDTA measured at nine different site across the cell culture (figure 6.9). Base on this observation, we speculate that when cell cultures were dosed with [76.7 pg of C_s + 4.3×10^{-1} pg Zn + 6.5 pg of PEG]$_p$, the zinc is able to leaches out of the particles, and was bio-available within a maximum region described by diffusion from the particle across the cell culture. However, when the cell culture was dosed with [76.7 pg of C_s + 4.3×10^{-1} pg of Zn + 6.5 pg of PEG + 2.3 pg of EDTA], though the Zn can be assumed able to leach from the particle and diffuse away, within the buffered serum free medium, the zinc component remained chelated by the EDTA and was therefore not bio-available across the cell culture. ICAM-1 expression was not observed at sites remote from where the particles had been deposited and adhered to the cells. Interestingly however, ICAM-1 was expressed at the site of particle deposition, which has been interpreted as being a result of the simultaneous uptake of Zn with Carbon by cells. Within a cell's lysozomes, where the pH was ~3, the [ZnEDTA] complex was not stable and the Zn^{2+} released.

6.5 Summary

Incorporation of PEG into [C_s]$_p$, [C_s+Zn+PEG]$_p$, [C_s+Na+PEG]$_p$, [C_s+NH_4+PEG]$_p$, or [C_s+Ni+PEG]$_p$ result in the adherence of the particle on the cell culture. Following a 72 h the incubation period, it was observed that the emission region of fluospheres in particles containing 76.7 pg of C_s, 4.3×10^{-1} pg of Zn, 6.5 pg of PEG, and 4.23×10^{-4} pg of fluospheres was the same and therefore it was speculated that the particle have not been broken down.

Dosing the cell culture with C_s particles containing PEG, fluosphere plus different metal salts result in the upregulation of ICAM-1 across the entire cell culture. Neither PEG particles nor C_s particles along result in the upregulation of ICAM-1.

Thru spectrofluorimeter, fluorescein containing C_s particles was detected in serum free medium following 5 min incubation period which suggest that the soluble components of the particles leaches out after 5 min incubation period.

Dosing the cell culture with either [76.7 pg of C_s + 6.5 pg of PEG + 2.3 pg of EDTA]$_p$ or [4.3×10^{-1} pg of Zn + 6.5 pg of PEG + 2.3 pg of EDTA]$_p$ was observed to not express ICAM-1, whereas when the cell culture dosed with [76.7 pg of C_s + 4.3×10^{-1} pg of Zn + 6.5 pg of PEG + 2.3 pg of EDTA]$_p$, ICAM-1 was upregulated at the site of deposition, but not at locations removed from the site of particle deposition. Based on the results of the fluorescein fluorescence emission data, we speculate that the zinc, in the C_s particle as Zn^{2+} or [$(ZnEDTA)^{2-}$], is able to leach out of the particles, and able to diffuse from the site of particle adherence across the cell culture. The difference in the ICAM-1 expression observed when adding the EDTA suggests that insoluble material in the particle is a necessary criteria to induce uptake of extracellular entities. Inside the cell, the vesicle docks with a lysozome and the pH drops, causing the release of Zn^{2+} from EDTA. This suggests that when particles containing Zn^{2+} and C_s are deposited onto a culture, there is co-operativity between these two components in activating cells at the site of particle adherence, and that the propagation of those mediators across the culture is promoted by soluble Zn^{2+} that has leached from the particle.

Chapter 7
Summary

The use of a levitation device enables the study of the effect of ambient particulate matter of known size and composition on lung cells. Dosing the cell culture with different coarse size and compositions of ambient particulate matter mimics, cause differential expression of biomolecules. Centrifugation and particle compositions are the two factors determining the adherence 2.4±0.1 μm particle onto a cell culture. Dosing the cell cultures with carbon particle containing LPS results in two distinct dose dependent regime. Furthermore, dosing the cell cultures with carbon particle containing bio-unavailable metal salt result in the expression of ICAM-1 over the entire cell culture where dosing the cell culture with carbon particle containing bio-unavailable metal salt caused ICAM-1 expression at the site where the particles deposited, but ICAM-1 differential expression was not observed at locations distant from the site of particle deposition.

Chapter 8
Future Directions

Numerous studies have demonstrated ambient particulate matter (PM) is a significant factor responsible for observed adverse health effects (increased morbidity and mortality). Most of the work undertaken during the course of this thesis related to the toxicology field revolved around the development of a method to deposit ambient particulate mimics ($PM_{2.5}$) and illustration that the role of a given component of particulate matter could be measured in an *in vitro* study through the measurement of a single pro-inflammatory mediator. In the future, the design of such studies could be extrapolated to incorporate the measurement of the differential expression of additional mediators *in vitro*, and then later followed by *in vivo* experiments that may provide data that can be extrapolated to known adverse health effects on humans following exposure to particulate air pollution.

The methodology developed through the course of this thesis enabled the detailed design of particles of known composition and the ability to deliver a known number of these particles to a cell culture followed by the capability to measure a cellular response. This capability has afforded us the opportunity to address hypotheses that had been challenging to directly test through experimentation. Ambient PM is complex mixture of solid and/or liquid particles of various size and compositions. It would be informative to investigate further the influence of other particle compositions based on compounds

measured to be present in EHC-93, and measure biological responses using other cell lines, and then later co-cultures.

The study involving the measurement of fluorescence emission of ICAM-1 intenstity was observed across the cell culture. The cells exhibiting ICAM-1 upregulation were separated from one another by many cells that themselves did not upregulate ICAM-1. To illustrate, the fluorescence emission of ICAM-1 was measured from the site of deposition to ~1.8 cm away from it in 4 orthogonal directions. Representative fluorescence image indicating ICAM-1 upregulation on the cell culture in one of the four orthogonal directions is presented in figure 7.1.

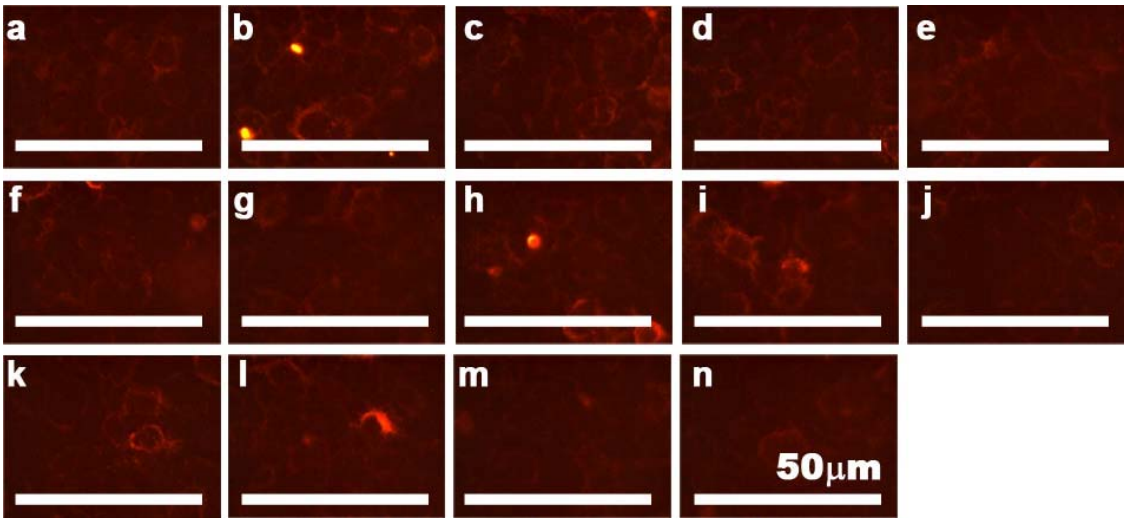

Figure 8.1 Representative fluorescence from one of 4 orthogonal directions (x direction) measure from the site of deposition to ~1.8 cm away from the site of deposition. a to n are fluorescence image captured every 169 μm.

The differential expression of ICAM-1 was determined based on the signal intensity of fluorescence emission. Differential ICAM-1 expression was calculated based on the fluorescence emission signal intensity at each pixel in each scan of a cell culture

using Image J software (Research Services branch, National Institute of Health, Bethesda, MD, USA) and the numerical values of the pixel signals were summed using Microsoft Excel. The summed ICAM-1 expression is reported as a percent of total signal intensity relative to A549 cell cultures treated with TNF-α as the positive control. Presented in figure 7.2, differential expression of ICAM-1 determined based on the signal intensity of fluorescence emission in four orthogonal directions. The fluorescence emission of ICAM-1 was observed to be dominated by the upregulation of individual cells, and periodic in amplitude of fluorescence emission signal intensity.

This observation may have importance with respect to understanding intercellular communication in cultures to which there was a dose of <100 particles. The diameter of the center-well where the cells are grown was ~ 2 cm, but the expression of ICAM-1 well removed from the site of particle deposition and adherence, and along its edge at the wall of the center well, was not measured.

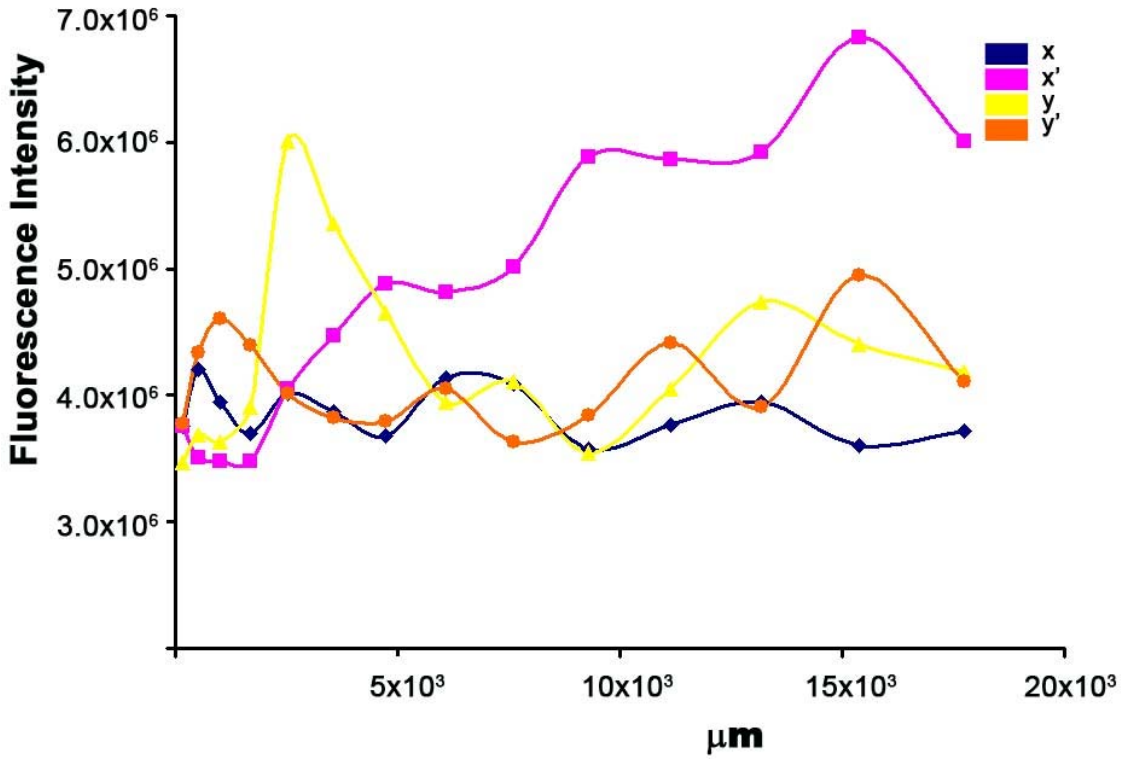

Figure 8.2 Expression of ICAM-1 measure from the site of deposition to ~1.8 cm away from the site of deposition. x, x', y, and y' are the expression of ICAM-1 measured outward from the site of particle deposition at normal angles with respect to each measurement track.

Throughout this study, the positive control used was A549 cell cultures treated with TNF-α. Another methodology for positive control was performed by depositing 6.5 or 13 pg of TNF-α particles onto cell cultures. Fluorescence emission of ICAM-1 intensity was observed across these cell cultures, also in a pattern not-unlike that observed previously for the upregulation of ICAM-1 in response to incubation with particles. This suggest that depositing TNF-α particles onto a cell culture could be a more appropriate positive control because the positive control is treated the same way as the cell culture dosed with different particle type mimics.

APPENDIX

Free Zinc ion concentrations in solution at pH ~ 7 (growth media) and pH ~3 (eg. in a lysozome).

$K_f = 10^{16.5} = [ZnY^{2-}] / [Zn^{2+}] [EDTA]$

$K_f = [ZnY^{2-}] / [Zn^{2+}] [\alpha_y^{4-}] [C_{EDTA}]$

	Zn^{2+} (M)	C_{EDTA} (M)	$[ZnY^{-2}]$ (M)
Initial	2.0×10^{-5}	2.1×10^{-4}	-
Change	-2.0×10^{-5}	1.9×10^{-4}	2.0×10^{-5}
Equilibrium	x	$1.9\times10^{-4} + x$	2.0×10^{-5}

at pH ~7, $\alpha_y^{4-} \sim 3.5\text{x}10^{-7}$, $Kf'(pH=7) = 10^{16.5} \text{ x } 3.5\text{x}10^{-7} = 1.1\text{x}10^{10}$, $[Zn^{2+}] \sim 8.6\times10^{-10}$ M

pH ~ 3, $\alpha_y^{4-} \sim 7.5\text{x}10^{-18}$, $Kf'(pH=3) = 10^{16.5} \text{ x } 7.5\text{x}10^{-18} = 2.4\text{x}10^{-1}$, $[Zn^{2+}] \sim 4\times10^{1}$ M

meaning that no Zn^{2+} is chelated to EDTA

REFERENCES

[1] Dockery, D.W. *et al.*, An Association between Air-Pollution and Mortality in 6 United-States Cities. *New Engl J Med* 329 (24), 1753-1759 (1993).

[2] Pope, C.A. *et al.*, Lung cancer, cardiopulmonary mortality, and long-term exposure to fine particulate air pollution. *Jama-J Am Med Assoc* 287 (9), 1132-1141 (2002).

[3] Zanobetti, A., Schwartz, J., & Dockery, D.W., Airborne particles are a risk factor for hospital admissions for heart and lung disease. *Environ Health Persp* 108 (11), 1071-1077 (2000).

[4] Raes, F. *et al.*, Formation and cycling of aerosols in the global troposphere. *Atmos Environ* 34 (25), 4215-4240 (2000).

[5] Pryor, S.C. & Sorensen, L.L., Nitric acid-sea salt reactions: Implications for nitrogen deposition to water surfaces. *J Appl Meteorol* 39 (5), 725-731 (2000).

[6] Galindo, I., Ivlev, L.S., Gonzalez, A., & Ayala, R., Airborne measurements of particle and gas emissions from the December 1994 January 1995 eruption of Popocatepetl Volcano (Mexico). *J Volcanol Geoth Res* 83 (3-4), 197-217 (1998).

[7] Delfino, R.J. *et al.*, The effect of outdoor fungal spore concentrations on daily asthma severity. *Environ Health Persp* 105 (6), 622-635 (1997).

[8] Huffman, G.P. *et al.*, Characterization of fine particulate matter produced by combustion of residual fuel oil. *J Air Waste Manage* 50 (7), 1106-1114 (2000).

[9] bin Abas, M.R., Oros, D.R., & Simoneit, B.R.T., Biomass burning as the main source of organic aerosol particulate matter in Malaysia during haze episodes. *Chemosphere* 55 (8), 1089-1095 (2004).

[10] Poschl, U., Atmospheric aerosols: Composition, transformation, climate and health effects. *Angew Chem Int Edit* 44 (46), 7520-7540 (2005).

[11] Napari, I., Noppel, M., Vehkamaki, H., & Kulmala, M., An improved model for ternary nucleation of sulfuric acid-ammonia-water. *J Chem Phys* 116 (10), 4221-4227 (2002).

[12] Shukla, A. *et al.*, Inhaled particulate matter causes expression of nuclear factor (NF)-kappa B-related genes and oxidant-dependent NF-kappa B activation in vitro. *Am J Resp Cell Mol* 23 (2), 182-187 (2000).

[13] Medzhitov, R., The Toll-like receptor family and innate immunity. *J Leukocyte Biol*, 11-11 (2000).

[14] Zhang, G.L. & Ghosh, S., Toll-like receptor-mediated NF-kappa B activation: a phylogenetically conserved paradigm in innate immunity. *J Clin Invest* 107 (1), 13-19 (2001).

[15] Baeuerle, P.A. & Henkel, T., Function Amd Activation of Nf-Kappa-B in the Immune-System. *Annu Rev Immunol* 12, 141-179 (1994).

[16] Backhed, F. *et al.*, Gastric mucosal recognition of Helicobacter pylori is independent of Toll-like receptor 4. *J Infect Dis* 187 (5), 829-836 (2003).

[17] Karin, M., Cao, Y.X., Greten, F.R., & Li, Z.W., NF-kappa B in cancer: From innocent bystander to major culprit. *Nat Rev Cancer* 2 (4), 301-310 (2002).

[18] Girardin, S.E., Hugot, J.P., & Sansonetti, P.J., Lessons from Nod2 studies: towards a link between Crohn's disease and bacterial sensing. *Trends Immunol* 24 (12), 652-658 (2003).

[19] Farrow, B. & Evers, B.M., Inflammation and the development of pancreatic cancer. *Surg Oncol* 10 (4), 153-169 (2002).

[20] Montefort, S., Holgate, S.T., & Howarth, P.H., Leukocyte-Endothelial Adhesion Molecules and Their Role in Bronchial-Asthma and Allergic Rhinitis. *Eur Respir J* 6 (7), 1044-1054 (1993).

[21] Fakler, C.R., McMicken, H.W., & Welty, S.E., Induction of lung ICAM-1 by lipopolysaccharide is associated with increased protein binding to an NF kappa B sequence. *Pediatr Res* 45 (4), 302a-302a (1999).

[22] Ley, K. *et al.*, Lectin-Like Cell-Adhesion Molecule-1 Mediates Leukocyte Rolling in Mesenteric Venules Invivo. *Blood* 77 (12), 2553-2555 (1991).

[23] Springer, T.A., Adhesion Receptors of the Immune-System. *Nature* 346 (6283), 425-434 (1990).

[24] Lane, C.S., Mass spectrometry-based proteomics in the life sciences. *Cell Mol Life Sci* 62 (7-8), 848-869 (2005).

[25] Aebersold, R. & Mann, M., Mass spectrometry-based proteomics. *Nature* 422 (6928), 198-207 (2003).

[26] Griffiths, W.J., Jonsson, A.P., Liu, S.Y., Rai, D.K., & Wang, Y.Q., Electrospray and tandem mass spectrometry in biochemistry. *Biochem J* 355, 545-561 (2001).

[27] March, R.E., An introduction to quadrupole ion trap mass spectrometry. *J Mass Spectrom* 32 (4), 351-369 (1997).

[28] Feng, X. & Agnes, G.R., Single isolated droplets with net charge as a source of ions. *J Am Soc Mass Spectr* 11 (5), 393-399 (2000).

[29] Bogan, M.J. & Agnes, G.R., Wall-less sample preparation of mu m-sized sample spots for femtomole detection limits of proteins from liquid based UV-MALDI matrices. *J Am Soc Mass Spectr* 15 (4), 486-495 (2004).

[30] Bogan, M.J., Agnes, G.R., Pio, F., & Cornell, R.B., Interdomain and membrane interactions of CTP : phosphocholine cytidylyltransferase revealed via limited proteolysis and mass spectrometry. *J Biol Chem* 280 (20), 19613-19624 (2005).

[31] Bogan, M.J. & Agnes, G.R., Time-of-flight mass spectrometric analysis of ions produced from adjacent sample spots irradiated simultaneously by a single 337 nm laser. *Rapid Commun Mass Sp* 17 (22), 2557-2562 (2003).

[32] Bogan, M.J. & Agnes, G.R., Preliminary investigation of electrodynamic charged droplet processing to couple capillary liquid chromatography with matrix-assisted laser desorption/ionization mass spectrometry. *Rapid Commun Mass Sp* 18 (22), 2673-2681 (2004).

[33] Bakhoum, S.F.W., Bogan, M.J., & Agnes, G.R., Archiving and absolute quantitation of solutes separated by single charged droplet coulomb explosion. *Anal Chem* 77 (11), 3461-3465 (2005).

[34] Bakhoum, S.F.W. & Agnes, G.R., Study of chemistry in droplets with net charge before and after Coulomb explosion: Ion-induced nucleation in solution and implications for ion production in an electrospray. *Anal Chem* 77 (10), 3189-3197 (2005).

[35] Haddrell, A.E., van Eeden, S.F., & Agnes, G.R., Dose-response studies involving controlled deposition of less than 100 particles generated and levitated in an ac trap onto lung cells, in vitro, and quantitation of ICAM-1 differential expression. *Toxicol in Vitro* 20 (6), 1030-1039 (2006).

[36] Haddrell, A.E., Ishii, H., van Eeden, S.F., & Agnes, G.R., Apparatus for preparing mimics of suspended particles in the troposphere and their controlled deposition onto individual lung cells in culture with measurement of downstream biological response. *Anal Chem* 77 (11), 3623-3628 (2005).

[37] Vastola, F.J., Mumma, R.O., & Pirone, A.J., Analysis of Organic Salts by Laser Ionization. *Org Mass Spectrom* 3 (1), 101-& (1970).

[38] Karas, M. & Hillenkamp, F., Laser Desorption Ionization of Proteins with Molecular Masses Exceeding 10000 Daltons. *Anal Chem* 60 (20), 2299-2301 (1988).

[39] Seliger, B. *et al.*, Identification of markers for the selection of patients undergoing renal cell carcinoma-specific immunotherapy. *Proteomics* 3 (6), 979-990 (2003).

[40] Hillenkamp, F., Karas, M., Beavis, R.C., & Chait, B.T., Matrix-Assisted Laser Desorption Ionization Mass-Spectrometry of Biopolymers. *Anal Chem* 63 (24), A1193-A1202 (1991).

[41] Strupat, K., Kampmeier, J., & Horneffer, V., Investigations of 2,5-DHB and succinic acid as matrices for UV and IR MALDI. Part II: Crystallographic and mass spectrometric analysis. *International Journal of Mass Spectrometry* 169, 43-50 (1997).

[42] Strupat, K., Karas, M., & Hillenkamp, F., 2,5-Dihydroxybenzoic Acid - a New Matrix for Laser Desorption Ionization Mass-Spectrometry. *Int J Mass Spectrom* 111, 89-102 (1991).

[43] Cadene, M. & Chait, B.T., A robust, detergent-friendly method for mass spectrometric analysis of integral membrane proteins. *Anal Chem* 72 (22), 5655-5658 (2000).

[44] Fenn, J.B., Ion Formation from Charged Droplets - Roles of Geometry, Energy, and Time. *J Am Soc Mass Spectr* 4 (7), 524-535 (1993).

[45] Knochenmuss, R. & Zenobi, R., MALDI ionization: The role of in-plume processes. *Chem Rev* 103 (2), 441-452 (2003).

[46] Zenobi, R. & Knochenmuss, R., Ion formation in MALDI mass spectrometry. *Mass Spectrom Rev* 17 (5), 337-366 (1998).

[47] Puretzky, A.A., Geohegan, D.B., Hurst, G.B., Buchanan, M.V., & Luk'yanchuk, B.S., Imaging of vapor plumes produced by matrix assisted laser desorption: A plume sharpening effect. *Phys Rev Lett* 83 (2), 444-447 (1999).

[48] Fujii, T. *et al.*, Interaction of alveolar macrophages and airway epithelial cells following exposure to particulate matter produces mediators that stimulate the bone marrow. *Am J Resp Cell Mol* 27 (1), 34-41 (2002).

[49] Fujii, T., Hayashi, S., Hogg, J.C., Vincent, R., & Van Eeden, S.F., Particulate matter induces cytokine expression in human bronchial epithelial cells. *Am J Resp Cell Mol* 25 (3), 265-271 (2001).

[50] Fujii, T. *et al.*, Adenoviral E1A modulates inflammatory mediator expression by lung epithelial cells exposed to PM10. *Am J Physiol-Lung C* 284 (2), L290-L297 (2003).

[51] Hetland, R.B. *et al.*, Release of inflammatory cytokines, cell toxicity and apoptosis in epithelial lung cells after exposure to ambient air particles of different size fractions. *Toxicol in Vitro* 18 (2), 203-212 (2004).

[52] Marano, F., Boland, S., Bonvallot, V., Baulig, A., & Baeza-Squiban, A., Human airway epithelial cells in culture for studying the molecular mechanisms of the inflammatory response triggered by diesel exhaust particles. *Cell Biol Toxicol* 18 (5), 315-320 (2002).

[53] van Eeden, S.F. *et al.*, Cytokines involved in the systemic inflammatory response induced by exposure to particulate Matter air pollutants (PM10). *Am J Resp Crit Care* 164 (5), 826-830 (2001).

[54] Eleghasim, N.M., Haddrell, A.E., van Eeden, S., & Agnes, G.R., The preparation of < 100 particles per trial having the same mole fraction of 12 inorganic compounds at diameters of 6.8, 3.8, or 2.6 mu m followed by their deposition onto human lung cells (A549) with measurement of the relative downstream differential expression of ICAM-1. *International Journal of Mass Spectrometry* 258 (1-3), 134-141 (2006).

[55] Mukae, H., Hogg, J.C., English, D., Vincent, R., & Van Eeden, S.F., Phagocytosis of particulate air pollutants by human alveolar macrophages stimulates the bone marrow. *Am J Physiol-Lung C* 279 (5), L924-L931 (2000).

[56] Atkinson, R.W. *et al.*, Acute effects of particulate air pollution on respiratory admissions - Results from APHEA 2 project. *Am J Resp Crit Care* 164 (10), 1860-1866 (2001).

[57] Dockery, D.W. & Pope, C.A., Acute Respiratory Effects of Particulate Air-Pollution. *Annu Rev Publ Health* 15, 107-132 (1994).

[58] Gauderman, W.J. *et al.*, Association between air pollution and lung function growth in Southern California children - Results from a second cohort. *Am J Resp Crit Care* 166 (1), 76-84 (2002).

[59] Chow, J.C. *et al.*, A Neighborhood-Scale Study of Pm-10 Source Contributions in Rubidoux, California. *Atmos Environ a-Gen* 26 (4), 693-706 (1992).

[60] Chow, J.C. *et al.*, Temporal and Spatial Variations of Pm(2.5) and Pm(10) Aerosol in the Southern California Air-Quality Study. *Atmos Environ* 28 (12), 2061-2080 (1994).

[61] Schappi, G.F., Monn, C., Wuthrich, B., & Wanner, H.U., Direct determination of allergens in ambient aerosols: Methodological aspects. *Int Arch Allergy Imm* 110 (4), 364-370 (1996).

[62] Becker, S., Soukup, J.M., Gilmour, M.I., & Devlin, R.B., Stimulation of human and rat alveolar macrophages by urban air particulates: Effects on oxidant radical generation and cytokine production. *Toxicol. Appl. Pharm.* 141 (2), 637-648 (1996).

[63] Pritchard, R.J. *et al.*, Oxidant generation and lung injury after particulate air pollutant exposure increase with the concentrations of associated metals. *Inhal Toxicol* 8 (5), 457-477 (1996).

[64] Monn, C. & Becker, S., Cytotoxicity and induction of proinflammatory cytokines from human monocytes exposed to fine (PM2.5) and coarse particles (PM10-2.5) in outdoor and indoor air. *Toxicol. Appl. Pharm.* 155 (3), 245-252 (1999).

[65] Adamson, I.Y.R., Prieditis, H., & Vincent, R., Pulmonary toxicity of an atmospheric particulate sample is due to the soluble fraction. *Toxicol. Appl. Pharm.* 157 (1), 43-50 (1999).

[66] Dreher, K.L. *et al.*, Soluble transition metals mediate residual oil fly ash induced acute lung injury. *J Toxicol Env Health* 50 (3), 285-305 (1997).

[67] Vincent, R. *et al.*, Acute pulmonary toxicity of urban particulate matter and ozone. *Am J Pathol* 151 (6), 1563-1570 (1997).

[68] Becher, R. *et al.*, Rat lung inflammatory responses after in vivo and in vitro exposure to various stone particles. *Inhal Toxicol* 13 (9), 789-805 (2001).

[69] Dye, J.A., Adler, K.B., Richards, J.H., & Dreher, K.L., Role of soluble metals in oil fly ash-induced airway epithelial injury and cytokine gene expression. *Am J Physiol-Lung C* 277 (3), L498-L510 (1999).

[70] Rice, T.M. *et al.*, Differential ability of transition metals to induce pulmonary inflammation. *Toxicol. Appl. Pharm.* 177 (1), 46-53 (2001).

[71] Eagle, H., Nutrition Needs of Mammalian Cells in Tissue Culture. *Science* 122 (3168), 501-504 (1955).

[72] Oyama, V.I. & Eagle, H., Measurement of Cell Growth in Tissue Culture with a Phenol Reagent (Folin-Ciocalteau). *P Soc Exp Biol Med* 91 (2), 305-307 (1956).

[73] Eagle, H., The Minimum Vitamin Requirements of the L-Cells and Hela Cells in Tissue Culture, the Production of Specific Vitamin Deficiencies, and Their Cure. *J Exp Med* 102 (5), 595-& (1955).

[74] Tozer, B.T. & Pirt, S.J., Suspension Culture of Mammalian Cells + Macromolecular Growth-Promoting Fractions of Calf Serum. *Nature* 201 (491), 375-& (1964).

[75] Guilbert, L.J. & Iscove, N.N., Partial Replacement of Serum by Selenite, Transferrin, Albumin and Lecithin in Hematopoietic Cell-Cultures. *Nature* 263 (5578), 594-595 (1976).

[76] Vogt, A., Mishell, R.I., & Dutton, R.W., Stimulation of DNA Synthesis in Cultures of Mouse Spleen Cell Suspensions by Bovine Transferrin. *Exp Cell Res* 54 (2), 195-& (1969).

[77] Haddad, J.J.E. & Land, S.C., O-2-evoked regulation of HIF-1 alpha and NF-kappa B in perinatal lung epithelium requires glutathione biosynthesis. *Am J Physiol-Lung C* 278 (3), L492-L503 (2000).

[78] Stiles, C.D. *et al.*, Dual Control of Cell-Growth by Somatomedins and Platelet-Derived Growth-Factor. *P Natl Acad Sci USA* 76 (3), 1279-1283 (1979).

[79] Folkman, J., Haudenschild, C.C., & Zetter, B.R., Long-Term Culture of Capillary Endothelial-Cells. *P Natl Acad Sci USA* 76 (10), 5217-5221 (1979).

[80] Kelley, D.S., Becker, J.E., & Vanpotter, R., Effect of Insulin, Dexamethasone, and Glucagon on Amino-Acid Transport Ability of 4 Rat Hepatoma Cell Lines and Rat Hepatocytes in Culture. *Cancer Res* 38 (12), 4591-4600 (1978).

[81] Ballard, P.L. & Tomkins, G.M., Hormone Induced Modification of Cell Surface. *Nature* 224 (5217), 344-& (1969).

[82] Fredin, B.L., Seifert, S.C., & Gelehrter, T.D., Dexamethasone-Induced Adhesion in Hepatoma-Cells - Role of Plasminogen Activator. *Nature* 277 (5694), 312-313 (1979).

[83] Lieber, M., Smith, B., Szakal, A., Nelsonrees, W., & Todaro, G., Continuous Tumor-Cell Line from a Human Lung Carcinoma with Properties of Type-Ii Alveolar Epithelial Cells. *Int J Cancer* 17 (1), 62-70 (1976).

[84] Limper, A.H., Tumor necrosis factor alpha-mediated host defense against Pneumocystis carinii. *Am J Resp Cell Mol* 16 (2), 110-111 (1997).

[85] Goto, Y. *et al.*, Exposure to ambient particles accelerates monocyte release from bone marrow in atherosclerotic rabbits. *Am J Physiol-Lung C* 287 (1), L79-L85 (2004).

[86] Foster, K.A., Oster, C.G., Mayer, M.M., Avery, M.L., & Audus, K.L., Characterization of the A549 cell line as a type II pulmonary epithelial cell model for drug metabolism. *Exp Cell Res* 243 (2), 359-366 (1998).

[87] Haddad, J.J., Antioxidant and prooxidant mechanisms in the regulation of redox(y)-sensitive transcription factors. *Cell Signal* 14 (11), 879-897 (2002).

[88] Bals, R., Lipopolysaccharide and the lung: a story of love and hate. *Eur Respir J* 25 (5), 776-777 (2005).

[89] Beinke, S. *et al.*, NF-kappa B1 p105 negatively regulates TPL-2 MEK kinase activity. *Mol Cell Biol* 23 (14), 4739-4752 (2003).

[90] Haddrell, A.E., van Eeden, S.F., & Agnes, G.R., Dose–response studies involving controlled deposition of less than 100 particles generated and levitated in an ac trap onto lung cells, in vitro, and quantitation of ICAM-1 differential expression. *Toxicol in Vitro* 20 (6), 1030-1039 (2006).

[91] Carty, C.L., Gehring, U., Cyrys, J., Bischof, W., & Heinrich, J., Seasonal variability of endotoxin in ambient fine particulate matter. *J Environ Monitor* 5 (6), 953-958 (2003).

[92] Heinrich, J., Pitz, M., Bischof, W., Krug, N., & Borm, P.J.A., Endotoxin in fine (PM2.5) and coarse (PM2.5-10) particle mass of ambient aerosols. A temporo-spatial analysis. *Atmos Environ* 37 (26), 3659-3667 (2003).

[93] Mueller-Anneling, L., Avol, E., Peters, J.M., & Thorne, P.S., Ambient endotoxin concentrations in PM10 from Southern California. *Environ Health Persp* 112 (5), 583-588 (2004).

[94] Schins, R.P.F. *et al.*, Inflammatory effects of coarse and fine particulate matter in relation to chemical and biological constituents. *Toxicol Appl Pharm* 195 (1), 1-11 (2004).

[95] Hasday, J.D., Bascom, R., Costa, J.J., Fitzgerald, T., & Dubin, W., Bacterial endotoxin is an active component of cigarette smoke. *Chest* 115 (3), 829-835 (1999).

[96] Alexis, N.E. *et al.*, Acute LPS inhalation in healthy volunteers induces dendritic cell maturation in vivo. *J Allergy Clin Immun* 115 (2), 345-350 (2005).

[97] Englert, N., Fine particles and human health - a review of epidemiological studies. *Toxicol Lett* 149 (1-3), 235-242 (2004).

[98] Schwarze, P.E. *et al.*, Particulate matter properties and health effects: consistency of epidemiological and toxicological studies. *Hum Exp Toxicol* 25 (10), 559-579 (2006).

[99] Ghio, A.J. & Huang, Y.C.T., Exposure to concentrated ambient particles (CAPs): A review. *Inhal Toxicol* 16 (1), 53-59 (2004).

[100] Ishii, H. *et al.*, Alveolar macrophage-epithelial cell interaction following exposure to atmospheric particles induces the release of mediators involved in monocyte mobilization and recruitment. *Resp Res* 6, - (2005).

[101] Omara, F.O., Fournier, M., Vincent, R., & Blakley, B.R., Suppression of rat and mouse lymphocyte function by urban air particulates (Ottawa dust) is reversed by N-acetylcysteine. *J Toxicol Env Heal A* 59 (2), 67-85 (2000).

[102] Biran, R., Tang, Y.Z., Brook, J.R., Vincent, R., & Keeler, G.J., Aqueous extraction of airborne particulate matter collected on Hi-Vol Teflon filters. *Int J Environ an Ch* 63 (4), 315-322 (1996).

[103] Mundandhara, S.D., Becker, S., & Madden, M.C., Effects of diesel exhaust particles on human alveolar macrophage ability to secrete inflammatory mediators in response to lipopolysaccharide. *Toxicol in Vitro* 20 (5), 614-624 (2006).

[104] Soukup, J.M. & Becker, S., Human alveolar macrophage responses to air pollution particulates are associated with insoluble components of coarse material, including particulate endotoxin. *Toxicol. Appl. Pharm.* 171 (1), 20-26 (2001).